UNIVERSIDADE FEDERAL DE SANTA CATARINA
CENTRO TECNOLÓGICO
PROGRAMA DE PÓS-GRADUAÇÃO EM ENGENHARIA DE AUTOMAÇÃO E SISTEMAS

Jackson Gonçalves Ernesto

Control Design for Constrained LTI and LPV Systems via Polyhedral Set Invariance

Florianópolis
2024

Jackson Gonçalves Ernesto

Control Design for Constrained LTI and LPV Systems via Polyhedral Set Invariance

Tese submetida ao Programa de Pós-Graduação em Engenharia de Automação e Sistemas da Universidade Federal de Santa Catarina para a obtenção do título de Doutor em Engenharia de Automação e Sistemas
Supervisor: Prof. Dr. Eugênio de Bona Castelan Neto
Co-supervisor: Prof. Dr. Eduardo Camponogara

Florianópolis
2024

Ficha catalográfica gerada por meio de sistema automatizado gerenciado pela BU/UFSC.
Dados inseridos pelo próprio autor.

Ernesto, Jackson Gonçalves
Control Design for Constrained LTI and LPV Systems via Polyhedral Set Invariance / Jackson Gonçalves Ernesto ; orientador, Eugênio de Bona Castelan Neto, coorientador, Eduardo Camponogara, 2024.
130 p.

Tese (doutorado) - Universidade Federal de Santa Catarina, Centro Tecnológico, Programa de Pós-Graduação em Engenharia de Automação e Sistemas, Florianópolis, 2024.

Inclui referências.

1. Engenharia de Automação e Sistemas. 2. Invariância de Conjuntos. 3. Realimentação de Saídas. 4. Sistemas LTI e LPV. 5. Controle sob Restrições. I. Neto, Eugênio de Bona Castelan. II. Camponogara, Eduardo. III. Universidade Federal de Santa Catarina. Programa de Pós-Graduação em Engenharia de Automação e Sistemas. IV. Título.

Jackson Gonçalves Ernesto

Control Design for Constrained LTI and LPV Systems via Polyhedral Set Invariance

O presente trabalho em nível de doutorado foi avaliado e aprovado por banca examinadora composta pelos seguintes membros:

Prof.(a) José Mário Araújo, Dr(a).
DAS - SSA - IFBA, Instituto Federal da Bahia

Prof.(a) Carlos Eduardo Trabuco Dórea, Dr(a).
DCA - CT - UFRN, Universidade Federal do Rio Grande do Norte

Prof.(a) Daniel Ferreira Coutinho, Dr(a).
DAS - CTC - UFSC, Universidade Federal de Santa Catarina

Prof.(a) César Cataldo Scharla, Dr(a).
EES - CTS - UFSC, Universidade Federal de Santa Catarina

Certificamos que esta é a **versão original e final** do trabalho de conclusão que foi julgado adequado para obtenção do título de Doutor em Engenharia de Automação e Sistemas.

ICP-Edu
Documento assinado digitalmente
Julio Elias Normey Rico
Data: 24/06/2024 15:54:59-0300
CPF: ***.840.859-**
Verifique as assinaturas em https://v.ufsc.br

Coordenação do Programa de
Pós-Graduação

GOV.BR
Documento assinado digitalmente
EUGENIO DE BONA CASTELAN NETO
Data: 21/06/2024 14:16:55-0300
CPF: ***.477.669-**
Verifique as assinaturas em https://v.ufsc.br

Prof. Dr. Eugênio de Bona Castelan Neto
Orientador

Florianópolis, 2024.

ACKNOWLEDGEMENTS

Gostaria de agradecer a todos os professores, familiares e amigos pelo apoio concedido durante a execução do meu doutorado. Em especial, gostaria de agradecer meu orientador, Prof. Dr. Eugênio de Bona Castelan Neto, pelo apoio, instruções e paciência durante todo o decorrer do doutorado. Também em especial aos meus pais Aldemir Ernesto e Júlia Aparecida Gonçalves Ernesto pelo carinho, cuidados e apoio, não apenas durante meu doutorado, mas também durante toda a minha vida. Não posso deixar também de agradecer ao meu amigo Feres Azevedo Salem que além do grande apoio concedido foi um dos grandes motivadores e incentivadores que me levaram a perseguir o aperfeiçoamento acadêmico e cursar o doutorado. Ao Prof. Dr. Walter Lucia que me apoiou e me acolheu, não somente, mas principalmente, durante o período de pesquisa realizado em Montreal no Canadá. Gostaria de agradecer também ao meu orientador do mestrado Prof. Dr. Cristiano Marcos Agulhari que sem dúvidas teve um papel importantíssimo em minha carreira acadêmica e me concedeu a coragem e confiança necessária para enfrentar o desafio de cursar o Doutorado. Gostaria de reforçar meu agradecimento a todos os meus amigos e familiares que apoiaram, Joshua, Douglas, Caio, Nilson, Leonel, Taynã, Bruno, Giuseppe, Surya, Christian, Anderson, Rafael, Denys, Vinícius, Adriano, Matheus, Geovana, Isabela, Amanda, Camila, Ingrid, Fânia, Giovanna e todos os outros que não foram nomeados aqui.

O presente trabalho foi realizado com apoio da Coordenação de Aperfeiçoamento de Pessoal de Nível Superior – Brasil (CAPES) – Código de Financiamento 001.
Adradeço também aos membros do programa de Pós-Graduação em Engenharia de Automação e Sistemas da UFSC e aos membros da banca.

O meu mais profundo
Obrigado!

RESUMO

Neste trabalho, os conceitos de invariância e contratividade aplicados a conjuntos poliedrais são utilizados para projetar leis de controle por realimentação de saídas e determinar regiões de estabilidade local para sistemas discretos lineares invariantes no tempo e sistemas lineares a parâmetros variantes no tempo. Os sistemas controlados podem estar sujeitos a restrições de estado, controle e variação do controle, e a perturbações persistentes limitadas.

Primeiramente, é utilizado a propriedade de Invariância Positiva Robusta (RPI), também chamada de Δ-Invariância, de conjuntos poliedrais para projetar uma lei de controle por realimentação estática de saídas para sistemas lineares e invariantes no tempo sujeitos a perturbações persistentes, garantindo que as restrições de estado e controle sejam satisfeitas. Condições algébricas são deduzidas para garantir que qualquer trajetória que se inicie no poliedro Δ-invariante permanece nele e convirja em tempo finito para outro conjunto poliedral ao redor da origem, onde a trajetória permanecerá ultimamente limitada. Assim, a solução por realimentação estática de saídas proposta para o sistema de controle restrito também requer a determinação dos conjuntos Δ-invariante e ultimamente limitado.

A seguir, são utilizados os conceitos conjuntos de conjuntos Robustos Controlados Invariantes (RCI) e Robustos Controlados a um Passo (ROSC) para obter um controlador chaveador por realimentação de saídas que guia as trajetórias do sistema restrito à origem em um certo número de passos amostrais. Um conjunto de ganhos estáticos de realimentação de saídas é computado de maneira *offline*, que mais tarde compõe o controlador chaveado.

Na sequência, baseado nas condições algébricas que descrevem de forma equivalente à invariância positiva de conjunto poliedrais para sistemas discretos Lineares a Parâmetros Variantes (LPV), é proposta a abordagem para o projeto de controladores incrementais por realimentação de saídas que garantam a estabilidade assintótica local em malha fechada, com o cumprimento das restrições de estado e controle. O controlador incremental por realimentação de saídas proposto realimenta as saídas medidas e as entradas de controle. O projeto de controle sob restrições permite, em particular, lidar com restrições na variação do controle por meio de uma lei de controle a parâmetros variantes. Finalmente, o projeto da lei de controle incremental LPV é estendida para lidar com perturbações limitadas persistentes. Neste caso, visando buscar soluções menos conservadores, propõe-se utilizar um ganho adicional à lei de controle.

As condições algébricas de projeto propostas são traduzidas em problemas bilineares de otimização bilineares. Cada Problema Bilinear (BP) considera uma função objetivo que otimiza o tamanho do poliedro em um conjunto dado de direções, ponderando o tamanho do poliedro associado (quando necessário), e suas restrições são formadas pelas condições de invariância positiva robusta e inclusões de conjuntos usadas para garantir o cumprimento das restrições. Um *solver* não-linear eficiente (KNITRO) e linguagem de programação AMPL são utilizados para lidar com as bilinearidades presentes nos problemas de otimização. Exemplos numéricos apresentados ao longo do documento demonstram o potencial e efetividade das técnicas propostas.

Palavras-chave: Invariância de Conjuntos. Invariância Robusta. Programação Bilinear. Realimentação de Saídas. Tempo Discreto. Sistemas LTI e LPV. Controle sob Restrições.

ABSTRACT

In this work, set invariance concepts applied to polyhedral sets are used to design stabilizing Output Feedback (*OF*) control laws for linear time-invariant (LTI) and linear parameter varying (LPV) discrete-time systems. The constrained controlled system may be subject to state, control amplitude, and control-rate constraints, and persistent disturbances.

Firstly, we use the Robust Positive Invariance (RPI) property (also called Δ-Invariance) of polyhedral sets to design a stabilizing static Output Feedback (*OF*) control law for linear discrete-time systems subject to persistent disturbances, assuring the states and control constraints fulfillment. We deduce algebraic conditions to guarantee that any trajectory emanating from the Δ-Invariant polyhedron remains in it and converges in finite time to another polyhedral set around the origin, where the trajectory remains ultimately bounded. Thus, the proposed static *OF* solution for the constrained control problem also requires determining the Δ-invariant and the ultimately bounded polyhedra.

Next, we use the joint concepts of Robust Control Invariant (RCI) set and Robust One-Step Controllable sets (ROSC) to obtain a switching output regulator that steers the constrained system's trajectory to the origin in a certain number of sample periods. A set of static output feedback control gains is computed offline, which later compose the online switching regulator.

Then, based on the necessary and sufficient algebraic conditions that describe the polyhedral positive-invariance for LPV systems, we propose an incremental controller design, guaranteeing the regional closed-loop stability and that the control and state constraints are all respected. The proposed incremental output feedback controller feeds back both the measured outputs and control inputs. The constrained control design allows, in particular, dealing with the control-rate variation bounds through a parameter-varying control law. Additionally, an alternative implementation is proposed, where the state and control constraints build part of the positive invariant set. Moreover, we extend the proposed LPV incremental control law design to deal with bounded persistent disturbances.

The proposed algebraic design conditions are translated into bilinear optimization problems. Each Bilinear Problem (BP) considers an objective function that optimizes the polyhedron size in given directions, weighting the size of associated polyhedral sets (when necessary), whose constraints are formed by the robust positive invariance conditions and set inclusions. An efficient non-linear optimization solver (KNITRO) is employed to tackle the present bilinearities through the AMPL language. Furthermore, numerical examples showcase the proposals' effectiveness and potential.

Keywords: Set invariance. Output Feedback. Discrete-time. LTI and LPV systems. Constrained Control.

RESUMO EXPANDIDO

Introdução

Lidar com restrições é uma tarefa essencial na análise e projeto de sistemas de controle. As restrições de estado e controle são ocorrências comuns devido a limites físicos ou de segurança dos elementos que compõe sistemas reais, também é comum a ocorrência de perturbações externas. Essas restrições e perturbações devem ser levadas em consideração no projeto de controladores, pois seus efeitos podem degradar ou, até mesmo, instabilizar os sistemas controlados. Na prática, essas variáveis possuem amplitudes limitadas, o que possibilita serem representadas por conjuntos poliedrais convexos (GONG; SHI, 2012; TARBOURIECH et al., 2011; BLANCHINI; MIANI, 2015).

Assim, para a compreensão e desenvolvimento deste trabalho, os seguintes conceitos são de extrema importância: a contratividade e invariância de conjuntos são fundamentais para garantir o cumprimento das restrições e determinar regiões de estabilidade locais. A invariância de conjuntos relaciona conjuntos convexos a sistemas dinâmicos. A propriedade de Invariância Positiva Robusta (RPI), também chamada de Δ-Invariância, garante que qualquer trajetória que se inicie em um dado conjunto dentro do espaço de estados permanecerá nesse conjunto, independentemente da presença de perturbações externas limitadas em amplitude; Caso o conjunto seja contrativo, essas trajetórias serão ultimamente limitadas em um subconjunto ao redor da origem. Na ausência de perturbações, a RPI se torna Invariância Positiva, onde a contratividade garante a convergência das trajetórias à origem. A Invariância Robusta Controlada (RCI) garante a existência de uma lei de controle que torne um conjunto RPI.

O trabalho se encontra organizado da seguinte maneira. No primeiro capítulo, após uma revisão bibliográfica, são apresentados os conceitos introdutórios e objetivos. No Capítulo 2, são apresentados os resultados do projeto de controladores por realimentação de saídas para sistemas discretos lineares invariantes no tempo sujeito a restrições de estado, controle e a perturbações persistentes limitadas. No Capítulo 3, é proposto a síntese de controladores chaveados por realimentação de saídas para o mesmo tipo de sistema do capítulo anterior. No Capítulo 4, são apresentados técnicas para síntese de controladores incrementais por realimentação de saídas para sistemas discretos lineares a parâmetros variantes no tempo sujeitos a restrições de estado, controle e variação do controle. No Capítulo 5, é proposto uma técnica para síntese de controladores incrementais para o mesmo sistema do capítulo anterior, mas agora também sujeitos a perturbações persistentes limitadas. Por fim, no último capítulo, são apresentadas conclusões, publicações realizadas pelo autor e trabalhos futuros.

Objetivos

O objetivo geral é utilizar propriedades de invariância de conjuntos poliedrais, através de condições algébricas de invariância e programação bilinear, para desenvolver estratégias de projeto de leis de controle por realimentação de saídas para sistemas lineares invariantes no tempo e lineares a parâmetros variantes sob restrições, em especial na presença de perturbações limitadas persistentes e restrições na variação do controle.

Metodologia

O método primordialmente aplicado é o analítico dedutivo, com teoremas e provas, assim como a utilização de casos de estudo e exemplos ilustrados por dados na forma gráfica e tabular, com comentários baseados na teoria de sistemas de controle. Com o intuito de desenvolver estratégias de projeto de controladores para sistemas sob restrições lineares e invariantes no tempo e lineares a parâmetros variantes, foram utilizados os conceitos de invariância positiva e aplicações do lema estendido de Farka's (HENNET, 1995). A partir dessas condições, são então construídos problemas de otimização bilineares que, de maneira geral, buscam a maximização do conjunto invariante positivo (e robusto, quando aplicável) em um conjunto de direções pré-determinados pelo projetista. Com intuito de ilustrar a capacidade das soluções propostas, são apresentados exemplos onde os problemas bilineares são solucionados utilizando o solver KNITRO (BYRD et al., 2006) através do AMPL (FOURER et al., 2003).

Resultados e Discussão

No segundo capítulo, a propriedade de Δ-Invariância de conjuntos poliédricos, também chamada de Invariância Positiva Robusta (RPI), é utilizada para o projeto de controladores por realimentação estática de saída para sistemas discretos lineares invariantes no tempo sujeitos a distúrbios limitados persistentes, garantindo que as restrições de estados e controle sejam respeitadas para toda trajetória que se inicia no conjunto invariante.

Primeiramente, é proposto um conjunto de condições algébricas equivalentes à propriedade de Δ-Invariância de um poliedro externo, a partir do qual as trajetórias do sistema convergem em tempo finito para um poliedro interno associado Ultimamente Limitado (UB). A partir dessas condições de Δ-Invariância e das relações algébricas que descrevem as condições de inclusão que garantem o cumprimento das restrições do estado e controle, são fornecidas condições necessárias e suficientes para a existência de uma lei de controle estática por realimentação de saídas e dois conjuntos invariantes que resolvem o problema de controle considerado. Além disso, é mostrado que, sob certas condições, as soluções propostas podem absorver distúrbios limitados de amplitude mais alta do que os especificados sem ultrapassar as restrições de estado e controle. Além da possibilidade de lidar com restrições assimétricas.

Em seguida, devido as bilinearidades inerentes das condições algébricas de inclusão e de Invariância Positiva Robusta, um problema de otimização bilinear é formulado para resolver o problema de controle sob restrições. O problema de otimização bilinear permite lidar com o tamanho de ambos conjuntos poliedrais invariantes, enquanto a matriz de ganho de controle aparece de forma explicita na formulação. A função objetivo proposta permite o projetista ponderar o tamanho relativo de ambos conjuntos invariantes. Para solucionar o problema bilinear é utilizado o solver KNITRO (BYRD et al., 2006). Adicionalmente, como é lidado com leis de controle por realimentação estática de saídas e a matriz de ganhos de controle aparece de forma explícita na formulação, a proposta permite o cômputo de leis de controle por Realimentação de Estados e Realimentação Dinâmica de Saídas. É demonstrado através de exemplos e comparações com outras técnicas que a estratégia de projeto de controladores proposta pode lidar eficientemente com os três

tipos de leis de controle e restrições estruturais sob essas leis, como a descentralização.

No Capítulo 3, é apresentada uma técnica para projeto de controladores chaveados por realimentação de saídas para sistemas discretos lineares invariantes no tempo sujeitos a restrições de estado e controle e sob o efeito de perturbações persistentes limitadas. O esquema proposto utiliza os conceitos de conjuntos Invariantes Robustos Controlados e conjuntos Robustos Controláveis a um Passo. Diferentemente do capítulo anterior, onde uma única lei de controle por realimentação de saídas e apenas dois conjuntos positivos invariantes são considerados, neste capítulo são construídos pares de conjuntos invariantes e ganhos de controle por realimentação de saídas associados. Assim, os conjuntos invariantes possuem sua própria lei de controle associada e, portanto, possibilitam obter conjuntos externos maiores e conjuntos internos menores quando comparados a aplicação de uma única lei de controle. Isto é possível devido à utilização das leis de controles chaveadas. Ressaltando que as restrições de estado e controle são respeitadas e que as perturbações persistentes são levadas em consideração durante o projeto dos controladores. Assim, para qualquer condição inicial no interior dos conjuntos invariantes, há garantias de que sua trajetória associada irá, em um número máximo e previamente conhecido de passos, convergir ao conjunto Robusto Positivo Controlado interno.

No capítulo 4, é proposta uma solução para o problema de estabilização de sistemas discretos Lineares a Parâmetros Variantes no tempo (LPV) sujeitos a restrições de estado, controle e, em especial, a variação do controle. A solução é construída utilizando a descrição do sistema LPV no espaço de estados estendido, composto pelas variáveis de estado e controle, onde a variação do controle age como a entrada de controle. A partir dessa formulação LPV estendida, são utilizadas as condições algébricas necessárias e suficientes para Invariância Positiva e contratividade de conjuntos poliedrais para propor um procedimento de projeto baseado em um problema otimização bilinear. É importante salientar que a técnica permite o cômputo simultâneo do conjunto positivo invariante e da lei de controle LPV por realimentação de saídas e, além de lidar com restrições assimétricas. Além disso, alguns graus de liberdade a mais aparecem devido à lei de controle realimentar não apenas as saídas da planta, mas também as variáveis de controle. Por fim, a função objetivo otimiza o tamanho do conjunto poliedral associado em algumas direções escolhidas pelo projetista e o problema de otimização bilinear é resolvido utilizando o solver KNITRO.

No Capítulo 5, os resultados do capítulo anterior são estendidos para lidar com sistemas discretos restritos e LPV sujeitos a perturbações limitadas persistentes. Assim, a solução proposta também considera as restrições de estado, controle e variação do controle. Também é construída a partir da descrição do sistema controlado LPV no espaço de estados aumentado, composto pelas variáveis de estado e controle, onde a variação do controle age como a entrada de controle. É utilizado as propriedades de Invariância Positiva Robusta (RPI) para construir um conjunto externo, grande, RPI de condições iniciais dos estados aumentados admissíveis e um conjunto interno, pequeno, onde as trajetórias serão ultimamente limitadas. Esta robustez do sistema a perturbações persistentes o torna mais aplicável em cenários reais.

Além disso, tentando obter mais graus de liberdade no projeto do controlador, foi considerado um ganho adicional constante e associado a saída do sistema no momento da

aplicação do sinal de controle. Este estudo mostra, em particular, que este termo independente da memória do sistema mantém o sistema em malha fechada representado como um sistema LPV politópico clássico. Assim, os resultados podem ser construídos a partir dos vértices das matrizes do sistema politópico em malha fechada, como no capítulo anterior. No entanto, o termo adicional não pode ser definido em alguns caso específicos, discutidos no decorrer do capítulo, e apontam para o uso de um ganho de controle dependente do parâmetro variante.

Considerações Finais

Nesta tese, foram propostas abordagens de projeto de controle inovadoras para sistemas lineares e invariantes no tempo (LTI) sujeitos a restrições de estado, controle e a perturbações limitadas, e para sistemas LPV sem e com perturbações limitadas. As abordagens de projeto são baseadas em invariância de conjunto, invariância positiva de conjuntos, invariância positiva robusta na presença de perturbações, e condições de inclusão de conjuntos para construir problemas de otimização bilinear para projetar os controladores. Exemplos foram fornecidos ao longo do documento para ilustrar as abordagens propostas, e o resumo de cada capítulo será apresentado a seguir.

Primeiro, no Capítulo 2, é proposto um novo conjunto de relações algébricas que descrevem conjuntamente a propriedade de Δ-Invariância (Invariância Positiva Robusta) de um poliedro e a convergência das trajetórias de sistemas lineares em tempo discreto para um poliedro associado Ultimamente Limitado (UB). As condições algébricas são então usadas para compor um problema de otimização bilinear que permite a ponderação entre a maximização do conjunto RPI externo em algumas direções escolhidas *a priori* e na minimização do conjunto UB interno. Os resultados deste Capítulo foram publicados em Briao et al. (2021).

Em seguida, no Capítulo 3, um controlador chaveado por realimentação de saída para sistemas lineares sujeitos a ruídos de processo e medição limitados foi apresentado. Utilizando o lema estendido de Farkas, argumentos de controlabilidade e invariância de conjunto, é proposto um conjunto de condições algébricas que garantem a controlabilidade em um passo para cada poliedro até que o conjunto mais interno seja alcançado, onde as trajetórias do sistema serão ultimamente limitadas. Finalmente, essas condições algébricas compõem um problema de otimização bilinear que visa minimizar o conjunto interno e construir iterativamente um conjunto controlável de um passo maior até que não seja mais possível encontrar um conjunto maior. Os resultados deste Capítulo foram publicados em Lucia et al. (2023).

No Capítulo 4, condições algébricas para um conjunto poliédrico ser positivamente invariante para um sistema LPV sujeito a restrições de estado, controle e taxa de variação do controle foram traduzidas em dois problemas de otimização bilinear. Duas possibilidades diferentes na estrutura dos conjuntos invariáveis positivos são propostas e comparadas. Além disso, as condições algébricas que garantem a estabilidade assintótica são usadas para construir problemas de otimização bilinear que visam maximizar o conjunto invariante positivo em algumas direções escolhidas *a priori*. O conteúdo deste Capítulo está relacionado às publicações Ernesto et al. (2021, 2022).

Além disso, no Capítulo 5, um controlador por realimentação de saída para sistemas LPV sujeitos a ruídos de processo e medição limitados foi apresentado. Utilizando o conceito de Invariância Positiva Robusta, é proposto um conjunto de condições algébricas que garantem que qualquer uma das trajetórias do sistema que começam dentro do conjunto mais externo serão ultimamente limitadas no conjunto mais interno. Finalmente, é proposto um problema de otimização bilinear baseado nessas condições algébricas que permite a ponderação na minimização do conjunto interno onde as trajetórias serão ultimamente limitadas e na maximização do conjunto externo em algumas direções escolhidas *a priori*, representando as condições iniciais estabilizáveis.

Em todos os capítulos, foram empregados o solver Knitro implementado através do AMPL, que permite várias configurações diferentes, incluindo processamento paralelo eficiente em alta velocidade, o que significa que é possível usar vários núcleos computacionais simultaneamente para resolver os problemas de otimização. Além disso, é importante ressaltar que o Knitro não garante a otimalidade global. No entanto, por meio de sua configuração *multistart*, o algoritmo parte de várias condições iniciais diferentes, cobrindo uma porção significativa do espaço de busca, e ao comparar os ótimos locais resultantes, o solver é capaz de fornecer resultados numericamente satisfatórios.

Como trabalhos futuros, recomenda-se: *i)* Estender a lei de controle incremental, utilizada no Capítulo 5 para o controle sob restrições de sistemas LPV discretos no tempo, para que o ganho adicional também seja dependente dos parâmetros variantes, com o objetivo de obter resultados menos conservadores em termos do tamanho do conjunto RPI; *ii)* Propor funções objetivo alternativas e considerar o uso de saturação, com o intuito de melhorar o tamanho dos conjuntos robustos invariantes positivos e a desempenho dos sistemas em malha fechada; e *iii)* Estender os resultados para tratar sistemas LTI discretos e sujeitos a atrasos variantes no tempo, assim como para sistemas de segunda-ordem, com foco em aplicações mecatrônicas.

Palavras-chave: Invariância de Conjuntos. Invariância Robusta. Programação Bilinear. Realimentação de Saídas. Tempo Discreto. Sistemas LTI e LPV. Controle sob Restrições.

LIST OF FIGURES

LIST OF TABLES

LIST OF ABBREVIATIONS AND ACRONYMS

BP	Bilinear Program
C-Sets	Convex-Sets
DoA	Domain of Atraction
DOF	Dynamic Output Feedback
EFL	Extended Farka's Lemma
GF	Gupta and Falcone
LMI	Linear Matrix Inequalities
LP	Linear Programming
LPV	Linear Parameter Varying
LTI	Linear Time-Invariant
MPC	Model Predictive Control
MPT3	Multi-Parametric Toolbox 3
NPP	Nonlinear Programming Problem
OF	Output Feedback
OFCI	Output Feedback-Controlled Invariant
PDC	Parallel-Distributed-Compensation
PI	Proportional Integral
RCI	Robust Controlled Invariant
ROSC	Robust One-Step Controllable
RPI	Robust Positive Invariance
SF	State Feedback
T-S	Takagi-Sugeno
UB	Ultimate Boundedness
UUB	Uniform Ultimate Boundedness
ZOH	Zero Order Holder

CONTENTS

1 INTRODUCTION

Dealing with constraints is an essential part of practical control system design (GONG; SHI, 2012, Chapter 7). The existence of hard constraints on state and control variables has often generated problems in the practical implementation of control laws. Unmodeled phenomena, such as the existence of practical bounds on the amplitude or rate-variation of the control variables and physical limitations on state variables, increase the risks of performance degradation and failure even for complex control designs that do not take them into account (TARBOURIECH et al., 2011; BLANCHINI; MIANI, 2015).

Such constrained control systems appear, for example, in modeling electrical circuits and nonholonomic mechanical systems, the analysis of minimum-phase behavior, and optimal control. For certain nonlinear constrained control systems, stability analysis can be done by using particular classes of candidate Lyapunov functions or by exploiting their structural properties (EBENBAUER; ALLGÖWER, 2007). Another possibility is to approximate or exactly describe the system's nonlinear model by a Linear Parameter Varying (LPV) or Quasi-LPV model, see for instance in Mohammadpour and Scherer (2012) and Tanaka and Wang (2004) and use the vast arsenal of tools for the control design, including Model Predictive Control (MPC).

Disturbances in the system states or in the output measurement (also called noise) are another common source of performance degradation or system instability. Notice that the disturbances are naturally bounded in amplitude in most physical processes, making it realistic to deal with persistent disturbances and noises. Integrating such constraints and disturbances in the control problem formulation is generally recommended and may lead to tractable solutions by optimization-based control designs. In special, the set-invariance theory has appeared as a powerful theoretical tool to guarantee the constraints fulfillment and regional stability or performance requirements (HENNET, 1995; TARBOURIECH et al., 2011; BLANCHINI; MIANI, 2015)

1.1 LPV

Besides the Linear Time-Invariant (LTI) systems treated in this work, we also treat LPV systems. LPV systems concern a class of linear dynamical systems whose state-space matrices depend linearly on parameters that change over time (BRIAT, 2014). Such characteristic allows a wide variety of time-varying and nonlinear plants to be modeled in this way.

The paradigm of LPV systems was first introduced by Shamma (1988) in his Ph.D. thesis for the systematic analysis and design of "gain-scheduled" controllers of nonlinear systems. In broad terms, the design of gain-scheduling control obtains a nonlinear controller from a family of linear controllers, each of which has been tuned to guarantee stability and a certain performance for specific operating conditions of the system. Ac-

cording to the current value of an online measured or estimated time-varying parameter, these linear controllers are combined (scheduled) using some interpolation or switching method. In this case, the closed-loop stability and performance are verified only by extensive simulations. Concerning the classical gain-scheduled control, the modern LPV control theory presents some advantages as the resulting controllers are automatically gain-scheduled and, besides, they guarantee stability, performance, and robustness properties for the closed-loop system. Moreover, modern LPV control exploits the computational tools of the convex optimization (MOHAMMADPOUR; SCHERER, 2012).

The scheduled parameters that govern the variation of the dynamics of an LPV system are usually unknown but bounded and supposed to be measured or estimated online. Moreover, these parameters can be classified into two types: i) exogenous, if they are a function of internal plant variables and exogenous signals, or ii) endogenous, if they are a function of the state variables. This latter case comes from the approximation of nonlinear systems as LPV systems, in which the nonlinear terms are used as scheduling variables. The resulting model is called quasi-LPV system (RUGH; SHAMMA, 2000).

Quasi-LPV and Takagi-Sugeno (T-S) models involve weighting functions that may depend on the state or input variables. Therefore, it is commonly argued that quasi-LPV and T-S models belong to the same class of convex polytopic systems. Especially when a T-S model is obtained from the sector nonlinearity approach from a nonlinear system, it is strictly equivalent to a quasi-LPV model (CHERIFI et al., 2015).

1.2 TAKAGI-SUGENO MODELS

Fuzzy T-S models provide a local representation of nonlinear plants as a convex combination of several linear models (TAKAGI; SUGENO, 1985). This feature has allowed the extension of linear systems analysis and design tools to handle nonlinear systems. In particular, the so-called Parallel-Distributed-Compensation (PDC) controllers can be designed to guarantee local asymptotical stability of a nonlinear system represented by a Fuzzy T-S model (WANG et al., 1996).

Most techniques described in the literature apply to continuous-time systems and consist in formulating analysis and synthesis conditions as convex optimization problems described in terms of Linear Matrix Inequalities (LMIs) (TANAKA; WANG, 2004; FENG, 2006). However, many of such techniques do not consider the fact that Fuzzy T-S models are usually valid only locally. Then, the performance computed through LMIs can only be achieved if the state trajectory is included in the region of validity of the Fuzzy T-S model (KLUG, 2015; KLUG et al., 2015b, 2015a). In (SILVA et al., 2020), a control design methodology is proposed for stabilizing nonlinear discrete-time systems with time-varying delay in the states under actuator saturation, which is based on the use of the fuzzy T–S model and a non-PDC controller. An extension of the previous work is presented in (SILVA et al., 2021), considering the effect of exogenous disturbances.

In both, the local stability of the system is associated with ellipsoidal attraction regions contained within the validity region of the model, and the design problem is formulated in terms of LMIs.

Recent work has been reported on constructing polyhedral invariant sets for discrete-time Fuzzy T-S systems. In Dórea et al. (2020), the constrained control of the Fuzzy Takagi-Sugeno system problem is solved with polyhedral Convex(C)-Sets (see also other related references in Dórea et al. (2020). In Isidório et al. (2023), a systematic design method of observer-based output feedback controllers based on the theory of invariant sets for fuzzy T–S systems with unmeasurable premise variables is formulated regarding a bilinear optimization problem.

1.3 MODEL PREDICTIVE CONTROL

One way to handle constraints and disturbances is by utilizing MPC (MAYNE et al., 2000). A basic design premise for MPC is that the disturbances are bounded, and the bounds are known. However, such control schemes generally imply considerable online computations and are not always robust enough. Nonetheless, robust MPC has been widely applied in control design problems (BORRELLI et al., 2017).

In Wan and Kothare (2002), the authors propose to decouple the state feedback controller and state estimator's design and then verify that robust stability is preserved when the resulting augmented output feedback controller is considered. In Findeisen et al. (2003), theoretical conditions are given to guarantee the stability of nonlinear MPC when used together with a state-observer. In Ding et al. (2008), a sequence of the output feedback controller is first offline designed for different bounds on the state-estimation error set and then online used according to the error realization. In Løvaas et al. (2008), a robust output-feedback MPC is designed, and the robust stability test is incorporated into a LMI condition that is proved to be feasible under an appropriate small-gain condition. In Mayne et al. (2009), the regulation problem is solved by employing a Luenberger state observer and a tube-based robust MPC. Along similar lines is Kögel and Findeisen (2017), where the conservativeness of the resulting tube-based MPC is reduced. In Subramanian et al. (2017), a tube-based MPC is also designed. However, different from other solutions, the proposed approach is independent of the used state-estimator algorithm. In Lorenzetti and Pavone (2020), a simplified single tube-based robust output feedback MPC is proposed, and it is shown that its computational complexity is equal to the one that would be obtained if the full state were available. In MORATO (2023), LPV models (and quasi-LPV embeddings) are used in order to model nonlinear and time-varying dynamics that can serve as a support to design real-time capable non-linear MPC algorithms.

1.4 SET INVARIANCE

Set-invariance is a powerful concept to treat various constrained control problems that deal with practical constraints. For systems subject to bounded disturbances, the so-called Robust Positive Invariance (RPI) (also called Δ-Invariance) property guarantees that any trajectory starting from a set inside the state space will remain in this set and, possibly, will be ultimately bounded in some of its subsets (BLANCHINI, 1990; MILANI, B. E. A.; DÓREA, 1996, 1996). In the absence of the disturbances, the Robust Positive Invariance (BLANCHINI; MIANI, 2015; GUPTA; FALCONE, 2019; KÖGEL; FINDEISEN, 2017), reduces to the classical Positive Invariance property, which guarantees the convergence to the origin when the related set is contractive along the trajectories of the system (HENNET, 1995; BLANCHINI, 1999; BITSORIS et al., 2014; TARBOURIECH et al., 2011).

The concept of positive invariance is, in principle, not associated with a Lyapunov function. Therefore, the idea of set-invariance can originate a much more general theory than Lyapunov Theory. For instance, the standard definition of a Lyapunov function requires positive definiteness. A Lyapunov function is typically used to assure the stability or boundedness of a system's solution. Still, the positive invariance conditions are pretty close (at least from a technical standpoint) to the known derivative conditions in Lyapunov theory (BLANCHINI; MIANI, 2015).

Several set-invariance techniques have been developed to solve control problems for linear systems subject to state and control constraints and to persistent disturbances (BLANCHINI; MIANI, 2015). In particular, polyhedral invariant sets have resulted in larger regions of attraction than the ellipsoidal sets obtained from quadratic Lyapunov functions delivered by LMI-based techniques. Most of the proposed constrained control techniques tackle the state and control limits using the positive-invariance and contractivity properties of C-sets, which allow the respect of constraints and guarantee closed-loop asymptotic stability.

Although the possibility of using LMI-based algorithms makes ellipsoidal sets and related composite structures more common in the literature (see, for instance, Hu and Lin (2001) and Tarbouriech et al. (2011)), polyhedral sets have been receiving a great deal of attention. Besides the fact that the shape of polyhedral sets fits best to the amplitude bounded constraints often encountered in practice, they can define level sets associated with a class of universal Lyapunov functions (see Blanchini (1999)).

In particular, the algebraic conditions that describe the RPI property of polyhedral sets for time-invariant and uncertain linear systems (BLANCHINI, 1990; MILANI, B. E. A.; DÓREA, 1996, 1996) can be used to treat some constrained control problems subject to persistent disturbances. For instance, by considering a given polyhedral set of state constraints and amplitude bounded control inputs, a Linear Constrained Control Problem consists of obtaining a linear state or output feedback control law that guarantees the

Δ-Invariance of that set of state constraints. In contrast, only admissible control inputs are applied. Thus, this kind of problem can be stated and solved by Linear Programming (LP), where the closed-loop RPI relations appear as part of the linear constraints of the associate LP optimization procedure, as in B. E. A. Milani and Dórea (1996) and M. M. D. Santos et al. (1997). In general, however, the set of state constraints cannot be made RPI by a linear or even a nonlinear feedback control law. In such cases, a possible solution is finding a feedback control law that makes RPI another *a*-priori unknown polyhedron, as large as possible but contained in the set of state constraints.

The concept of Robust Controlled Invariant (RCI) sets allows us to look for the existence of the maximal RCI set contained in the set of state constraints. Such a maximal RCI set can be determined by a sequence of LP problems that generates a family of one-step controlled invariant sets. Thus, a series of static state-feedback control actions can be generated online from the state's knowledge. Furthermore, the extension of this RCI set approach for dealing with output feedback control is not direct and turns out to be theoretically more involving, as well as its online application since only partial information about the states is available (see, for instance, Dantas et al. (2018) and Dórea et al. (2020) and references therein). Notice also that, in general, a linear state or, even less, static output feedback does not exist that can make Robust invariant the maximal RCI set. However, the optimization procedure mentioned in the above paragraph is readily available and adapted to look for those feedback matrices. We should also remember that the maximal RCI set approach may generate complex polyhedral sets regarding the polyhedron's vertices or faces.

Another approach consists of the numerical determination of an unknown robust invariant polyhedral set with guaranteed complexity using algebraic relations that ensure the Δ-invariance of polyhedral sets. Thus, using the LMI design technique in Gupta and Falcone (2019) (see also other author's references mentioned therein), it is possible to find a linear state-feedback control law and an associated Δ-invariant set, with optimized size and given complexity. Notice that this technique is based on a sufficient condition that guarantees the Robust/Δ-invariance of polyhedral sets does not deal with the design of an associated Ultimate Boundedness (UB)-set and does not deal with output feedback.

Another possibility is using the necessary and sufficient algebraic conditions that describe the robust invariance property to look for linear control laws and an associated robust invariant polyhedron, with guaranteed complexity, that satisfies the state and control constraints. As mentioned before, it results in more sophisticated optimization techniques than a single LP, primarily to deal with some inherent bilinear products among the matrix and vector variables involved in the algebraic relations (see, for instance, Blanchini and Miani (2015) and Brião et al. (2018)). Furthermore, using this last technique for tackling the mentioned control problem by linear static Output Feedback *(OF)* control law, which by itself characterizes a non-convex stabilization problem (SADABADI; PEAU-

CELLE, 2016), and jointly considering the determination of an associated set for UB is a more challenging problem. Besides, by considering solutions through *static OF*-control laws, the obtained results can readily be adapted to deal with State Feedback *(SF)* and Dynamic Output Feedback *(DOF)* control laws. A related control problem using T-S fuzzy modeling was treated in Dórea et al. (2020), see also Isidório et al. (2023).

Utilizing the positive invariance concepts, some recent works pursuing the design of Proportional Integral (PI) or PI-like controllers to tackle the tracking problem for LTI systems have already been developed (see França et al. (2021), Geovana Franca dos Santos et al. (2024), Dos Santos et al. (2023) and Geovana Franca dos Santos et al. (2023)). Through the positive invariance and set inclusion conditions, these works solved the tracking problem for constrained systems subject to different types of reference signals. For example, Geovana Franca dos Santos et al. (2024) tackles the tracking problem for ramp and sinusoidal references, reinforcing the potential of using polyhedral invariance concepts in designing controllers.

BILINEAR PROGRAMMING

As in Brião (2019), Dórea et al. (2020), França et al. (2021) and Isidório et al. (2023), the optimization techniques in the present document take the form of a Bilinear Program (BP).

A BP is a kind of Nonlinear Programming Problem (NLP) in which all nonlinear terms consist of products of two variables. From an initial guess, local algorithms can take advantage of derivatives to reach a locally optimal solution relatively fast but without a certificate of solution quality. Sequential quadratic programming and interior-point methods are two efficient local algorithms available in software (WÄCHTER; BIEGLER, 2006; WALTER et al., 2005). However, the dependency on the initial guess can compromise the quality and even feasibility of the local algorithm's trial solution, especially when the problem is highly nonlinear and when local minima abound. Conversely, global algorithms are less dependent on initial guesses, such as spatial branch-and-bound, which can find a globally optimal solution (FLOUDAS, 2005) by iteratively partitioning the search space and relying on lower and upper bounding procedures. However, owing to the complexity involved that can lead to an exponential search, global optimization is primarily effective in low-dimensional problems.

This work follows an optimization strategy halfway between local and global algorithms, which applies a local solver with multistart capabilities. It means that the local algorithm is invoked from multiple initial guesses in an attempt to provide a proper cover of the decision space. More precisely, we generate the results using the KNITRO solver (BYRD et al., 2006), which implements a multistart strategy in tandem with four state-of-the-art algorithms for solving continuous, nonlinear optimization problems. Among them, the Interior/CG algorithm proved to be the most efficient and robust for solving

the proposed bilinear programming problem. Ultimately, it should be noted that KNITRO does not guarantee to find globally optimal solutions, however, local minima are found upon convergence. Furthermore, the nonlinear optimization problem present in this work, whose constraints are formulated by a matrix form, can be expressed in the element-wise form that is more suitable for the language AMPL (FOURER et al., 2003) that employs KNITRO.

1.5 OBJECTIVES

The general objective is to use the invariance property of polyhedral sets through the so-called algebraic invariance conditions and bilinear programming to develop output feedback design strategies for constrained LTI and LPV control systems, especially those that include exogenous bounded disturbances and control rate constraints.

More specifically, I pursue the following complementary objectives

1.5.1 Specific Objectives

1. To develop output feedback control design conditions for discrete-time LTI systems subject to disturbances, measurement noises, state, and control constraints, that, if fulfilled, guarantee the local closed-loop system's ultimate boundedness stability.
2. To develop design conditions for a switching output feedback control problem for constrained discrete-time LTI systems subject to bounded disturbances, which, if fulfilled, guarantee the local closed-loop system's stability.
3. To develop conditions for incremental control feedback design problem for discrete-time LPV systems subject to state and control constraints (amplitude and rate) that, if fulfilled, guarantee the local closed-loop system's asymptotic stability.
4. To develop conditions for incremental control feedback design problem for constrained discrete-time LPV systems subject to bounded disturbances and control amplitude and rate constraints, such that, if fulfilled, guarantee the local closed-loop system's ultimate boundedness stability.
5. To implement all the proposed conditions computationally and compare with other approaches in the literature.

1.6 ORGANIZATION AND CONTRIBUTIONS

The next four chapters are aligned with the previous objectives. These chapters and the Conclusion one are organized as follows:

In chapter 2, based in (BRIAO et al., 2021), we use the Δ-Invariance property of polyhedral sets to design a stabilizing static OF for linear discrete-time systems subject

to persistent disturbances, assuring the states and control constraints fulfillment. We deduce new algebraic conditions to guarantee that any trajectory emanating from the Δ-Invariant polyhedron remains in it and converges in finite time to another polyhedral set around the origin, where the trajectory remains ultimately bounded. Thus, the proposed *static OF* solution for the constrained control problem also requires determining the Δ-invariant and the ultimately bounded polyhedra. Therefore, the proposal considers a bilinear optimization problem whose objective function weighs the two associated polyhedral sets' size and whose constraints are formed by the invariance relation.

In chapter 3, based in (LUCIA et al., 2023), we use the joint concepts of the RCI set and Robust One-Step Controllable (ROSC) sets to offline design a family of robust switching static output feedback controllers for constrained linear systems subject to persistent bounded process and measurement noises. The resulting necessary and sufficient algebraic conditions are then used to propose a bilinear optimization problem to design each static output feedback controller. Finally, the constrained system's trajectory is steered to the origin in a certain number of sample periods by switching the static output feedback controllers online.

In chapter 4, based in Ernesto et al. (2021, 2022), we describe the constrained control system in the extended state space composed of the system's state and control variables, in which the control variations act as the control inputs. From this extended LPV formulation, we use the algebraic conditions for positive invariance and contractivity to propose two bilinear optimization problems to design the controller. The second bilinear optimization problem is an alternative implementation, proposing a different structure to the positive invariant set. In the LPV setting, the varying parameters are considered to be measured or computed online, which allows for dealing with LPV control laws such that the gains depend on such varying parameters. The proposed bilinear optimization problem for the controller design guarantees regional closed-loop stability for LPV systems, respecting state amplitude, control amplitude, and control rate constraints.

In Chapter 5, similar to the previous chapter, we describe the constrained control system in the extended state space composed of the system's state and control variables, in which the control variations act as the control inputs. This time, we use the RPI property to propose a new set of conditions for LPV discrete-time systems subject to persistent disturbances, guaranteeing the state, control, and control variation constraints fulfillment. The resulting algebraic conditions are then used to propose a bilinear optimization problem that jointly computes an external set of admissible initial conditions, an internal set where the system's trajectories will be ultimately bounded, and the necessary control gains to guarantee regional closed-loop stability.

Finally, in Chapter 6, we summarized the thesis document contributions, along with a list of the author's publications throughout the doctorate and some recommendations for future works.

It is worth noting that the contents of Chapters 2 to 4 are strongly based on the author's publications. As a consequence, each chapter is almost self-contained. However, some notations may differ from chapter to chapter, in which cases we warn the reader. Thus, this first chapter finishes with some basic notation and concepts shared in this doctorate thesis.

SOME BASIC NOTATION AND CONCEPTS

Notation:

The sets of real numbers, real-values column vectors of dimension $n_v > 0$ and real-values matrices of dimension $n_r \times n_c$, $n_r, n_c > 0$ are denoted with $\mathbb{R}$, $\mathbb{R}^{n_c}$ and $\mathbb{R}^{n_r \times n_c}$, respectively. The entries of a matrix M are denoted M_{ij}, $\forall i, j$. The vectors $\mathbf{0}_p \in \mathbb{R}^p$, $\mathbf{1}_p \in \mathbb{R}^p$ denote columns of vectors containing only zeros or ones in all the components. Given a vector $v \in \mathbb{R}^{n_v}$, v_k represents the value of v at the discrete time instant $k \in \mathbb{Z}_+ := \{0, 1, ...\}$. Given an invertible square matrix M, M^{-1} denotes its inverse.

The following definitions and lemma can be found in Hennet (1995) and Blanchini and Miani (2015).

Definition 1 *(Convex Polyhedral Set) Any closed and convex polyhedral set $\mathcal{P}(\phi) \subseteq \mathbb{R}^n$ can be characterized by a shaping matrix $P \in \mathbb{R}^{l_p \times n}$ and a vector $\phi \in \mathbb{R}^{l_p}$, with l_p and n being positive integers, i.e.,*

$$\mathcal{P}(\phi) = \{x \in \mathbb{R}^n : Px \leq \phi\}. \tag{1}$$

Note that $\mathcal{P}(\phi)$ in (1) includes the origin as an interior point if $\phi > 0$. In the sequel, if $\phi = \mathbf{1}_* = [1\ 1 \dots\ 1]^T \in \mathbb{R}^*$, the resulting polyhedral set $\mathcal{P}(\mathbf{1}_*)$ will be simply denoted as $\mathcal{P}$. Additionally, a convex polyhedral set is also said to be compact if it is bounded and closed, which requires that $rank(P) = n$.

Definition 2 *(Non-negative Matrix) A matrix M is non-negative, if all elements satisfy $M_{ij} \geq 0, \forall i, j$.*

Lemma 1 *Extended Farkas'Lemma (EFL) (HENNET, 1995): Consider two polyhedral sets of $\mathbb{R}^n$, defined by $\mathcal{P}_i = \{x : P_i x \leq \phi_i\}$, for $i = 1, 2$, with $P_i \in \mathbb{R}^{l_{p_i} \times n}$ and positive vectors $\phi_i \in \mathbb{R}^{l_{p_i}}$. Then $\mathcal{P}_1 \subseteq \mathcal{P}_2$ or, equivalently, $P_2 x \leq \phi_2, \forall x : P_1 x \leq \phi_1$, if and only if there exists a non-negative matrix $Q \in \mathbb{R}^{l_{p_2} \times l_{p_1}}$ such that*

$$\begin{aligned} QP_1 &= P_2, \\ Q\phi_1 &\leq \phi_2. \end{aligned}$$

2 OUTPUT FEEDBACK DESIGN FOR DISCRETE-TIME CONSTRAINED LTI SYSTEMS VIA BILINEAR PROGRAMMING

In this chapter, we use the Δ-Invariance property of polyhedral sets, also called RPI to design a stabilizing *static OF* for linear discrete-time systems subject to persistent disturbances, assuring the states and control constraints fulfillment.

We first propose a new set of algebraic conditions equivalent to the Δ-Invariance property of an external polyhedron from which the system trajectories converge in finite time to an associated internal UB-polyhedron. From these Δ-Invariance and the algebraic relations that describe the inclusion conditions that guarantee the state and control fulfillment, we give necessary and sufficient conditions for the existence of a *static OF*-control law and two invariant sets that solve the considered constrained control problem. Also, under certain conditions, we show that the proposed solutions can absorb higher amplitude-bounded disturbances than the specified ones without overshooting the state and control constraints.

Further, due to the inherent bilinearities in the Δ-Invariance and the inclusion conditions, a bilinear optimization problem is formulated to solve the associated constrained control problem. The proposed bilinear optimization design strategy allows dealing with the two invariant polyhedra sizes, while the control gain matrix appears explicitly in the formulation. Then, the proposed objective function allows the designer to *trade-off* the relative sizes of the two invariant sets. To tackle the bilinear approach proposed in this chapter, the efficient KNITRO solver (BYRD et al., 2006) is used.

Additionally, since we deal with *static OF*-control laws and the control gain matrix appears explicitly in the formulation, our proposal also allows computing *SF* and *DOF*-control laws. We show that the proposed control design strategy can efficiently deal with the three fundamental control laws and structural constraints, such as decentralization, through numerical examples, also comparing with some existing techniques.

Thus, the present chapter closely follows the contents of our first journal contribution (BRIAO et al., 2021). It improves the results presented in Brião's thesis, (BRIÃO, 2019, Chapter 5), by developing new Δ-invariance conditions, numerically implementing a set of directions instead of a shape-set to promote the growth of the invariant sets, and by extending the control design to DOF and Decentralized DOF controllers.

The chapter is organized as follows. The next section is devoted to the formulation of the considered control problem. Section 2.2 proposes the new Δ-Invariance algebraic conditions and presents other basics for the proposed design approach. Section 2.3 is devoted to the presentation of the bilinear optimization design strategy and contains a discussion of design principles and implementation aspects, including the ability to deal with *SF* and *DOF*-control laws. Section 2.4 reports two numerical examples, including comparisons with two other proposals from the literature and exploiting different features allowed by the design approach. A Conclusion finishes the chapter.

2.1 PROBLEM STATEMENT

Consider the following linear time-invariant discrete-time system:

$$x_{k+1} = Ax_k + Bu_k + B_p p_k \tag{2a}$$
$$y_k = Cx_k + D_\eta \eta_k, \tag{2b}$$

where $k \in \mathbb{N}$ is the time index, $x_k \in \mathbb{R}^n$ is the state, $u_k \in \mathbb{R}^m$ is the control input, $y_k \in \mathbb{R}^p$ is the measured output, and $p_k \in \mathbb{R}^s$ and $\eta_k \in \mathbb{R}^q$ are exogenous disturbances. The system matrices have the appropriate dimensions and the pairs (A, B) and (C, A) are controllable and observable, respectively.

Furthermore, the states and control inputs are constrained to evolve within given polyhedral sets, and the disturbances are considered to be persistent (*i.e.*, amplitude bounded). Thus, without loss of generality, these constraints are represented by the following polyhedral sets:

$$\mathcal{X} = \{x_k : Xx_k \leq \mathbf{1}_{l_x}\}, \text{ with } X \in \mathbb{R}^{l_x \times n}, \tag{3a}$$
$$\mathcal{U} = \{u_k : Uu_k \leq \mathbf{1}_{l_u}\}, \text{ with } U \in \mathbb{R}^{l_u \times m}, \tag{3b}$$
$$\mathcal{P} = \{p_k : Pp_k \leq \mathbf{1}_{l_p}\}, \text{ with } P \in \mathbb{R}^{l_p \times s}, \tag{3c}$$
$$\mathcal{N} = \{\eta_k : N\eta_k \leq \mathbf{1}_{l_n}\}, \text{ with } N \in \mathbb{R}^{l_n \times q}. \tag{3d}$$

Notice that the adopted set representation allows describing a broad range of practical constraints and amplitude-bounded disturbances, as symmetrical, dissymmetrical, and asymmetrical ones (BLANCHINI; MIANI, 2015; TARBOURIECH et al., 2011).

In this chapter, we primarily consider a stabilizing linear *static OF* control law

$$u_k = Ky_k, \quad K \in \mathbb{R}^{m \times p}, \tag{4}$$

such that the corresponding closed-loop system is given by:

$$x_{k+1} = (A + BKC)x_k + Dd_k, \tag{5}$$

where $(A + BKC)$ is Schur stable, $D = [B_p \mid BKD_\eta] \in \mathbb{R}^{n \times l_d}$, with $l_d = s + q$, and $d_k = [p_k^T \ \eta_k^T]^T \in \mathbb{R}^{l_d}$ verifies, from (3c) and (3d):

$$\Delta = \{d_k : \Pi d_k \leq \mathbf{1}_{l_\pi}\}, \text{ with } \Pi = diag\{P, N\} \in \mathbb{R}^{l_\pi \times l_d}, \ l_\pi = l_p + l_n. \tag{6}$$

Thus, by considering the state and control constraints, and that the closed loop-system is subject to persistent exogenous disturbances, the following control problem is considered in the sequel.

Problem 1 *Find a stabilizing linear static OF matrix K in* (4)*, a* large *set $\mathcal{L}_0 \subseteq \mathcal{X}$ and a* small *set $\mathcal{L}_\infty \subseteq \mathcal{L}_0$, such that for any initial condition $x_0 \in \mathcal{L}_0 \backslash \mathcal{L}_\infty$ and for any persistent disturbances $d_k \in \Delta$, the control variable is admissible,* i.e. *$u_k \in \mathcal{U}$, and the associated state trajectory does not leave $\mathcal{X}$, converge to $\mathcal{L}_\infty$ in a finite time $\tilde{k}$, and does not leave $\mathcal{L}_\infty$ for all $k \geq \tilde{k}$.*

Inspired by Brião (2019, Chapter 5), the proposed solution is mainly based on the concept of Δ-invariant polyhedral sets, with associate UB-sets, to define $\mathcal{L}_0$ and $\mathcal{L}_\infty$, while guaranteeing the local closed-loop stability and constraints fulfillment required in Problem 1. Thus, the following two sections present the theoretical basis of our proposal and the bilinear optimization design technique for jointly synthesizing the *static OF* control law and the two invariant sets. In parallel, the publication (DE ALMEIDA; DOREA, 2020) considered the same problem set-up and used the concept of Output Feedback-Controlled Invariant (OFCI)-sets to propose another type of *static OF* solution to Problem 1. The reader is referred to Subsection 2.4.1.2 for a numerical comparison between the proposal in (DE ALMEIDA; DOREA, 2020) and ours, and additional comments.

2.2 Δ-INVARIANCE AND CONSTRAINTS FULFILLMENT

To obtain appropriate solutions to Problem 1, we consider polyhedral sets to describe the set of initial conditions $\mathcal{L}_0$, and the associated set $\mathcal{L}_\infty$ where the trajectories should remain ultimately bounded, as follows:

$$\mathcal{L}_0 = \{x_k : Lx_k \leq \mathbf{1}_{l_r}\}, \tag{7a}$$

$$\mathcal{L}_\infty = \{x_k : Lx_k \leq \boldsymbol{\rho}\}, \tag{7b}$$

with $L \in \mathbb{R}^{l_r \times n}$, $l_r > n, rank(L) = n$, and $\mathbf{0}_{l_r} < \boldsymbol{\rho} \in \mathbb{R}^{l_r}$, such that $\boldsymbol{\rho} = \bar{\rho}\mathbf{1}_{l_r}$ for some real scalar $\bar{\rho} \in (0, 1]$, which guarantees $\mathcal{L}_\infty \subseteq \mathcal{L}_0$. Notice that $\mathcal{L}_0$ and $\mathcal{L}_\infty$ may have some redundant constraints. Thus, we consider that r, which is an upper bound for the maximum number of faces of these polyhedral sets, defines their *complexity*.

More specifically, to guarantee the fulfillment of the state-constraints, we shall impose the following Δ-Invariance property to $\mathcal{L}_0$, with the ultimate boundedness property associated to $\mathcal{L}_\infty$.

Definition 1 *A set $\mathcal{L}_0$ is a contractive Δ-invariant set of the system* (5)*, with UB-set $\mathcal{L}_\infty \subseteq \mathcal{L}_0$, if for any initial condition $x_0 \in \mathcal{L}_0 \backslash \mathcal{L}_\infty$ and for any $d_k \in \Delta$, the corresponding trajectory remains inside $\mathcal{L}_0$ and converges to $\mathcal{L}_\infty$ in finite time $\tilde{k} \geq 0$, and does not leave $\mathcal{L}_\infty$ for all $k \geq \tilde{k}$.*

Notice that, without considering the UB-set $\mathcal{L}_\infty$, Definition 1 corresponds to the classical Δ-Invariance property considered, for instance, in (BLANCHINI, 1990; MILANI, B. E. A.; DÓREA, 1996). It is also worth to notice that the contractivity property mentioned in the above definition must occur in $\mathcal{L}_0 \backslash \mathcal{L}_\infty$ to guarantee the convergence of the trajectories to the UB-set $\mathcal{L}_\infty$ which, itself, has to be a Δ-invariant set. At last, if $d_k = \mathbf{0}\ \forall k$, then $\mathcal{L}_\infty$ equals the origin of the state space and, hence, we retrieve the classical positive-invariance property, with contractivity, of $\mathcal{L}_0$.

Furthermore, to guarantee that the control constraints (3b) are fulfilled, we also impose the following admissibility condition to $\mathcal{L}_0$ (MILANI, B. E. A.; DÓREA, 1996),

which is obtained from (2b), (3b) and (4):

$$\left[\begin{array}{cc} x_k^T & \eta_k^T \end{array}\right]^T \in \mathcal{U}_y, \text{ for all } x_k \in \mathcal{L}_0 \text{ and } \eta_k \in \mathcal{N}, \tag{8}$$

where

$$\mathcal{U}_y = \left\{ \left[\begin{array}{c} x_k \\ \eta_k \end{array}\right] : UK \left[\begin{array}{cc} C & D_\eta \end{array}\right] \left[\begin{array}{c} x_k \\ \eta_k \end{array}\right] \leq \mathbf{1}_{l_u} \right\}.$$

Thus, the following type of solution to Problem 1 is considered in this work:

Find a triplet $(K, \mathcal{L}_0, \mathcal{L}_\infty)$ *composed by a stabilizing* static OF *matrix* K *and a large admissible contractive* Δ*-invariant polyhedral set such that* $\mathcal{L}_0 \subseteq (\mathcal{X} \cap \mathcal{U}_y)$*, with an associated small polyhedral UB-set* $\mathcal{L}_\infty \subseteq \mathcal{L}_0$.

The extended Farka's Lemma (EFL) (see Hennet (1995)), here recalled through its application for describing the inclusion $\mathcal{L}_0 \subseteq \mathcal{X}$, plays a key role to develop the results presented henceforth.

Lemma 1 *The inclusion* $\mathcal{L}_0 \subseteq \mathcal{X}$ *is verified, or, equivalently,* $x_k \in \mathcal{X}$ *for all* $x_k \in \mathcal{L}_0$*, if and only if there exists a non-negative matrix* $T \in \mathbb{R}^{l_x \times l_r}$*, such that:*

$$TL = X, \tag{9a}$$

$$T\mathbf{1}_{l_r} \leq \mathbf{1}_{l_x}. \tag{9b}$$

□

Thus, from Lemma 1, the admissibility of $\mathcal{L}_0$, in (8), is assured if and only if there exist non-negative matrices $Q_1 \in \mathbb{R}^{l_u \times l_r}$ and $Q_2 \in \mathbb{R}^{l_u \times l_n}$, such that:

$$Q_1 L = UKC \tag{10a}$$

$$Q_2 N = UKD_\eta \tag{10b}$$

$$Q_1 \mathbf{1}_{l_r} + Q_2 \mathbf{1}_{l_n} \leq \mathbf{1}_{l_u}. \tag{10c}$$

Furthermore, from Definition 1, the following algebraic characterization of the Δ-Invariance property of the polyhedral set $\mathcal{L}_0$, with UB-set $\mathcal{L}_\infty$, is proposed.

Proposition 1 *For* $\lambda \in [0, 1)$*, the polyhedron* (7a) *is a contractive* Δ*-invariant set of the system* (5)*, with UB-set given by* (7b)*, if and only if there exist non-negative matrices* $H \in \mathbb{R}^{l_r \times l_r}$ *and* $V \in \mathbb{R}^{l_r \times (l_p + l_n)}$*, and a non-negative vector* $\boldsymbol{\rho} \leq \mathbf{1}_{l_r} \in \mathbb{R}^{l_r}$*, such that:*

$$HL = L(A + BKC), \tag{11a}$$

$$V\Pi = LD, \tag{11b}$$

$$H\mathbf{1}_{l_r} + V\mathbf{1}_{l_\pi} \leq \lambda \mathbf{1}_{l_r}, \tag{11c}$$

$$H\boldsymbol{\rho} + V\mathbf{1}_{l_\pi} \leq (1 - \epsilon)\boldsymbol{\rho}, \tag{11d}$$

where $0 < \epsilon \in \mathbb{R}$ *is a sufficiently small scalar.*

Proof.

Firstly, notice that the relations (11a)-(11c) give necessary and sufficient conditions for the contractive Δ-Invariance of the polyhedral set $\mathcal{L}_0$. They can be obtained by applying the EFL to the following one-step admissibility condition (see B. E. A. Milani and Dórea (1996) and M. M. D. Santos et al. (1997)):

$$L \begin{bmatrix} (A+BKC) & D \end{bmatrix} \begin{bmatrix} x_k \\ d_k \end{bmatrix} \leq \lambda \mathbf{1}_{l_r},$$
$$\forall \begin{bmatrix} L & \mathbf{0} \\ \mathbf{0} & \Pi \end{bmatrix} \begin{bmatrix} x_k \\ d_k \end{bmatrix} \leq \begin{bmatrix} \mathbf{1}_{l_r} \\ \mathbf{1}_{l_\pi} \end{bmatrix}.$$

Thus, such inclusion condition is equivalent to the existence of a non-negative matrix $\begin{bmatrix} H & V \end{bmatrix} \in \mathbb{R}^{l_r \times (l_r+l_p+l_n)}$ verifying the following algebraic relations, from which (11a)-(11c) follows:

$$\begin{bmatrix} H & V \end{bmatrix} \begin{bmatrix} L^T & \mathbf{0} \\ \mathbf{0} & \Pi^T \end{bmatrix}^T = L \begin{bmatrix} (A+BKC) & D \end{bmatrix}$$
$$\begin{bmatrix} H & V \end{bmatrix} \begin{bmatrix} \mathbf{1}_r \\ \mathbf{1}_{l_\pi} \end{bmatrix} \leq \lambda \mathbf{1}_r.$$

Next, by using similar arguments as above, the relations (11a), (11b) and (11c) guarantees that $\mathcal{L}_\infty$ is a Δ-invariant polyhedron, with guaranteed contractive factor $(1-\epsilon)$. Hence, any trajectory that reaches or emanates from $\mathcal{L}_\infty \leq \mathcal{L}_0$ remains inside in it for any $d_k \in \Delta$, which proves the part *i)* above.

Finally, it remains to show the finite-time convergence of the trajectories starting from $\mathcal{L}_0 \backslash \mathcal{L}_\infty$ to $\mathcal{L}_\infty$. To this end, notice that $\tau\mathcal{L}_\infty = \{x_k : Lx_k \leq \tau\boldsymbol{\rho}\}$, with $1 \leq \tau \leq \bar{\rho}^{-1}$, is also a Δ-invariant set of the system (5) and shares the guaranteed contractivity coefficient $\tilde{\lambda} = (1-\epsilon) < 1$ of $\mathcal{L}_\infty$; please refer to the inequality (13) in the proof of Corollary 1. Thus, as in De Almeida and Dorea (2020), we assume that $x_0 \in \tau_0\mathcal{L}_\infty$ and $x_k \in (\tilde{\lambda}^k\tau_0)\mathcal{L}_\infty \subseteq \mathcal{L}_\infty$, $\forall d_k \in \Delta$ with $k > 0$. It can be observed that $x_k \in \mathcal{L}_\infty$ when $\tilde{\lambda}^k\tau_0 \leq 1 \Rightarrow \tilde{\lambda}^k \leq \tau_0^{-1}$, and solving it for k, we can conclude that for $k \geq \tilde{k} = -\log_{\tilde{\lambda}} \tau_0 \Rightarrow x_k \in \mathcal{L}_\infty$. The number of steps $\tilde{k}$ should be seen as a reference value because the trajectory may reach the set $\mathcal{L}_\infty$ in a number of steps k less than $\tilde{k}$. □

The Schur stability of $(A+BKC)$ can also be shown from the algebraic conditions in Proposition 1. To this end, first recall that, by assumption, $l_r > n$ and $rank(L) = n$ which, from the inequality (11a), imply that $\sigma(A+BKC) \subset \sigma(H)$. Also, from (11c) we have $H\mathbf{1}_{l_r} \leq \lambda\mathbf{1}_{l_r}$, which guarantees that $\sigma(H)$ belongs to the interior of the unit circle because, by construction, $H \geq \mathbf{0}_{l_r}$ (BERMAN; PLEMMONS, 1994; HENNET, 1995). Furthermore, it has a real positive eigenvalue, noted $\tilde{\mu}$, that equals its spectral radius and satisfies $\tilde{\mu} \leq \lambda$. Hence, $(A+BKC)$ is necessarily Schur stable. More specifically, for any $\mu_i \in \sigma(A+BKC)$, $i = 1, \ldots, n$, this shows that $|\mu_i| \leq \tilde{\mu}$.

Let us also recall in (7), that the matrix $L \in \mathbb{R}^{l_r \times n}$ has full column rank, if and only if it admits a (left) pseudo-inverse $J \in \mathbb{R}^{n \times l_r}$ such that:

$$JL = I_n. \tag{12}$$

The following Proposition summarizes the considered solutions to Problem 1, which proof directly follows from the concepts and necessary and sufficient algebraic conditions for constraint fulfillment and Δ-invariance shown in this Section.

Proposition 2 *For given system* (2)*, constraints* (3)*, and complexity $l_r > n$, Problem 1 has a solution with a Δ-invariant polyhedron* (7a) *and associated UB-set* (7b)*, with $\mathcal{L}_0 \subseteq (\mathcal{X} \cap \mathcal{U}_y)$, if and only if there exist matrices K, L and J, non-negative matrices H, V, T, Q_1, Q_2, a non-negative vector ρ, and a real scalar $\lambda \in [0, 1)$ such that* (9)-(12) *are verified.*

Before proposing an optimization-based design strategy, let us present the following Corollary of Proposition 2, which shows that under the specific condition $\bar{\rho} < 1$, the considered solutions allow absorbing more significant persistent disturbances than the ones considered in the design procedure while fulfilling the state and control constraints. This property has practical interest in such cases where the disturbances eventually overshoot the amplitude limits during the process evolution.

Corollary 1 *For a given system* (2) *under constraints* (3)*, let a triplet (K, $\mathcal{L}_0$,$\mathcal{L}_\infty$) be obtained from Proposition 2. Also, suppose that for some $\bar{k} > 0$ and for some sequence $d_k \in \Delta$, $k = 1, ..., \bar{k}$, the closed-loop system's current state $x_{\bar{k}}$ is such that $x_{\bar{k}} \in \mathcal{L}_\infty$. Then, if for $k > \bar{k}$, $d_k \in \tau\Delta = \{d_k : Dd_k \leq \tau\mathbf{1}\}$, with $\tau \in (1, \bar{\rho}^{-1}]$, the corresponding closed-loop trajectory remains ultimately bounded inside the set $\tau\mathcal{L}_\infty = \{x_k : Lx_k \leq \tau\mathbf{1}\} \subseteq \mathcal{L}_0$, for all $k > \bar{k}$, thus fulfilling the state and control constraints.*

Proof. By multiplying inequality (11d) by $\tau \in (1\ ,\ \rho^{-1}]$, one gets

$$H\rho_\tau + V\mathbf{1}_\tau \leq (1 - \epsilon)\rho_\tau, \tag{13}$$

where, by definition, $\rho_\tau = \tau\rho$ and $\mathbf{1}_\tau = \tau\mathbf{1}$. Thus, together with (11a) and (11b), inequality (13) means that $\tau\mathcal{L}_\infty$ is a Δ-invariant polyhedron of the closed-loop system (5) and, by construction, $\tau\mathcal{L}_\infty \subseteq \mathcal{L}_0 \subseteq (\mathcal{X} \cap \mathcal{U}_x)$ for any τ in the considered interval $(1\ ,\ \rho^{-1}]$, which completes the proof. □

2.3 BILINEAR OPTIMIZATION DESIGN STRATEGY

The use of Proposition 1 to synthesize solutions to Problem 1 carries some products among pairs of matrix variables to be synthesized, including the control gain K and the matrix L that defines the sets $\mathcal{L}_0$ and $\mathcal{L}_\infty$, as well as bilinear terms arising from products with the unknown vector ρ. Namely, the matrix and vector variables appear

in bilinear products as follows: *i)* T and L in (9a); *ii)* Q_1 and L in (10a), and Q_2 and N in (10b); *iii)* H and L in the left-hand side of equation (11a), and L and K in its right-hand; *iv)* L and K, from the product LD present in (11b); *v)* H and ρ in inequality (11d); and *vi)* J and L in (12). However, these bilinear products can be considered as design constraints of the optimization program proposed in the sequel and adapted nonlinear optimization techniques can be used to find solutions to Problem 1, as discussed later in this section.

2.3.1 Control Design Principles

In the design strategy of this section we propose enlarging the size of the set of admissible initial conditions $\mathcal{L}_0$ along some directions in $\mathbb{R}^n$ (TARBOURIECH et al., 2011), while guaranteeing a pre-specified relative size of the UB-set $\mathcal{L}_\infty$ with regards to $\mathcal{L}_0$. This strategy allows the designer to exploit a range of different solutions $(K, \mathcal{L}_0, \mathcal{L}_\infty)$ to Problem 1 that trade-off the relative sizes of the two invariant sets. For this purpose, the set of directions is defined by

$$\mathcal{V} = \{\gamma_t v_t, t = 1, \ldots, \bar{t}\},$$

where $v_t \in \mathbb{R}^n$ are given vectors and $0 < \gamma_t \in \mathbb{R}$ are scaling factors to be optimized, such that the inclusion $\mathcal{V} \subseteq \mathcal{L}_0$ is satisfied or, equivalently:

$$L\gamma_t v_t \leq \mathbf{1}_{l_r}, \ t = 1, \ldots, \bar{t}. \tag{14}$$

Among possible choices for the set $\mathcal{V}$, the designer may choose, for instance, a set of directions defined from the vertices of $\mathcal{X}$, or a set of normalized directions, possibly equally spaced in the state-space and covering a significant number of directions for the optimization process. Notice also that the inequalities (14) bring bilinear products among the matrix variable L and the scaling factors γ_t to be synthesized.

Notice that, from our experience with different numerical experiments, the directions' method proposed in this chapter has performed better than the shape set method formerly used in Brião (2019, Chapter 5), which made us choose the present method over the former one.

Next, assume the scalar variable $\bar{\rho} \in (0, 1]$ defining a limit for the relative size of the UB-set $\mathcal{L}_\infty \subseteq \mathcal{L}_0$. Furthermore, consider that following design parameters are chosen *a priori*: *a)* allowed complexity (*i.e* the maximum number of faces) for the invariant sets, by choosing $l_r > n$; *b)* $\bar{t}$ directions v_t used to enlarge $\mathcal{L}_0$; *c)* maximum contractivity factor $\bar{\lambda} < 1$; and *d)* weighting factor $0 \leq \alpha \in \mathbb{R}$, to be used in objective function suggested below. Thus, we propose the following basic bilinear optimization problem to

find solutions to the design Problem 1:

$$\begin{aligned} \underset{\Gamma}{\text{maximize}} \quad & \Phi(\gamma_t, \bar{\rho}) = \phi(\gamma_t) - \alpha\bar{\rho} \\ \text{subject to} \quad & (9)\text{–}(14), \\ & 0 \leq \lambda \leq \bar{\lambda}, \\ & f_\ell(\cdot) \leq \varphi_\ell, \quad \ell = 1, \ldots, \bar{\ell}, \end{aligned} \tag{15}$$

with $\Gamma = (K, L, H, T, J, Q_1, Q_2, V, \lambda, \gamma_t, \bar{\rho})$ collecting all of the scalar and matrix variables, and where:

i) the proposed weighted objective function $\Phi(\gamma_t, \bar{\rho})$ allows to trade-off the maximization of the external set $\mathcal{L}_0$ through the scaling factors associated to the directions in $\mathcal{V}$, by considering $\phi(\gamma_t) = \Sigma_{t=1}^{\bar{t}} \gamma_t$, and the relative size of a internal set $\mathcal{L}_\infty$, represented by $\bar{\rho}$; notice that, for different choices of the weighting parameter α, the optimization program (15) can provide different solutions to Problem 1, which may also depend on the designer choices of $\mathcal{V}$ and l_r.

ii) the additional constraints, represented by $f_\ell(\cdot) \leq \varphi_\ell$, may be imposed on the decision variables for different purposes, including the numerical ones discussed later in this section.

In the next two remarks, we show that it is also possible to use the bilinear optimization problem (15) to deal with Problem 1 by using two other fundamental classical control laws.

Remark 1 *The design of SF control laws through* (15)*, with $K \in \mathbb{R}^{m \times n}$, can be readily treated by letting $C = I_n$.*

Remark 2 *We can also consider Problem 1 using DOF control laws, by considering n_c-order DOF controllers described by:*

$$x_{k+1}^c = A_c x_k^c + B_c y_k \tag{16a}$$
$$u_k = C_c x_k^c + D_c y_k, \tag{16b}$$

where $x_k^c \in \mathbb{R}^{n_c}$, and A_c, B_c, C_c and D_c have compatible dimensions. Classically, we can define the following augmented vectors, which allow us to consider the static OF control of system (2) *augmented by a n_c-dimensional unit-delay system:*

$$x_k^a = \begin{bmatrix} x_k \\ x_k^c \end{bmatrix} \in \mathbb{R}^{n_a}, \; u_k^a = \begin{bmatrix} u_k \\ \bar{u}_k \end{bmatrix} \in \mathbb{R}^{m_a}, \; y_k^a = \begin{bmatrix} y_k \\ \bar{y}_k \end{bmatrix} \in \mathbb{R}^{p_a},$$

where $\bar{u}_k$ and $\bar{y}_k$ are "dummy" control and output vectors, respectively, and $n_a = n + n_c$, $m_a = m + n_c$, $p_a = p + n_c$. Thus, the design of DOF controllers using (15) *considers the*

following substitutions:

$$A \leftarrow \begin{bmatrix} A & 0 \\ 0 & 0 \end{bmatrix}, B \leftarrow \begin{bmatrix} B & 0 \\ 0 & I_{n_c} \end{bmatrix}, B_p \leftarrow \begin{bmatrix} B_p \\ 0 \end{bmatrix},$$
$$C \leftarrow \begin{bmatrix} C & 0 \\ 0 & I_{n_c} \end{bmatrix}, D_\eta \leftarrow \begin{bmatrix} D_\eta \\ 0 \end{bmatrix}, K \leftarrow \begin{bmatrix} D_c & C_c \\ B_c & A_c \end{bmatrix},$$
$$X \leftarrow \begin{bmatrix} X & 0 \\ 0 & \tilde{X} \end{bmatrix}, U \leftarrow \begin{bmatrix} U & 0 \end{bmatrix}.$$

where the choice of $\tilde{X}$ defines auxiliary constraints over x^a, which are used for design purposes.

It is worth noticing that the corresponding sets $\mathcal{L}_0$ and $\mathcal{L}_\infty$ (see Eq. (7)) should now belong to the augmented state-space $\mathbb{R}^{n_a}$, with $r > n_a$. Similarly, $\mathcal{V} \subset \mathbb{R}^{n_a}$, although the coordinates of $v_s \in \mathbb{R}^{n_a}$ associated to x^c can be set to zero for favoring the directions associated to the original state-space.

The following remark points out another interesting extension of our proposal to deal with richer constrained control problems, which will be explored in the context of parameter varying systems (see Chapters 4 and 5).

Remark 3 *Another possible dynamical control law, which structure is particularly interesting to include control-rate constrains in the design process, consists in the incremental output-feedback control law $u_{k+1} = u_k + \delta u_k$, with $\delta u_k = Ky_k + \bar{K}u_k$, with $K \in \mathbb{R}^{m\times p}$ and $\bar{K} \in \mathbb{R}^{m\times p}$. As in Blanchini and Miani (2015), we can re-define $x_k^a = \begin{bmatrix} x_k^T & u_k^T \end{bmatrix}^T \in \mathbb{R}^{n+m}$, $u_k^a = \delta u_k \in \mathbb{R}^m$, and, in addition, $y_k^a = \begin{bmatrix} y_k^T & u_k^T \end{bmatrix}^T \in \mathbb{R}^{p+m}$. Thus, the optimization design Problem* (15) *can be adapted to compute the augmented* static OF *matrix $K^a = \begin{bmatrix} KC & \bar{K} \end{bmatrix}$ and consider additional control-rate constraints under the form $\mathcal{U}_\delta = \{\delta u_k : U_\delta \delta u_k \leq 1_{l_\delta}\}$, with $U_\delta \in \mathbb{R}^{l_\delta \times m}$.*

2.3.2 Implementation Details

For simplicity, only relations (11a)-(11c) are considered in the sequel. We assume the indexes $i \in \{1, \ldots, l_r\}$, $j \in \{1, \ldots, n\}$, and $s \in \{1, \ldots, m\}$. Let $\Theta \in \mathbb{R}^{n\times n}$ be given by $\Theta = BKC$, so the term $L\Theta$ is bilinear. Then, in the element-wise form, the matrix equality (11a) is rewritten by $l_r.n$ equations, such that for each i and j:

$$\sum_{\kappa=1}^{l_r} h_{i\kappa} l_{\kappa j} - \sum_{\kappa=1}^{n} [l_{i\kappa}(a_{\kappa j} + \theta_{\kappa j})] = 0,$$

where $\theta_{\kappa j} = \sum_{s=1}^{m} b_{\kappa s} f_{sj}$, with $f_{sj} = \sum_{\kappa=1}^{p} k_{s\kappa} c_{\kappa j}$. Analogously, for $\omega \in \{1, \ldots, l_d\}$, (11b) is recast as:

$$\sum_{\kappa=1}^{l_\pi} v_{i\kappa} \pi_{\kappa\omega} - \sum_{\kappa=1}^{n} l_{i\kappa} d_{\kappa\omega} = 0.$$

Also, the element-wise formulation of the inequality (11c) becomes:

$$\sum_{\kappa=1}^{r} h_{i\kappa} + \sum_{\kappa=1}^{l_\pi} v_{i\kappa} \leq \lambda.$$

In addition, for $\nu \in \{1, \ldots, l_r\}$ and $\iota \in \{1, \ldots, p\}$ the constraints $f_\ell(\cdot) \leq \varphi_\ell$ are established, in order to determine lower and upper bounds to the elements of K and L:

$$\underline{k} \leq k_{s\iota} \leq \bar{k} \text{ and } \underline{l} \leq l_{ij} \leq \bar{l}$$

where $\underline{k}, \bar{k}, \underline{l}, \bar{l} \in \mathbb{R}$. Likewise, upper and lower limits are also determined for the elements of the other involved vector and matrix decision variables.

Remark 4 *Imposing upper and lower bounds to the elements of the decision variables, as considered before, is a key strategy used in mathematical programming to deal with non-linear or non-convex optimization problems, to reduce the search space, thus promoting a more efficient search for solutions of the considered problem. For instance, convex relaxations for bilinear terms with bounded variables can be derived from McCormick envelopes (MC-CORMICK, 1976), the effectiveness of which depend on how tight these bounds are. Thus, aside from the choice of the control design parameters, the user's experience on choosing the mentioned upper and lower bounds also impacts the computational search and time to get solutions efficiently.*

It is worth mentioning that some decision variables of the optimization problem (15) *are limited by definition or by construction. For instance, the elements of matrices H, V, T, and $[Q_1 \; Q_2]$ are all non-negative, by definition. From equations* (9b), (10c), (11c) *and* (11d), *it can be verified that they are upper-limited by* 1. *Similarly, the involved scalar variables λ, γ_t and $\bar{\rho}$ should be non-negative. Besides, the given state and control constraint amplitudes can guide the designer for choosing compatible limits for L and, in consequence, J.*

2.4 NUMERICAL EXAMPLES

In this section, we deal with a 2*nd*-order and a 4*th*-order example systems. The first example is presented throughout three subsections concerning the *SF*, *static OF*, and *DOF* designs, respectively. In particular, in the first two ones, we compare our proposal with two existing approaches which deal with *i)* an *SF*-design by an LMI-based approach, and *ii)* an implicit *static OF*-design which requires the *on-line* computation of the control action. In the second example, we consider a higher-order example and show our proposal's ability to deal with more complex and realistic systems, including the design of decentralized output feedback control laws.

In the numerical examples shown in this section, the following lower and upper [–1000 1000] bounds are assigned to the elements of K and J. Similar upper and lower bounds, $\underline{l}$ and $\bar{l}$, are used in the *SF* and *static OF* designs shown in the sequel and modified

as explained in the *DOF*-designs. The non-negative scalar λ is upper limited by $\bar{\lambda} = 0.9999$. The numerical results are obtained by using the KNITRO solver (BYRD et al., 2006).

2.4.1 Example 1

Consider the system (2) and constraints (3) represented by the following matrices

$$A = \begin{bmatrix} 1 & 1 \\ 0 & 1 \end{bmatrix},\ B = \begin{bmatrix} b \\ 1 \end{bmatrix} \text{ and } B_p = \begin{bmatrix} 1 \\ 1 \end{bmatrix},$$

for which the persistent disturbances are defined from $P^T = \begin{bmatrix} 10 & -10 \end{bmatrix}^T$ and $N^T = [\ 10 \quad -10\ ]$, meaning that $|p_k| \leq 0.1$ and $|\eta_k| \leq 0.1$. The state and control constraints are defined from $X^T = \begin{bmatrix} g & 0 & -1 & 0 \\ 0 & 1 & 0 & -1 \end{bmatrix}$ and $U^T = \begin{bmatrix} 1 & -z \end{bmatrix}$. Furthermore, the output matrices C and D_η, and the parameters b, g and z are defined depending on each one of three cases exemplified in the sequel, which consider not only *static OF* design but also *SF* and *DOF* ones.

2.4.1.1 SF Design

We firstly make some comparisons between our proposal and the LMI-based one by Gupta and Falcone (GF) from Gupta and Falcone (2019). The latter is capable to compute uniquely symmetric invariant sets, only by using a state-feedback control law $u_k = Kx_k$, and without considering measurement noises. Thus, according to Remark 1, we set $C = I_2$ and let $D_\eta^T = [\,0 \;\; 0\,]$. Furthermore, to get the same system and symmetrical constraints considered in Example B of Gupta and Falcone (2019), we let $b = 0$ and $g = z = 1$.

The results obtained from solving (15), for different choices of the optimization parameter α, are summarized in Tables 1 and 2, for $l_r = 4$ and $l_r = 6$, respectively, which correspond to $n_p = 2$ and $n_p = 3$ in Gupta and Falcone (2019). The first row in each table corresponds to the result reported in Gupta and Falcone (2019), where we consider $\bar{\rho} = 1$ because their design procedure does not deal with the UB-set $\mathcal{L}_\infty$. Our results were obtained by using both $\bar{t} = 8$ and $\bar{t} = 16$ normalized vectors v_t, equally spaced in the state-space, thus defining the corresponding sets $\mathcal{V}$; only the results obtained with $\bar{t} = 16$ are reported in Table 2, for $l_r = 6$. Accounting for the area[1] of $\mathcal{L}_0$, it should be first noticed that by setting $\alpha = 0$ or $\alpha = 1$, with $\bar{t} = 16$, our approach was able to obtain better results than in Gupta and Falcone (2019) for $l_r = 4$, and similar ones for $l_r = 6$.

We can observe that the area of $\mathcal{L}_0$ and the value $\bar{\rho}$, which gives an upper bound for the relative size of $\mathcal{L}_\infty$, may vary with the choice of the set $\mathcal{V}$, through $\bar{t}$, and the choice

[1] As in Gupta and Falcone (2019), the calculation of polyhedron areas is performed by using the Multi-Parametric Toolbox 3 (MPT3).

Table 1 – *SF* designs with $l_r = 4$

α	$\bar{t}$	Area	$\bar{\rho}$	K
		1.8000	1	[–0.8630 –1.7407]
0	8	1.6990	1	[–0.9000 –1.6586]
	16	1.9172	1	[–0.2047 –1.0466]
1	8	1.6661	0.9391	[–0.8935 –1.6547]
	16	1.9028	0.8526	[–0.2466 –1.1021]
5	8	1.5279	0.4236	[–0.6180 –1.6180]
	16	1.6614	0.5834	[–0.3909 –1.2802]
20	8	1.5279	0.4236	[–0.6180 –1.6180]
	16	1.3177	0.3828	[–0.7071 –1.7071]

Table 2 – *SF* designs with $l_r = 6$

α	$\bar{t}$	Area	$\bar{\rho}$	K
		2.6100	1	[–0.2251 –1.2219]
0	16	2.6100	1	[–0.2285 –1.2215]
1	16	2.6099	0.9999	[–0.3792 –1.2026]
5	16	2.2121	0.4813	[–0.5623 –1.5111]
20	16	2.0234	0.3828	[–0.7071 –1.7071]

of the weighting factor α, which allows to trade-off the relative sizes of the two sets. In particular, we see that smaller is α, bigger is the area of $\mathcal{L}_0$. Instead, more significant is α, smaller is the relative size of the UB-set $\mathcal{L}_\infty$.

More specifically, for $l_r = 4$ Figure 1 allows a geometrical comparison between GF's solution, depicted in red, and ours for ($\alpha = 0, \bar{t} = 16$) and ($\alpha = 5, \bar{t} = 16$), in black and blue lines, respectively. The innermost set, in dash-dotted blue lines, corresponds to $\mathcal{L}_\infty$ obtained for $\alpha = 5$. The associated matrices L are, respectively:

$$L_{GF}^T = \begin{bmatrix} 1.0000 & 1.2222 & -1.0000 & -1.2222 \\ 0.0000 & 2.2222 & 0.0000 & -2.2222 \end{bmatrix},$$

$$L_{0,16}^T = \begin{bmatrix} 0.9389 & -0.9389 & -1.1476 & 1.1476 \\ -0.6111 & 0.6111 & -1.4753 & 1.4753 \end{bmatrix},$$

and

$$L_{5,16}^T = \begin{bmatrix} 1.2828 & -1.2828 & -0.8701 & 0.8701 \\ 1.6497 & -1.6497 & 0.7579 & -0.7579 \end{bmatrix}.$$

Note that in Figure 1, the normalized vectors v_t used for optimizing the size of $\mathcal{L}_0$ are depicted by dotted lines.

Now, Figure 2 aims at comparing GF's and our solution for ($\alpha = 5, \bar{t} = 16$). The trajectories around the origin, which emanate from $x_0 = [0\ 0]^T$, were simulated by considering a particular random disturbance sequence that takes its values only in the allowable limits ± 0.1. As expected from the theory, the closed-loop trajectory in blue, obtained from our solution, remains inside the corresponding UB-set $\mathcal{L}_\infty$. The trajectory

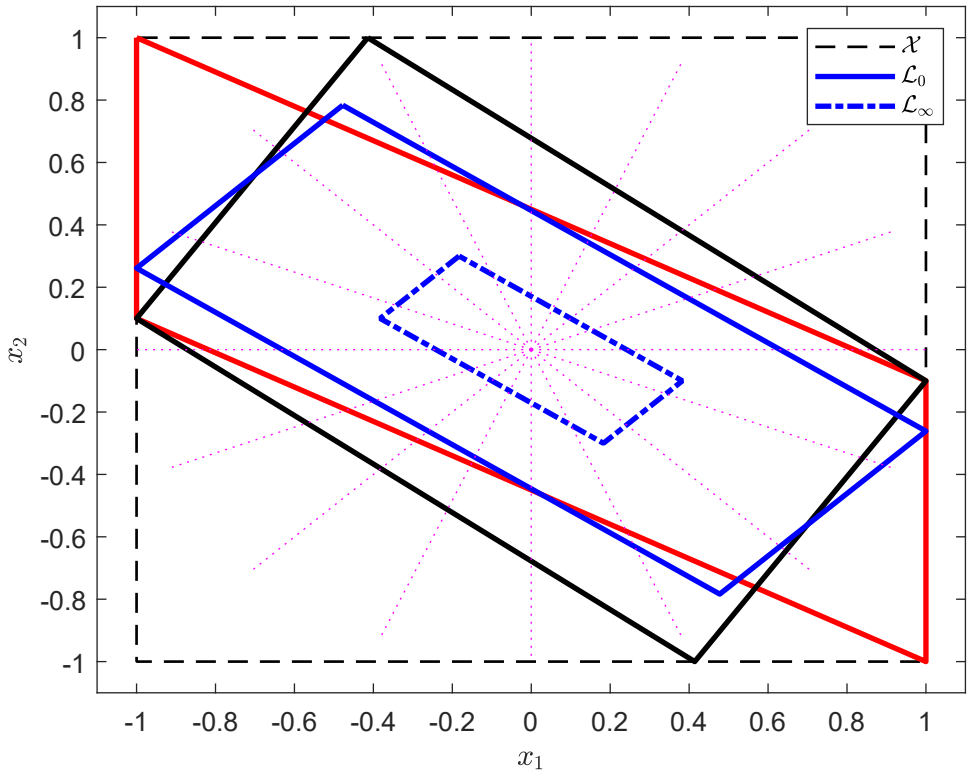

Figure 1 – Invariant sets with $l_r = 4$, for $\alpha = 0$ (black) and $\alpha = 5$ (blue), and from Gupta and Falcone (2019) (red)

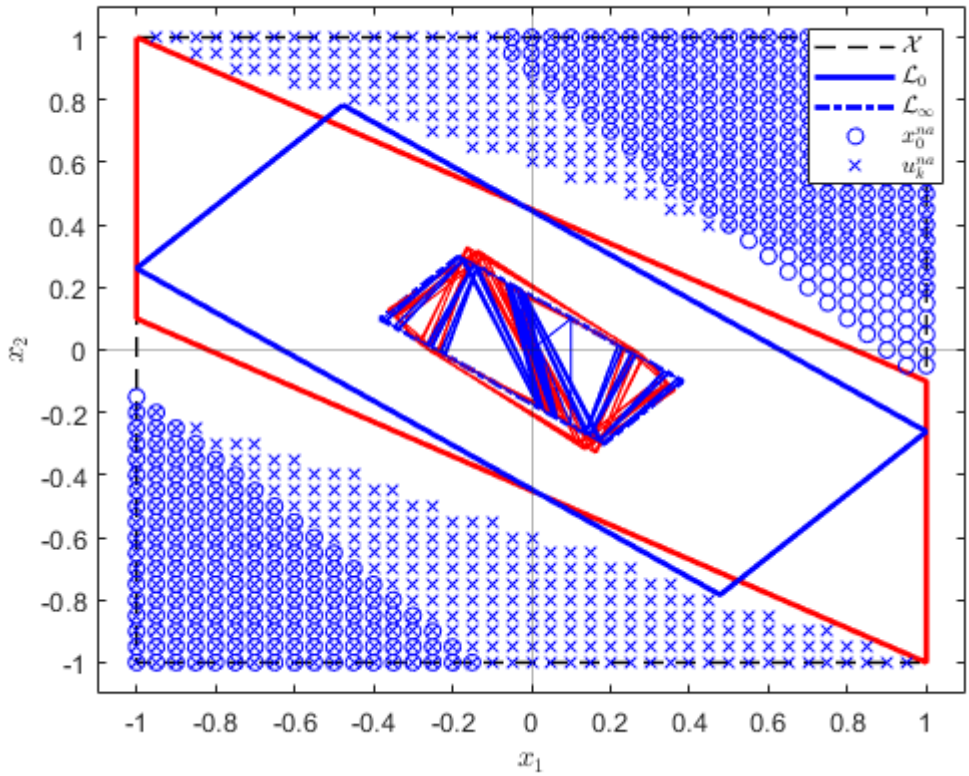

Figure 2 – *StF* design for $l_r = 4$, $\alpha = 5$, with trajectories information

around the origin corresponding to GF's result is depicted in red. Besides, for the same disturbance sequence, Figure 2 also depicts initial conditions generating trajectories that do not respect the state constraints and trajectories that imply non-admissible control input (see (8)) and (10)). Such non-admissible initial conditions are referenced as x_0^{na} and u_0^{na} in the figure's legends, and represented by $\circ$ and $\times$, respectively[2]. Thus, roughly, the non-marked part of the set $\mathcal{X}$ corresponds to the set of initial conditions that are admissible both in terms of state and control constraints, considering the particular disturbance sequence.

Let us now consider $l_r = 6$ and the same disturbance sequence as before. Firstly, in Figure 3, the set depicted with black lines corresponds to $\mathcal{L}_0$ obtained both in Gupta and Falcone (2019) and by our approach with ($\alpha = 0$, $\bar{t} = 16$), where:

$$L_{GF}^T = L_{0,16}^T = \begin{bmatrix} -0.2222 & -1 & -1.1111 & 0.2222 & 1 & 1.1111 \\ -1.2222 & 0 & -1.1111 & 1.2222 & 0 & 1.1111 \end{bmatrix}.$$

As before, non-admissible solutions are marked on the graph, showing that the obtained solution $\mathcal{L}_0$ covers a significant part of this particular set of initial admissible conditions. Further, Figure 4 depicts the solution we obtained with ($\alpha = 20, \bar{t} = 16$), where

$$L_{20,16}^T = \begin{bmatrix} 0.7071 & -1.3536 & -0.7071 & -1 & 1.3536 & 1 \\ 1.7071 & -1.3536 & -1.7071 & 0 & 1.3536 & 0 \end{bmatrix}.$$

Comparing with the previous result for $\alpha = 0$, we observe that the smaller UB-set $\mathcal{L}_\infty$ is obtained at the expense of a less significant set $\mathcal{L}_0$ and, hence, a smaller set of initial admissible conditions.

Finally, we utilize this last *SF*-design to illustrate the ability to admit disturbance and noise with higher amplitude bounds, as established by Corollary 1. Figure 5 depicts the closed-loop system's trajectory due to the application of disturbance and noise sequences, with $x_0^T = \begin{bmatrix} 0 & 0 \end{bmatrix}$, that obeys the considered design limits of p_k and η_k for $k = 0, \ldots 14$, but may take more significant amplitude values for $k \geq 15$, within $|p_k| = |\eta_k| \leq 0.1\bar{\rho}^{-1}$, with $\bar{\rho}^{-1} = 2.6123$. The trajectory is depicted in green for $k = 1, \ldots, \bar{k}$, which remains inside $\mathcal{L}_\infty$, and in red for $k \geq 15$, which now remains in $\mathcal{L}_0 = \bar{\rho}^{-1}\mathcal{L}_\infty$, thus respecting the state constraints. The corresponding control actions are depicted in Figure 6, showing that the control constraints are still fulfilled.

2.4.1.2 Static OF Design

In this subsection, we firstly want to show some specific features of our proposal that cannot be dealt with by other works proposed in the literature, together with the

[2] These marks are obtained by considering all the initial conditions in $\mathcal{X}$ spaced by 0.05 in both horizontal and vertical directions, simulating the respective closed-loop trajectories, and marking the ones that do not respect the state and control constraints.

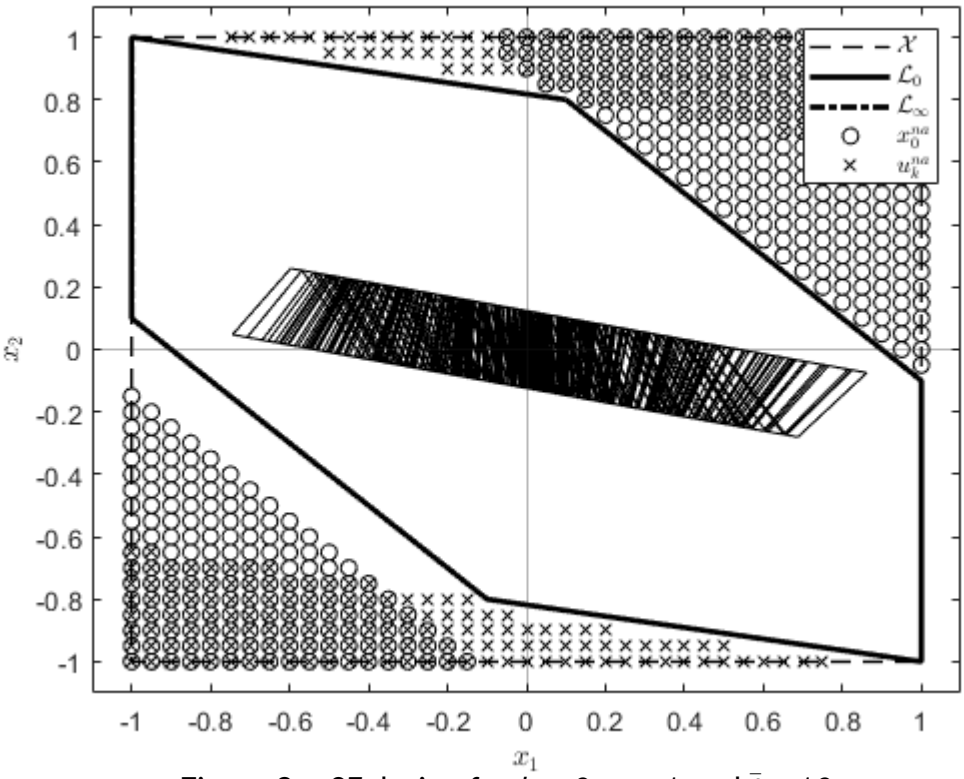

Figure 3 – *SF* design for $l_r = 6$, $\alpha = 1$ and $\bar{t} = 16$

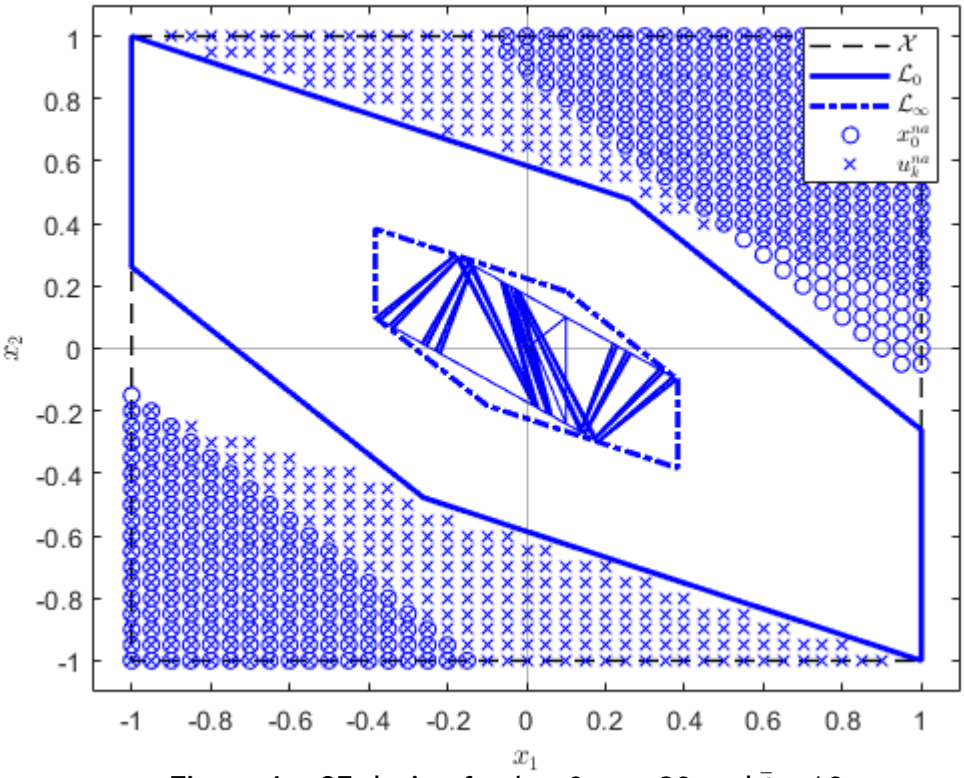

Figure 4 – *SF*-design for $l_r = 6$, $\alpha = 20$ and $\bar{t} = 16$

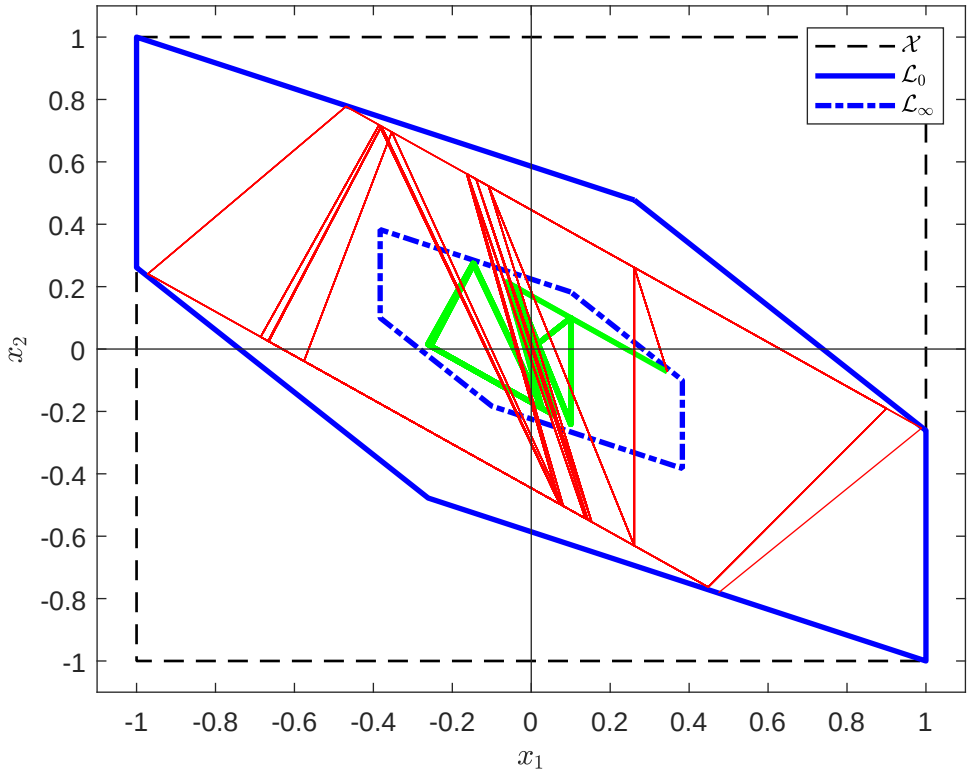

Figure 5 – *SF*-design for $l_r = 6$, $\alpha = 20$ Simulation with disturbance and noise within and outside the design specifications

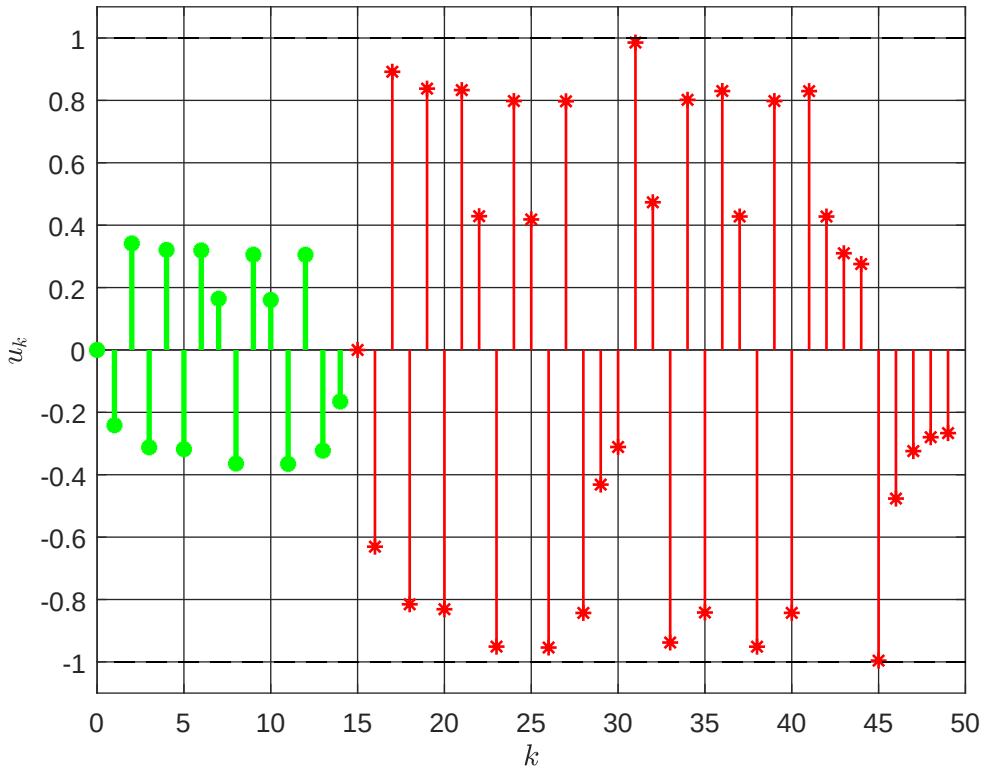

Figure 6 – Control actions for the simulation in Fig. 5

Table 3 – *static OF* designs with $l_r = 6$ and $\bar{t} = 16$

α	Area	$\bar{\rho}$	K
1	3.1113	1	[–0.6111]
5	2.9312	0.8409	[–0.6192]
20	1.9873	0.5126	[–0.6862]

explicit computation of a *static OF*-control gain. Secondly, we compare our bilinear optimization design approach, which requires only the *off-line* computation of the controller's gains, with the proposal recently presented in De Almeida and Dorea (2020), which aims at solving Problem 1 using the concept of OFCI sets. This last implicit technique, differently from ours, requires the *on-line* computation of a static output control action $u_k = f(y_k)$ at each sampling-time by solving an LP problem.

Thus, let us now consider $b = 2$ and the output matrix $C = [1 \;\; 0]$, which guarantee the given system can be stabilized by *static OF* in the absence of disturbances and constraints. Also, to deal with a noise measurement, $D_\eta = [1]$ and $N^T = \begin{bmatrix} 10 & -10 \end{bmatrix}$. Furthermore, because our proposal allows non-symmetrical state-constraints and Δ-invariant sets, the following constraint parameters are now considered in matrices X and U, respectively: $g = 0.8$ and $z = 1.25$.

Firstly, different *static OF* designs were synthesized from (15) by using the parameters: $l_r = 6$, $\bar{t} = 16$, and $\alpha = 1$, 5 and 20, yielding to different solutions $(K, \mathcal{L}_0, \mathcal{L}_\infty)$. Part of the obtained numerical results are reported in Table 3. In Figure 7, we show the corresponding invariant sets, which corresponding matrices L are, respectively:

$$L_1^T = \begin{bmatrix} 0.8271 & 0.0000 & -0.7285 & 0.8434 & 0.2857 & -1.0000 \\ 0.0000 & 1.0000 & 1.1921 & -1.1678 & -1.2857 & 0.0000 \end{bmatrix},$$

$$L_5^T = \begin{bmatrix} 0.0000 & -0.7668 & 0.3248 & -1.0000 & 0.8389 & 0.9300 \\ 1.0000 & 1.2385 & -1.3627 & 0.0000 & 0.0000 & -1.2596 \end{bmatrix},$$

and

$$L_{20}^T = \begin{bmatrix} 1.4386 & -0.6173 & 0.6930 & -1.0000 & -1.2262 & 0.9382 \\ -1.6492 & 1.6580 & -1.8614 & 0.0000 & 1.4057 & 0.0000 \end{bmatrix}.$$

Furthermore, the sets represented in red concern a *SF*-design obtained with $\alpha = 1$, showing that the whole set of state-constraints, $\mathcal{X}$, could be made Δ-invariant by the state-feedback matrix $K = [-0.1667 \; -0.5000]$, with associated UB-set $\mathcal{L}_\infty$ such that $\bar{\rho} = 0.4$ [3]. However, since the feedback information concerns the single state x_1, only part of $\mathcal{X}$ could be made Δ-invariant by *static OF*.

Notice that *static OF*-designs with better estimations of the UB-sets $\mathcal{L}_\infty$ are obtained for more significant values of the weight parameter α, although at the expense

[3] For the *SF*-design, following Remark 1, we used $C = I_2$ and $D_\eta = [1 \; 0]^T$.

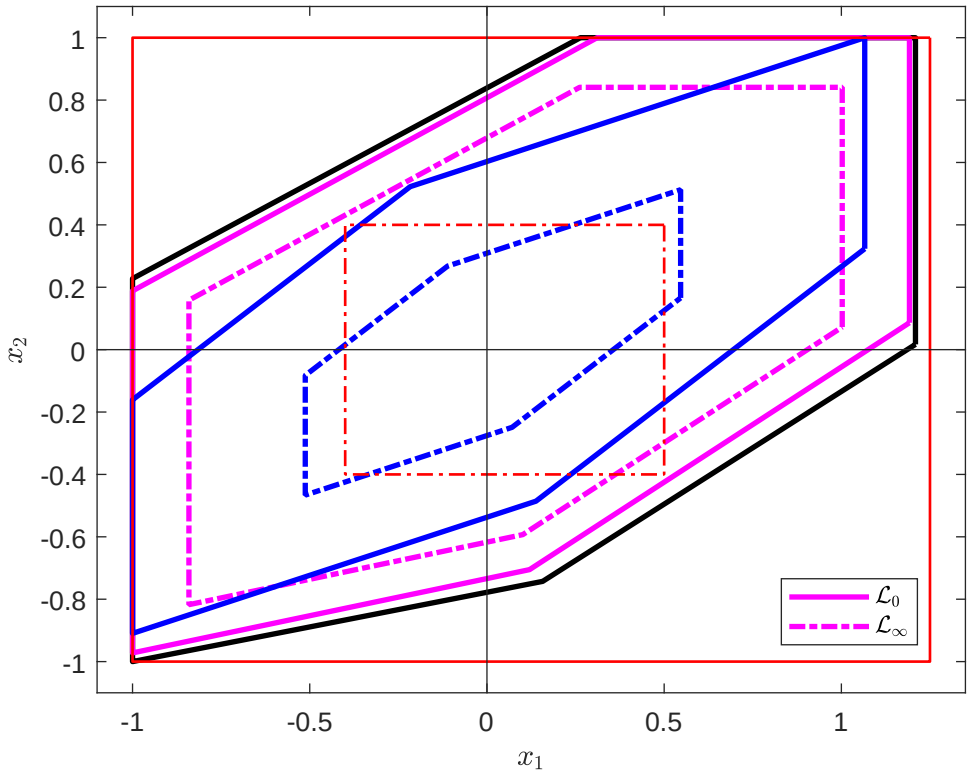

Figure 7 – *static OF* designs with $l_r = 6$: Invariant sets $\mathcal{L}_0$ and $\mathcal{L}_\infty$ for $\alpha = 0$ (black), $\alpha = 5$ (magenta), and $\alpha = 20$ (blue). Also, the *StF* design with $\alpha = 1$ (red)

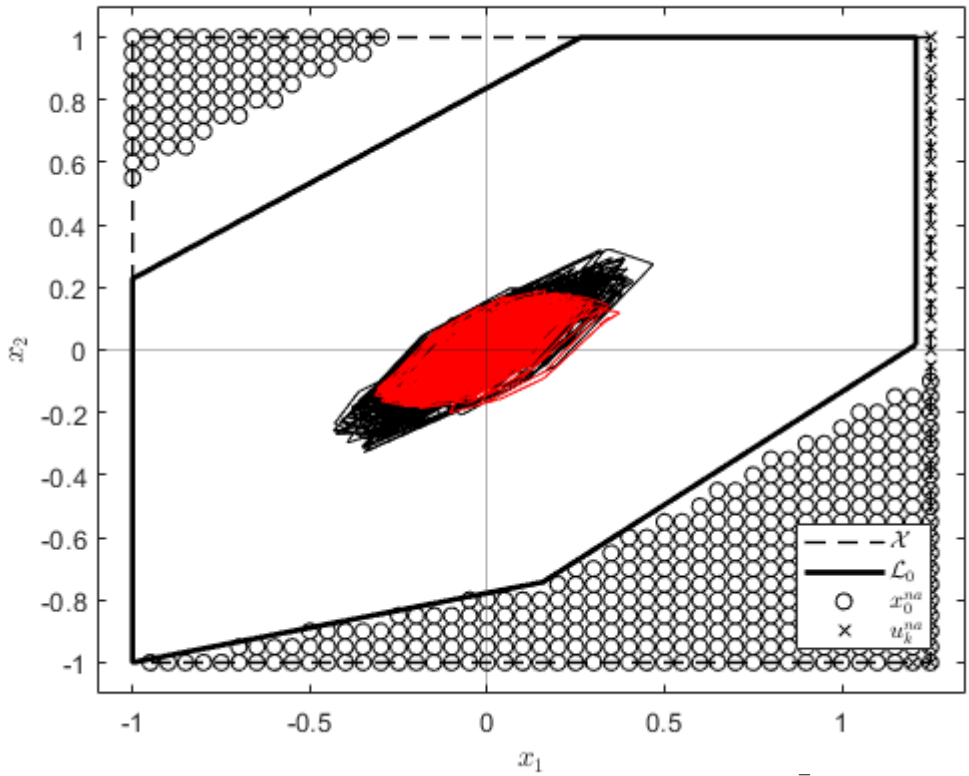

Figure 8 – *static OF* design for $l_r = 6$, $\alpha = 0$ and $\bar{t} = 16$

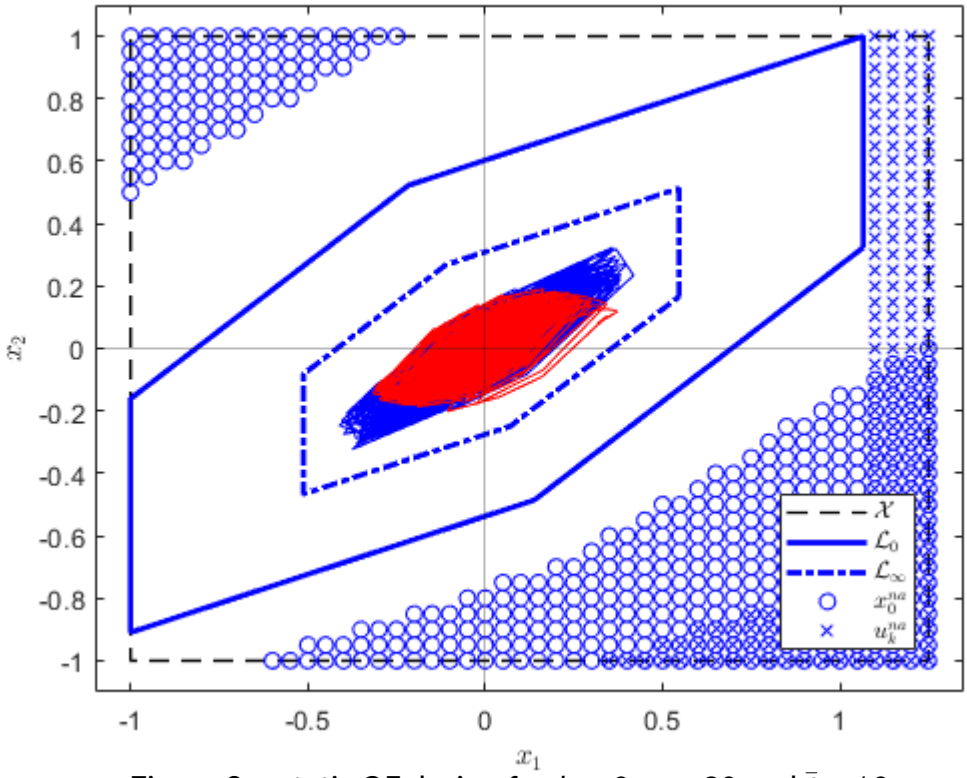

Figure 9 – *static OF* design for $l_r = 6$, $\alpha = 20$ and $\bar{t} = 16$

of less significant areas for the corresponding $\mathcal{L}_0$ sets. Finally, Figures 8 and 9 depict the trajectories around the origin, in black and blue, respectively, which were obtained from the application of the same disturbance sequence, p_k, used before, and of a noise sequence η_k, similarly randomly generated by taking only the values ± 0.1. We verify that both trajectories remain close around the origin, independently of the estimated value for $\bar{\rho}$. For comparison purpose, we also plot in red the closed-loop trajectory obtained from the above mentioned *SF*-design. Finally, we can also observe that the set of initial admissible conditions obtained with $\alpha = 20$ is significantly smaller than the one with $\alpha = 1$, especially by comparing the right-hand strips of non-admissible initial conditions present in both Figures 8 and 9.

Next, we compare our bilinear design approach, which requires only the *off-line* computation of the controller's gains, with the Almeida and Dorea (AD) proposal (DE ALMEIDA; DOREA, 2020) [4] that, besides an *off-line* design phase, requires the *on-line* computation of a static output control action $u_k = f(y_k)$ at each sampling-time by solving an LP problem. Thus, using the approach described in Section III of De Almeida and Dorea (2020), we find the OFCI-set $\mathcal{L}_{AD} = \{x : L_{AD}x \leq 1\}$ with complexity $l_{rAD} = 7$, painted with green color in Figure 10, where

$$L_{AD}^T = \begin{bmatrix} 0.0000 & -1.0000 & 0.0000 & -1.3679 & 1.3681 & 0.8689 & 0.4872 \\ 1.0000 & 0.0000 & -1.0000 & 1.3679 & -1.3681 & 0.0000 & 0.4872 \end{bmatrix}.$$

[4] We acknowledge the help of the authors, especially in the code implementation

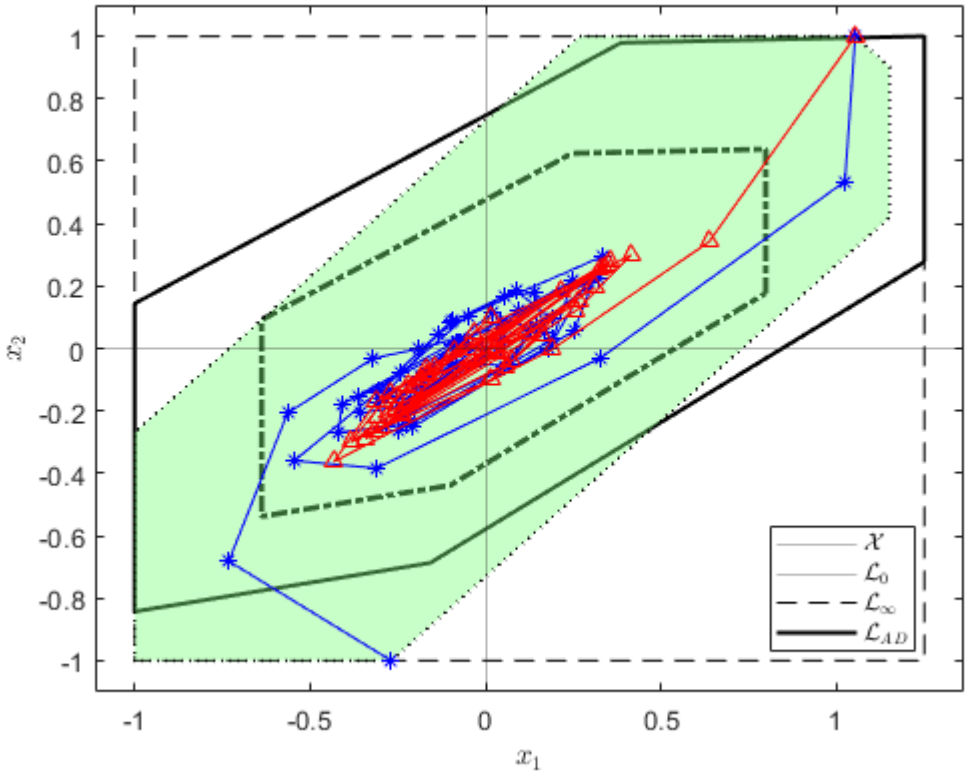

Figure 10 – Designed sets $\mathcal{L}_{AD}$, $\mathcal{L}_0$, and $\mathcal{L}_\infty$, with state trajectories

Table 4 – *Static OF*-designs: AD from De Almeida and Dorea (2020) and bilinear optimization approach (15)

Design	α	l_r	$\bar{t}$	Area	$\bar{\rho}$	K
AD	–	7	–	2.4837	–	–
(15)	10	6	16	2.5654	0.6383	[–0.5926]

Figure 10 also depicts the sets $\mathcal{L}_0$ and $\mathcal{L}_\infty$, with assigned complexity $l_r = 6 < l_{rAD}$, obtained from (15) for $\alpha = 10$ and $\bar{t} = 16$, yielding to

$$L_{10,16}^T = \begin{bmatrix} -0.0249 & 0.2816 & -0.8073 & 0.8000 & 1.1840 & -1.0000 \\ 1.0312 & -1.5206 & 1.3394 & 0.0000 & -1.7280 & 0.0000 \end{bmatrix}.$$

For comparative purpose, notice that the areas of the OFCI-set and Δ-invariant polyhedron $\mathcal{L}_0$ are similar, about 2.5, although the polyhedron $\mathcal{L}_0$ obtained from (15) is less complex than the OFCI-set. It can also be observed from previous results that our design with $\alpha = 1$ generated a bigger Δ-invariant set than the one with $\alpha = 10$, whereas the latter provided a better estimation of the UB-set $\mathcal{L}_\infty$ than that one.

In Figure 10 we show state-trajectory simulations obtained by applying the *on-line* control actions from (DE ALMEIDA; DOREA, 2020), in red and marked with $\triangle$, and the *static OF*-design from (15), in blue and marked with $*$. In these simulations, we consider two different initial conditions and apply the same random sequences p_k and η_k used before. The first initial condition, $x_0^T = [1.053 \;\; 1]$, is inside the obtained OFCI-set and Δ-invariant polyhedron $\mathcal{L}_0$, and both designs yield state trajectories that converge and

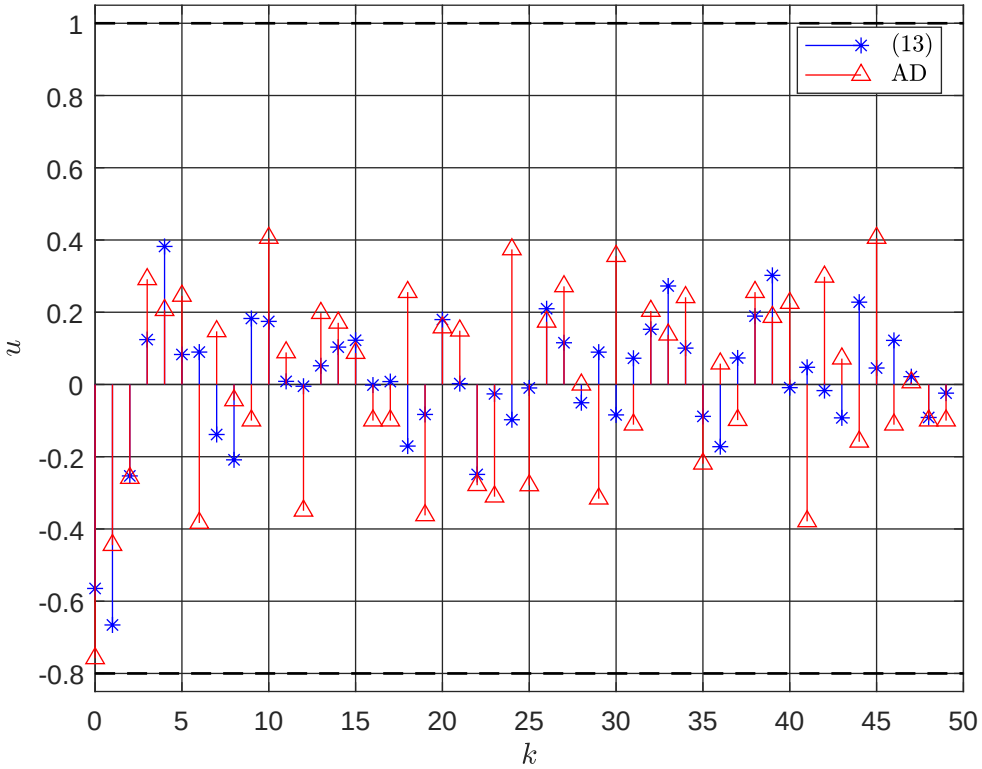

Figure 11 – Control actions for simulations with $x_0^T = [1.053 \;\; 1]$

remain bounded around the origin; particularly, the blue trajectory converge to the estimated UB-set $\mathcal{L}_\infty$. Figure 11 depicts the corresponding control actions that are within the control limits, which generated the two different state behaviors in Figure 10.

The other trajectory emanating from $x_0^T = [-0.2691 \;\; -1]$, which is still inside the OFCI-set but outside Δ-invariant sets, aims at emphasizing that the *static OF*-control gain obtained from (15) is capable of stabilizing every trajectory that emanates from the $\mathcal{L}_{AD}$ but outside $\mathcal{L}_0$ without exceeding the states and control constraints. Conversely, for initial conditions outside the $\mathcal{L}_{AD}$, it is not possible to generate adequate control actions since the *on-line* computations depend on the designed OFCI-set.

2.4.1.3 DOF Design

Now, by following Remark 2, we demonstrate the possibility of designing *DOF*-controllers from our proposal, by considering the same system, constraints, and output matrices $C = [1 \;\; 0]$ and D_η of the last case. To this purpose, we present different designs of reduced-order *DOF*-controllers, hence with $n_c = 1$, by considering the following design parameters: $l_r = 9$, the same $\bar{t} = 16$ directions used before under the augmented form $[\upsilon_t^T \; 0] \in \mathbb{R}^3$, and different values of the weighting factor α. Furthermore, we set $\tilde{X} = [0.2 \; -0.2]^T$, which corresponds to using the auxiliary constraint $|x_k^c| \leq 5$. Besides, differently from the two previous cases, we set $\underline{l} = -100$ and $\bar{l} = 100$ to get more comprehensive sets $\mathcal{L}_0$ and, as a by-product, numerically well-behaved controller parameters.

Table 5 – *DOF* designs with $l_r = 9$ and $\bar{t} = 16$

α	Volume	Area	$\bar{\rho}$	$\begin{bmatrix} D_c & C_c \\ B_c & A_c \end{bmatrix}$
1	2.6749	3.1589	1	$\begin{bmatrix} -0.6055 & -0.1372 \\ -0.1461 & 0.0508 \end{bmatrix}$
5	0.1943	2.9213	0.7522	$\begin{bmatrix} -0.5926 & 2.3181 \\ 0.0228 & -0.2854 \end{bmatrix}$
10	4.3415	2.6799	0.6551	$\begin{bmatrix} -0.6081 & -0.0969 \\ -0.6237 & 0.0875 \end{bmatrix}$
20	0.6347	2.0940	0.4927	$\begin{bmatrix} -0.6504 & -1.1125 \\ -0.0846 & 0.2452 \end{bmatrix}$

These choices yield to the *DOF*-controllers, defined in (16), and associated results summarized in Table 5. In particular, it shows the volume of each set $\mathcal{L}_0$ belonging to $\mathbb{R}^3$, and the area of the section of each $\mathcal{L}_0$ on the system state-subspace $\mathbb{R}^2$. Notice that each mentioned section of $\mathcal{L}_0$ is not necessarily invariant but defines a set of initial admissible conditions under the form $x_0^c = [x_0^T \; 0]^T$ such that the corresponding closed-loop trajectories evolve inside the augmented-state limits, hence respecting the original state constraints $\mathcal{X} \subset \mathbb{R}^2$, for any $d_k \in \Delta$. Furthermore, these trajectories converge in finite-time to $\mathcal{L}_\infty \subset \mathbb{R}^3$, and remain in it. In the same manner, the section of the UB-set $\mathcal{L}_\infty$ is not invariant either, but for any initial condition $x_0^c = [x_0^T \; 0]^T$ belonging to it, the corresponding trajectories do not leave $\mathcal{L}_\infty \subset \mathbb{R}^3$. It is worth mentioning that the area of these sections of $\mathcal{L}_0$ are all bigger than the areas of the sets $\mathcal{L}_0$ obtained in the *SOF*-designs presented before, showing that the additional degrees-of-freedom in *DOF*-designs can be used to obtain, in particular, larger sets of initial admissible conditions by considering that the *DOF*-controller system is at rest. Besides, smaller values for $\bar{\rho}$ could be associated to less significant values of the optimization weighting parameter α.

Finally, the two Figures 12 and 13, depict the sets $\mathcal{L}_0$ and $\mathcal{L}_\infty$ obtained for $\alpha = 1$ and 10, both in blue, as well as their sections on the original state-space, which are in red. In black, we represent the trajectories obtained, for each case, by considering the same sequences of input disturbances p_k and η_k, with null-initial conditions. The corresponding matrices L are as follows:

$$L_{1,16}^T = \begin{bmatrix} 0.271 & -0.221 & -0.605 & -1.000 & -0.721 & 0.000 & 0.779 & 0.819 & 0.517 \\ -1.284 & -0.582 & -0.325 & 0.000 & 1.191 & 1.000 & -1.179 & 0.000 & 0.000 \\ 0.352 & 1.807 & -1.869 & 0.000 & -0.163 & 0.000 & 0.139 & 0.185 & -2.791 \end{bmatrix}$$

and $L_{10,16}^T =$

$$\begin{bmatrix} -1.000 & 0.823 & 0.790 & 0.727 & -0.857 & -0.103 & -1.000 & 0.867 & 0.327 \\ 1.000 & 0.000 & 0.000 & -1.338 & 1.345 & 1.125 & 0.000 & -1.543 & -1.511 \\ -1.586 & 0.131 & -0.055 & 1.198 & -0.119 & -0.016 & 0.000 & 0.142 & 0.293 \end{bmatrix}.$$

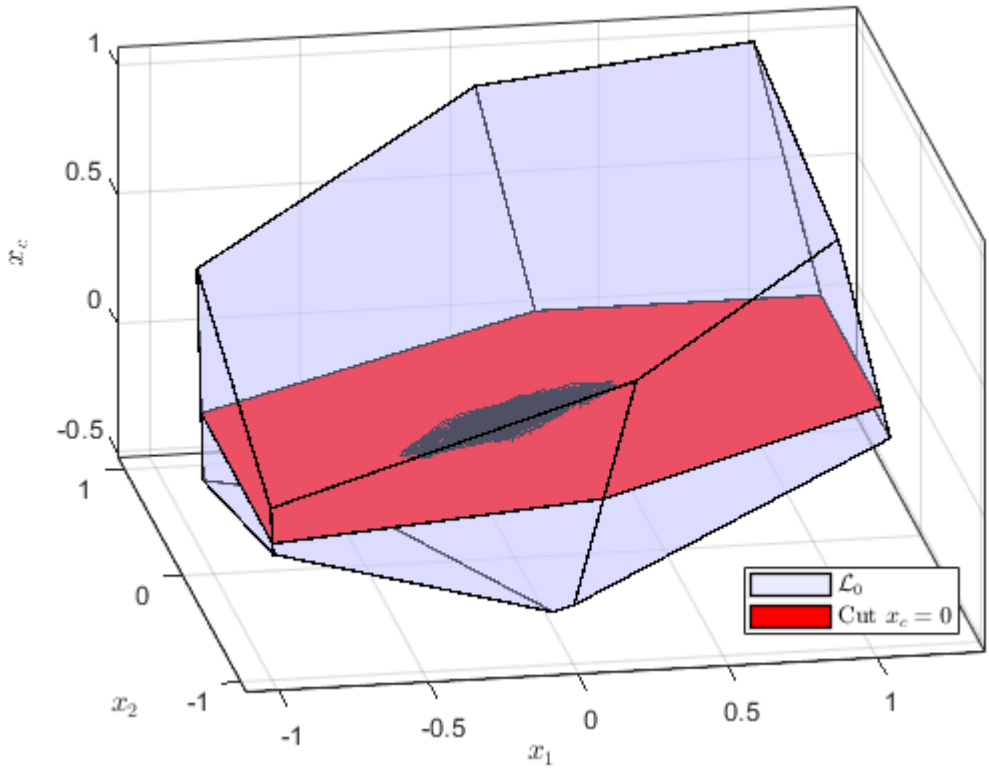

Figure 12 – *DOF*-design for $\alpha = 1$

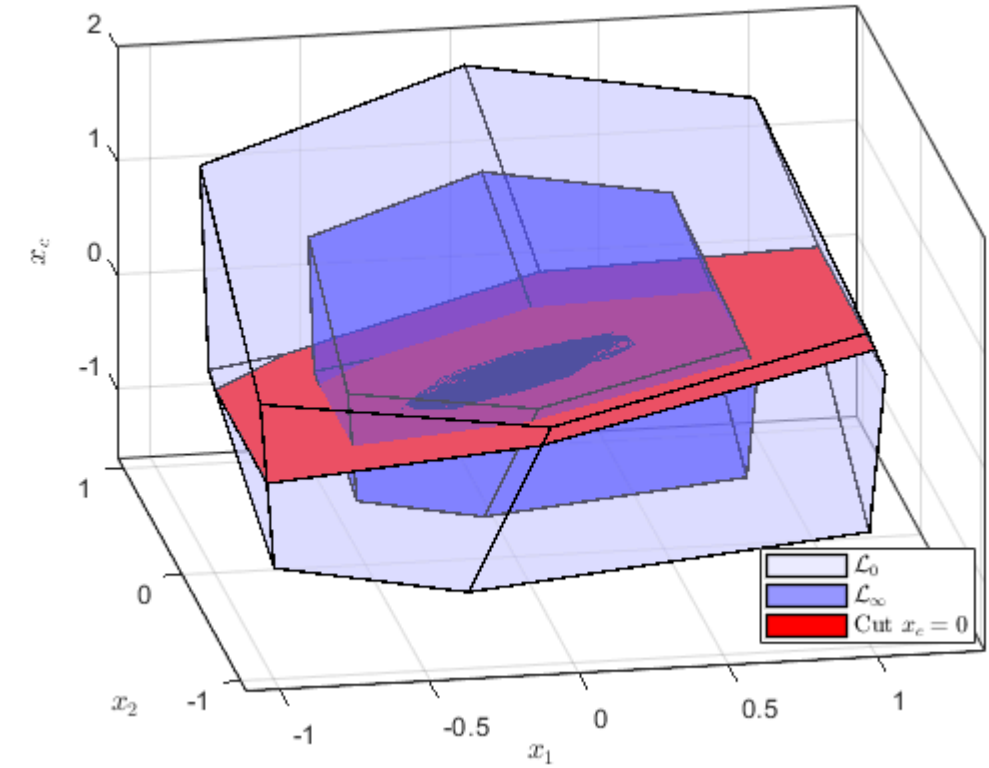

Figure 13 – *DOF*-design for $\alpha = 10$

2.4.2 Example 2

Let us now consider the continuous-time model of a hydraulic application with a four-tank system whose parameters, and state and control constraints are borrowed from Zhou et al. (2015). The corresponding fourth-order discrete-time system, obtained from the Zero Order Holder (ZOH)-discretization of the continuous-time model, with sampling period $T_s = 5$ seconds, has the following system's matrices:

$$A = \begin{bmatrix} 0.9705 & 0 & 0.0207 & 0 \\ 0 & 0.9663 & 0 & 0.0195 \\ 0 & 0 & 0.9790 & 0 \\ 0 & 0 & 0 & 0.9802 \end{bmatrix}, \; B = \begin{bmatrix} 24.6291 & 0.5213 \\ 0.5737 & 32.7684 \\ 0 & 49.4735 \\ 57.7531 & 0 \end{bmatrix}, \; C^T = \begin{bmatrix} 1 & 0 \\ 0 & 1 \\ 0 & 0 \\ 0 & 0 \end{bmatrix}.$$

Notice that this open-loop system, with eigenvalues corresponding to the diagonal terms of matrix A, is asymptotically stable. But it has the following set of transmission-zeros, $\{0.9425\,,\ 1.0181\}$, one of which is outside of the unit-circle, thus with a non-minimum phase characteristic. Moreover, the associated state and control constraints, (3a) and (3b), are described from

$$X = \begin{bmatrix} 1.4085 & 0 & 0 & 0 \\ 0 & 1.4286 & 0 & 0 \\ 0 & 0 & 1.5385 & 0 \\ 0 & 0 & 0 & 1.5625 \\ -2.2222 & 0 & 0 & 0 \\ 0 & -2.1739 & 0 & 0 \\ 0 & 0 & -2.2222 & 0 \\ 0 & 0 & 0 & -2.1739 \end{bmatrix}, \text{ and } \; U = \begin{bmatrix} 2.2086 & 0 \\ 0 & 1.8 \\ -2.2086 & 0 \\ 0 & -1.8 \end{bmatrix} \times 10^3.$$

Additionally, we consider that the system is subject to external disturbances acting on the control inputs, thus implying $B_p = B$, and that the output measurements are noiseless, that is $D_\eta = \mathbf{0}$. Thus, by admitting that due to the external disturbances, the actual control inputs can vary $\pm 2.5\%$ around the computed values, the considered set $\mathcal{P}$, eq. (3c), of admissible disturbances is described by

$$P^T = \begin{bmatrix} 8.8344 & 0 & -8.8344 & 0 \\ 0 & 7.2 & 0 & -7.2 \end{bmatrix} \times 10^4.$$

By considering this realistic example, our single objective in the sequel is to demonstrate the possibility of dealing with a more complex case, both in terms of the system's order and controller's complexities (dimension or structure), thus not to compare it with other techniques. In particular, we want to show the ability to use the bilinear optimization problem (15) to synthesize both centralized and decentralized solutions for the considered constrained control problem. Therefore, for decentralized solutions, two independent controllers are to be applied to the input-output pairs (u_i, y_i), for $i = 1, 2$,

which require to obtain some control gains equal to zero in both *static OF* and *DOF* designs. However, because the elements of the output feedback matrix explicitly appear as decision variables in (15), the mentioned decentralization constraints can be directly imposed by setting the required elements of the considered feedback matrix to zero.

Therefore, for the *static OF* and *DOF* designs presented in the sequel, we set $l_r = 3n = 12$ and $l_r = 3n_a = 18$, respectively, and determine the set $\mathcal{V}$, of directions to be optimized (see (14)), composed by the $\bar{t} = 16$ vertices of the state constraints set $\mathcal{X}$. In this way, by setting $\alpha = 0$ in the objective function of the optimization procedure (15), we ultimately seek to obtain the scaling factors γ_i in (14) as close as possible to 1. Thus, in the particular case of *static OF*-designs, we want to get the set $\mathcal{L}_0$ as close as possible to $\mathcal{X}$.

2.4.2.1 Static OF Designs

In Table 6 that summarizes the *static OF*-designs, the second and third columns aims at putting in evidence the values of the scaling factors $0 \leq \gamma_i \leq 1$, $i = 1, \ldots, 16$, such that their sum (second column) cannot be greater than 16, as well as cannot be the number of such elements that reach the unity (third column). Thus, in the centralized case where all the elements of K are decision variables, we obtain:

$$K_{cent} = \begin{bmatrix} -0.2306 & 0.0365 \\ 0.0198 & -0.3189 \end{bmatrix} \times 10^{-4},$$

and in the decentralized case, by imposing a diagonal structure to the *static OF*-matrix, we get:

$$K_{dec} = \begin{bmatrix} k_{11} & 0 \\ 0 & k_{22} \end{bmatrix} = \begin{bmatrix} 0.5256 & 0.0000 \\ 0.0000 & -0.6394 \end{bmatrix} \times 10^{-4}.$$

From the second and third columns of Table 6, we can firstly remark that the centralized solution rendered Δ-invariant the whole set of state constraints, that is $\mathcal{L}_0 = \mathcal{X}$. We can also deduce that the set $\mathcal{L}_0 \subseteq \mathcal{X}$ obtained in the decentralized case is less significant than in the centralized case, the latter also giving a smaller estimation of the relative size for $\mathcal{L}_\infty$.

It is also interesting to remark the relatively small control gains obtained in both designs, which are due to implicit control objective of maximizing the size of $\mathcal{L}_0$ with respect to $\mathcal{X}$, leading to the corresponding spectra to be close to the open-loop one: $\sigma(A + BK_{cent}C) = \{0.9705, 0.9663, 0.9790, 0.9802\}$ and $\sigma(A + BK_{dec}C) = \{0.9664 \pm j0.0027, 0.9812 \pm j0.0043\}$.

Table 6 – *Static OF*-designs with $\alpha = 0$, $l_r = 12$, and $\bar{t} = 16$

Type	$\Sigma_{i=1}^{t}\gamma_i$	$\#\gamma_i$	$\bar{\rho}$
Central.	16.0000	16	0.9550
Decent.	6.4609	4	0.9996

Table 7 – Decentralized *DOF*-design with $l_r = 12$ and $\bar{t} = 16$

Type	$\Sigma_{i=1}^{t}\gamma_i$	$\#\gamma_i$	$\bar{\rho}$
Decent.	12.5888	12	0.975

2.4.2.2 Decentralized DOF-design

Now, following Remark 2, we consider the decentralized *DOF*-design of two 1*st*-order controllers, thus considering structured control gains as follows

$$K \leftarrow \begin{bmatrix} D_c & C_c \\ B_c & A_c \end{bmatrix} = \begin{bmatrix} d_{c,11} & 0 & c_{c,11} & 0 \\ 0 & d_{c,22} & 0 & c_{c,22} \\ b_{c,11} & 0 & a_{c,11} & 0 \\ 0 & b_{c,22} & 0 & a_{c,22} \end{bmatrix}.$$

Furthermore, we set auxiliary constraints to $x_c \in \mathbb{R}^2$, by assigning $\tilde{X}^T = \begin{bmatrix} 2 & 0 & -2 & 0 \\ 0 & 2 & 0 & -2 \end{bmatrix}$ and establishing $\underline{l} = -50$ and $\bar{l} = 50$. The result is summarized by Table 7, and the decentralized control gain matrix obtained is as follows

$$K_0 \leftarrow \begin{bmatrix} -0.0653 & 0.0000 & -0.2339 & 0.0000 \\ 0.0000 & -0.0548 & 0.0000 & 0.1979 \\ -16.2634 & 0.0000 & 36.9928 & 0.0000 \\ 0.0000 & 54.3233 & 0.0000 & 44.4147 \end{bmatrix} \times 10^{-4}.$$

By comparing the decentralized solutions reported by Tables 6 and 7, we verify that the *DOF*-design produces a more relevant set of admissible initial conditions in the x_k-plane than in the decentralized *static OF* case, due to considering two first-order dynamical controllers instead of two proportional gains. Finally, the closed-loop spectrum is now composed by 6 Eigenvalues, as follows: {0.9661, 0.9705, 0.9804, 0.9787, 0.0037, 0.0044}.

Remark 5 *The average computational time varies according to the different solver configurations, upper and lower bounds of variables, and the number of constraints of the bilinear optimization problem* (15)*, which turns out to be a function of the system's order and polyedral constraints* (3)*, and the user's choices for the control design parameters. Keep in mind that the Knitro solver (BYRD et al., 2006) implemented through AMPL (FOURER et al., 2003) allows for efficient parallel processing, with a high speed up, meaning that you can use multiple cores simultaneously to solve the optimization problem.*

Table 8 shows the average computation time, in seconds, to solve each of control designs in the examples. The control design problems were solved on a Ubuntu 20.04.1 LTS server, with two Intel Core Xeon E5-2630 v4 Processors (2.20GHz) and 64 GB of RAM. The AMPL language was used to implement the mathematical models.

Table 8 – Average computation time in Example 1

Example	Control Type	Average Time
5.1	*SF*	100s
	Static OF	80s
	DOF	220s
5.2	*Static OF*	680s
	DOF	1360s

2.5 CONCLUSION

In this chapter, inspired by Brião (2019, Chapter 5), we have proposed a new set of algebraic relations that jointly describe the Δ-Invariance property of a polyhedron and the convergence of the trajectories of linear discrete-time systems to an associate UB polyhedron. Further, we have developed a bilinear optimization design approach to find a stabilizing linear *static OF* control law for state and control constrained linear discrete-time systems subject to persistent disturbances, which defines the important class of amplitude-bounded exogenous signals present in most practical processes. Differently from Brião (2019), the proposed objective function allows weighing the maximization of the Δ-invariant set in given directions and an upper-bound for the relative size of the internal UB-set. In this optimization approach, the control gain matrix appears explicitly in the formulation, allowing the consideration of structured control laws, and it also applies to design *StF* and *DOF* controllers, thus covering the ability to deal with these three fundamental classical controllers. Additionally, it also allows the design of reduced-order *DOF*-controllers, which is not a feature often encountered in other optimization approaches such as LMI-based ones (see, for instance, Silva Jr et al. (2013)). Furthermore, from the proposed improvements, we reached less conservative results than the ones presented in Brião (2019, Chapter 5).

3 SET-THEORETIC OUTPUT FEEDBACK CONTROL: A BILINEAR PROGRAMMING APPROACH

In this chapter, a novel Set-Theoretic (ST)-Output Feedback(OF) controller is proposed to deal with the robust output regulation problem of systems subjects to process and measurement disturbances and state and input constraints. The proposed scheme resorts to the joint use of the concepts of robust control invariant (RCI) set and robust one-step controllable sets (ROSC). In the state-feedback case, such a paradigm has been successfully employed to develop a computationally low-demanding MPC solution known as dual-mode set-theoretic MPC, see, e.g. Bertsekas and Rhodes (1971), Blanchini and Miani (2015), Angeli et al. (2008) and Lucia et al. (2017). However, such a framework has not been used to deal with the output regulation problem. In this chapter, following our second journal publication (LUCIA et al., 2023), we show that a computationally affordable switching output regulator can still be obtained in the output feedback case and that the design of such a controller can be obtained by jointly leveraging extended Farkas's lemma arguments and bilinear programming tools. This differs from the previous chapter, where a single output feedback control and only two associated positive invariant sets are considered.

The main features of the proposed controller can be summarized as follows: (i) state/input constraints, as well as plant and measurement disturbances, can be all taken into account, (ii) most of the required computations are moved into an offline phase, so leaving online the computation of simple set-membership tests, (iii) for any initial condition belonging to the controller's domain of attraction, the controller ensures that the state trajectory is uniformly ultimately bounded into a small RCI set in a finite and offline known number of steps.

The chapter is organized as follows: first, by considering the class of static output feedback controllers, we geometrically characterized the RCI and ROSC set concepts and we present the proposed switching output feedback control strategy. Then, by resorting to the extended Farkas lemma and bilinear optimization tools, we provide a detailed computable control scheme. Finally, simulation results are presented to contrast the proposed solution with existing approaches.

3.1 PRELIMINARIES

Consider again the following Linear Time-Invariant (LTI) discrete-time system:

$$x_{k+1} = Ax_k + Bu_k + B_p p_k \tag{17}$$

$$y_k = Cx_k + D_\eta \eta_k \tag{18}$$

where $u_k \in \mathbb{R}^m$ is the control input, $x_k \in \mathbb{R}^n$ the state space vector, $y_k \in \mathbb{R}^p$ the output vector, and (A, B, C) are the system matrices of suitable dimensions with $rank(C) = p$. The input and the state vectors $(u_k,\ x_k)$ are subject to the following constraints

$$u_k \in \mathcal{U}, \quad x_k \in \mathcal{X}, \quad \forall k \geq 0, \tag{19}$$

where $\mathcal{U} \subset \mathbb{R}^m$, $\mathcal{X} \subset \mathbb{R}^n$ are compact subsets with $\mathbf{0}_m \in \mathcal{U}$ and $\mathbf{0}_n \in \mathcal{X}$. Moreover, $p_k \in \mathbb{R}^s$, $\eta_k \in \mathbb{R}^r$ are exogenous and bounded process and measurement disturbances, with

$$p_k \in \mathcal{P}, \quad \forall k \geq 0 \tag{20}$$

$$\eta_k \in \mathcal{N}, \quad \forall k \geq 0 \tag{21}$$

and $\mathcal{P} \subset \mathbb{R}^s$ and $\mathcal{N} \subset \mathbb{R}^r$ compact subsets with $\mathbf{0}_s \in \mathcal{P}$ and $\mathbf{0}_r \in \mathcal{N}$, respectively. Thus, we assume that all the bounding sets are described as the following polyhedra:

$$\begin{aligned} \mathcal{X} &= \{x \in \mathbb{R}^n : Xx \leq \mathbf{1}_{l_x}\}, \quad X \in \mathbb{R}^{l_x \times n} \\ \mathcal{U} &= \{u \in \mathbb{R}^m : Uu \leq \mathbf{1}_{l_u}\}, \quad U \in \mathbb{R}^{l_u \times m} \\ \mathcal{P} &= \{p \in \mathbb{R}^s : Pp \leq \mathbf{1}_{l_p}\}, \quad P \in \mathbb{R}^{l_p \times s} \\ \mathcal{N} &= \{n \in \mathbb{R}^r : N\eta \leq \mathbf{1}_{l_p}\}, \quad N \in \mathbb{R}^{l_n \times r} \end{aligned} \tag{22}$$

The following definitions are used along the rest of the chapter:

Definition 3 *Let $\mathcal{Q} \subset \mathcal{X}$ be a region of interest. The closed-loop trajectory of (17), is said to be Uniformly Ultimately Bounded (UUB) in $\mathcal{Q}$ if for all $\mu > 0$, there exists a function $T(\mu) > 0$ such that $\forall \|x_0\| \leq \mu \rightarrow x_k \in \mathcal{Q}, \forall d_k \in \mathcal{D}$ and $\forall\, k \geq T(\mu)$ (BLANCHINI; MIANI, 2015).*

Definition 4 *A set $\mathcal{Q} \subseteq \mathcal{X}$ is said Robust Control Invariant (RCI) for (17) under (19)-(21) if (BORRELLI et al., 2017):*

$$\begin{gathered} \forall x \in \mathcal{Q} \rightarrow \exists u \in \mathcal{U} : \\ Ax + Bu + B_p p \in \mathcal{Q}, \ \ \forall p \in \mathcal{P} \end{gathered} \tag{23}$$

□

Definition 5 *Consider the plant model (17) under (19)-(21), and a set $\mathcal{L}_i \subset \mathcal{X}$. The set of states Robustly One-Step Controllable (ROSC) to $\mathcal{L}_i$ in one-step, namely $\mathcal{L}_{i+1} \subset \mathcal{X}$, is defined as (BORRELLI et al., 2017):*

$$\mathcal{L}_{i+1} := \{x \in \mathcal{X}, \exists u \in \mathcal{U} : Ax + Bu + B_p p \in \mathcal{L}_i, \ \forall p \in \mathcal{P}\} \tag{24}$$

□

The extension of the Farkas' Lemma (see, for instance, Hennet (1995) and Blanchini and Miani (2015)) plays a fundamental role in describing the inclusion of two polyhedral sets. In this chapter, we re-state such a result and use it to describe algebraically the previous definitions of RCI and ROSC sets.

Definition 6 *Given two sets $\mathcal{S}_1, \mathcal{S}_2 \subset \mathbb{R}^{n_s}$, their Minkowski/Pontryagin set sum ($\oplus$) and difference ($\sim$) are (BORRELLI et al., 2017):*

$$\mathcal{S}_1 \oplus \mathcal{S}_2 = \{s_1 + s_2 : s_1 \in \mathcal{S}_1, s_2 \in \mathcal{S}_2\}$$
$$\mathcal{S}_1 \sim \mathcal{S}_2 = \{s_1 \in \mathcal{S}_1 : s_1 + s_2 \in \mathcal{S}_1, \forall s_2 \in \mathcal{S}_2\}$$

3.2 PROBLEM FORMULATION

Consider the problem of stabilization of the constrained system (17)-(21) by means of an output feedback control law

$$u_k = f(y_k) \tag{25}$$

where $f(y_k) : \mathbb{R}^p \to \mathbb{R}^m$ is a function characterizing the output control logic.

The control problem addressed in this chapter can be stated as follows:

Problem 1 *Find a stabilizing output feedback control function (25) and an associated domain of attraction $\mathcal{L}_D \subseteq \mathcal{X}$, $0_n \in \mathcal{L}_D$ such that $\forall\, x_0 \in \mathcal{L}_D$ and persistent disturbances (20)-(21), the following properties are met:*

- *$\mathcal{L}_D$ is a RCI set.*
- *There exist a small RCI region $\mathcal{L}_0 \subseteq \mathcal{L}_D$, $\mathbf{0}_n \in \mathcal{L}_0$ where the state trajectory is UUB in a finite and a-priori known numbers of steps.*
- *The state and input constraints (19) are fulfilled.*

To improve as much as possible the clarity of the presentation, the rest of the two following sections are organized as follows. First, by neglecting the computational details, the proposed solution is geometrically described and its properties formally proved (Section 3.3). Then, all the computational aspects are presented (Section 3.4).

Notation Warning: It is worth noticing that the notation $\mathcal{L}_0$ given here for the innermost set differs from the notation used in the previous chapter, where $\mathcal{L}_\infty$ and $\mathcal{L}_0$ defined an innermost and the outermost invariant sets, respectively. The present notation, associating $\mathcal{L}_0$ to the innermost robust positively invariant set, will also be valid in the next chapters.

3.3 PROPOSED SOLUTION

We propose solving *Problem* 1 by means of a switching output feedback controller exploiting set-theoretic controllability arguments. The family of switching static Output Feedback (OF) controllers is offline designed as follows:

- First, by considering a single static OF control law

$$u_k = K_0 y_k \tag{26}$$

the gain $K_0 \in \mathbb{R}^{m\times n}$ is optimized to obtain a small RCI region $\mathcal{L}_0 \subseteq \delta\mathcal{X}, 0_n \in \mathcal{L}_0$, $0 < \delta_0 \leq 1$ for (17)-(21) satisfying the conditions (27)-(29):

$$(A + BK_0C)\mathcal{L}_0 \oplus B_p\mathcal{P} \oplus BK_0D_\eta\mathcal{N} \subseteq \mathcal{L}_0 \tag{27}$$

$$\mathcal{L}_0 \subseteq \delta_0\mathcal{X} \tag{28}$$

$$K_0C\mathcal{L}_0 \oplus K_0D_\eta\mathcal{N} \subseteq \mathcal{U} \tag{29}$$

Notice that the conditions (27)-(28) enforce that $\mathcal{L}_0$ is an admissible small RCI set under (26) and (20)-(21), and (29) guarantees that the input constraints are fulfilled regardless any admissible measurement error (21). It is worth to remark that the related computational details are addressed in subsection 3.4.1.

- Second, the domain of the terminal controller, i.e. $\mathcal{L}_0$, is enlarged by recursively computing a family of robust one-step controllable (ROSC) sets, namely $\{\mathcal{L}_i\}_{i=0}^{\bar{N}}$, $\bar{N} > 0$ where each set $\mathcal{L}_i \subseteq \mathcal{X}$ is associated to a different static OF gain $K_i \in \mathbb{R}^{m\times n}$. Each pair $(\mathcal{L}_i, K_i)$ is computed to satisfy the inclusion conditions (30)-(33):

$$(A + BK_iC)\mathcal{L}_i \oplus B_p\mathcal{P} \oplus BK_iD_\eta\mathcal{N} \subseteq \mathcal{L}_{i-1} \tag{30}$$

$$\mathcal{L}_i \subseteq \mathcal{X} \tag{31}$$

$$K_iC\mathcal{L}_i \oplus K_iD_\eta\mathcal{N}\mathcal{L}_i \subseteq \mathcal{U} \tag{32}$$

$$\mathcal{L}_{i-1} \subseteq \mathcal{L}_i \tag{33}$$

while $\bar{N}$ (i.e., the number of ROSC sets computed) is constructively obtained by recursively applying (30)-(33) until the the set growth saturates, i.e.,:

$$\bar{N} = \left(\min_{j\geq 1} j - 1\right) \text{ s.t.}$$
$$\mathcal{L}_j = \mathcal{L}_{j-1} \tag{34}$$

Therefore, $\mathcal{L}_D := \bigcup_{i=1}^{\bar{N}} \mathcal{L}_i \subseteq \mathcal{X}$ defines the domain of attraction associated to the family of Sof controllers $\{K_i\}_{i=0}^{\bar{N}}$.

Remark 6 *Please note that the set containment conditions (30)-(32) are necessary to define a robust one-step controllable set (see Definition 5) under the static OF law $u_k = K_i y_k$. On the other hand, (33) is not strictly necessary, however, it is instrumental to ensure the feasibility of the proposed output feedback controller if $\text{rank}(C) < n$ and/or $\mathcal{N} \neq \mathbf{0}_r$, see, e.g., Proposition 3. The computational details related to the geometrical conditions (30)-(33) are given in subsection 3.4.2.*

3.3.1 Set-theoretic output feedback with $rank(C) < n$

Proposition 3 *Consider the plant model (17)-(21) with $rank(C) < n$, a family of static OF controllers $\{K_i, \mathcal{L}_i\}_{i=0}^{\bar{N}}$ satisfying the conditions (26)-(34) and an initial condition $x_0 \in \mathcal{L}_D$. If at each time instant the $\bar{i}_k$–th Sof controller (i.e., $u_k = K_{\bar{i}_k} y_k$) is selected according to the switching rule (35)*

$$\bar{i}_k = \begin{cases} \bar{N} & \textbf{if } k = 0 \\ \max(\bar{i}_{k-1} - 1, 0) & \textbf{otherwise} \end{cases} \tag{35}$$

then $u_k \in \mathcal{U}$ and $x_{k+1} \in \mathcal{L}_{max(0,\, \bar{i}_k - 1)}$, $\forall\, k$. Moreover, $\mathcal{L}_D$ is a RCI set and the state trajectory is Uniform Ultimate Boundedness (UUB) into the terminal set $\mathcal{L}_0$ in at most $\bar{N}$ steps.

Proof If $rank(C) < n$, then we cannot accurately determine the set $\mathcal{L}_i$ containing x_0. However, by taking a worst-case approach and exploiting the set-inclusion condition (33), we can safely assume that $x_0 \in \mathcal{L}_N$. This choice, by construction, ensures that $u_0 = K_{\bar{N}} y_0$ is admissible (i.e., $u_0 \in \mathcal{U}$) and that the one-step evolution is constrained into the predecessor set $\mathcal{L}_{\bar{N}-1}$ (i.e., $x_1 \in \mathcal{L}_{\bar{N}-1}$) regardless of any admissible disturbance realization (20)-(21), see (30)-(33). As a consequence, the set $\mathcal{L}_D$ is a RCI set. Moreover, at $k = 1$, we can use the Sof controller $u_1 = K_{\bar{N}-1} y_1$ that ensures that $u_1 \in \mathcal{U}$ and $x_2 \in \mathcal{L}_{\bar{N}-2}$. By recursively applying the same procedure for $k > 1$, i.e., by using the monotonically decreasing switching law (35), the RCI region $\mathcal{L}_0$ is guaranteed to be reached in $\bar{N}$ steps and the UUB property fulfilled.

3.3.2 Set-theoretic output feedback with $rank(C) = n$

Proposition 4 *Consider the plant model (17)-(21) with $C \in \mathbb{R}^{n \times n}$ and $rank(C) = n$, a family of static OF controllers $\{K_i, \mathcal{L}_i\}_{i=0}^{\bar{N}}$ satisfying the conditions (26)-(34), the sets $\{\tilde{\mathcal{L}}_i\}_{i=0}^{\bar{N}}$, $\tilde{\mathcal{L}}_i := \mathcal{L}_i \sim C^{-1} D_\eta \mathcal{N}$, and an initial condition $x_0 \in \mathcal{L}_D$.*
If at each time instant the $\underline{i}_k$–th static OF controller (i.e., $u_k = K_{\underline{i}_k} y_k$) is selected according to the switching rule (36)

$$\underline{i}_k = \begin{cases} \min\left(J(y_k, \bar{N}),\, \bar{N}\right) & \textbf{if } k = 0 \\ \min\left(J(y_k, \underline{i}_{k-1} - 1),\, \max(\underline{i}_{k-1} - 1, 0)\right) & \textbf{if } k > 0 \end{cases} \tag{36}$$

$$J(y_k, i_{max}) := \min_{0 \le i \le i_{max}} i \quad s.t. \quad C^{-1} y_k \in \tilde{\mathcal{L}}_i \tag{37}$$

then $u_k \in \mathcal{U}$ and $x_{k+1} \in \mathcal{L}_{max(0,\, \underline{i}_k - 1)}$, $\forall\, k$. Moreover, the state trajectory is UUB into the terminal set $\mathcal{L}_0$ in at most $\underline{i}_0$ steps.

Proof If $C \in \mathbb{R}^{n \times n}$ and $rank(C) = n$, then we can estimate x_k from y_k as follows:

$$\hat{x}_k = C^{-1} y_k \tag{38}$$

By expanding the right hand side, we obtain that

$$\begin{aligned} \hat{x}_k &= C^{-1}(C x_k + D_\eta \eta_k) \\ \hat{x}_k &= x_k + C^{-1} D_\eta \eta_k \end{aligned} \tag{39}$$

Therefore, since $\eta_k \in \mathcal{N}$, the resulting estimation error is bounded by the set $\mathcal{E}_k = C^{-1} D_\eta \mathcal{N}$. By resorting to Minkowski set difference arguments, we can conclude that

$$\textbf{if } \hat{x}_k \in \tilde{\mathcal{L}}_{i-1} := \mathcal{L}_i \sim C^{-1} D_\eta \mathcal{N} \textbf{ then } x_k \in \mathcal{L}_{i-1} \tag{40}$$

As a consequence, the switching control logic (36) determines the smallest set $\mathcal{L}_i$ ensuring that $x_k \in \mathcal{L}_i$. Notice that in the worst-case scenario (following the same arguments used in the proof of Proposition 3), $\underline{i}_0 = \bar{N}$ and that $\underline{i}_k$ must decrease by one unit at each step. The latter ensures that $\mathcal{L}_0$ is reached in at most $\underline{i}_0$ steps and that the UUB property holds true.

Remark 7 *In the worst-case scenario, the switching signal $\underline{i}_k$ obtained by (36) is upper bounded by $\bar{i}_k$ computed as in (35), i.e. $\underline{i}_k \leq \bar{i}_k$, $\forall\, k$. As a consequence, the switching logic (35) can still be used if $\mathrm{rank}(C) = n$. On the other hand, the logic (36), by exploiting that C is invertible, is capable of better estimating the set containing the current measurement y_k. As a consequence, with (36), a faster convergence to $\mathcal{L}_0$ is expected.*

Remark 8 *Note that the containment condition (33) can be removed/relaxed if $\mathrm{rank}(C) = n$ and $\mathcal{N} = \mathbf{0}_r$. The main rationale is that in this case there is no ambiguity to determine (using the switching logic (36)) to which set the state x_k belongs $\forall\, k$.*

3.3.3 Algorithm

The complete control algorithm is here summarized:

Algorithm 1 Set-Theoretic Output Feedback (ST-OF)

−Offline (given (17)-(21))−

1: Build a small terminal RCI region $\mathcal{L}_0$ and associated static OF gain K_0 pair $(\mathcal{L}_0, K_0)$ as in (27)-(29);
2: Build a family of ROSC sets $\{\mathcal{L}_i\}$ and associated static OF controller gains $\{K_i\}$ as in (30)-(33), until the stopping condition (34) is satisfied;
3: **if** $rank(C) = n$ **then** compute

$$\{\tilde{\mathcal{L}}_i\}_{i=0}^{\bar{N}},\ \tilde{\mathcal{L}}_i := \mathcal{L}_i \sim C^{-1} D_\eta \mathcal{N}$$

4: **end if**
5: Store $\{K_i, \tilde{\mathcal{L}}_i^y\}_{i=0}^{\bar{N}}$ for online use.

−Online ($\forall\, k$, $x_0 \in \mathcal{L}_D$)−

1: Given y_k, compute i_k as follows:

$$i_k = \begin{cases} \bar{i}_k \text{ by (35)} & \textbf{if } rank(C) < n \\ \underline{i}_k^f \text{ by (35) } or \text{ (36)} & \textbf{if } rank(C) = n \end{cases} \tag{41}$$

2: Compute $u_k = K_{i_k} y_k$;
3: Apply u_k.

Remark 9 *Please note that if $rank(C) = n$ and $\mathcal{N} = \mathbf{0}_r$ then the ST-OF algorithm defines a switching set-theoretic state-feedback (ST-SF) controller, similar to the dual-mode solution proposed in Angeli et al. (2008). Differently from Angeli et al. (2008), the proposed algorithm does not require the online solution of an optimization problem to compute the control action. Indeed, the controller gains K_i are offline computed along with the controllable sets $\mathcal{L}_i$.*

3.4 IMPLEMENTATION DETAILS

In this section, the geometric conditions (27)-(29) and (30)-(33) are translated into computable algebraic relations.

From now on, we assume that the controllable sets $\mathcal{L}_i$, for $i = 0, \ldots, \bar{N}$, are compact.

According to (28), (29), (31) and (32), any candidate set $\mathcal{L}_i$ must satisfy $\mathcal{L}_i \subseteq \mathcal{X}$ and the control admissibility condition

$$x_k \in \mathcal{U}_i^x, \forall x_k \in \mathcal{L}_i \text{ and } \eta_k \in \mathcal{N}, \tag{42}$$

where, by definition,

$$\mathcal{U}_i^x = \{x_k \in \mathbb{R}^n, \eta_k \in \mathbb{R}^r : U(K_i C x_k + D_\eta \eta_k) \leq \mathbf{1}_{l_u}, \forall \eta_k \in \mathcal{N}\} \tag{43}$$

Since any admissible RCI and ROSC set must satisfy the state constraints $\mathcal{X}$, the inclusion $\mathcal{L}_i \subseteq \mathcal{X}$ must be imposed. Moreover, to provide some degrees of freedom in

the shape of $\mathcal{L}_i$, we add further auxiliary constraints defined by the following closed polyhedral set $\mathcal{R}_i$,

$$\mathcal{R}_i = \{x \in \mathbb{R} : R_i x_k \leq \mathbf{1}_{r_i}\}, R_i \in \mathbb{R}^{r_i \times n} \tag{44}$$

As a consequence, $\mathcal{L}_i$ is described as

$$\mathcal{L}_i = \{x \in \mathbb{R} : L_i x_k \leq \mathbf{1}_{l_{r,i}}\}, L_i \in \mathbb{R}^{l_{r,i} \times n}, rank(L_i) = n, \tag{45}$$

where, by construction,

$$L_i = \begin{bmatrix} R_i \\ \delta_i X \end{bmatrix}, \text{ and } \mathbf{1}_{l_{r,i}} = \begin{bmatrix} \mathbf{1}_{r_i} \\ \mathbf{1}_{l_x} \end{bmatrix}, \tag{46}$$

with $l_{r,i} = r_i + l_x > n$, and $0 < \delta_i \leq 1, \forall\, i$.

Remark 10 *A necessary and sufficient condition for matrix $L_i \in \mathbb{R}^{l_{r,i} \times n}$ be full-column rank is the existence of a left-inverse matrix $J_i \in \mathbb{R}^{n \times l_{r,i}}$ such that $J_i L_i = I_n$ (STRANG, 2006).*

3.4.1 Small Robust Control Invariant Region $\mathcal{L}_0$ and K_0

The small RCI-set $\mathcal{L}_0$, can be obtained from (45)-(46) and, in addition, by imposing the inclusion:

$$\mathcal{S} \subseteq \mathcal{L}_0, \tag{47}$$

where $\mathcal{S}$ is a given compact and small shape-set used to obtain well-conditioned initial solutions, defined by the polyhedron

$$\mathcal{S} = \left\{x \in \mathbb{R}^n : Sx \leq \mathbf{1}_{l_s}\right\}, S \in \mathbb{R}^{l_s \times n}, l_s > n. \tag{48}$$

Thus, the real non-negative scalar $\delta_0 \leq 1$ in (28) is minimized to obtain a small RCI set $\mathcal{L}_0$.

The following algebraic relations, obtained by applying the Extended Farkas' Lemma (refer to Remark 11 and to the proof of Proposition 5 for further details) describe, in a matrix form, the conditions that the pair $(\mathcal{L}_0, K_0)$ must satisfy:

- the RCI conditions (27)-(29) $\Leftrightarrow \exists$ non-negative matrices $H_0 \in \mathbb{R}^{l_{r,0} \times l_{r,0}}$, $V_0 \in \mathbb{R}^{l_{r,0} \times l_p}$, $W_0 \in \mathbb{R}^{l_{r,0} \times l_\eta}$, $M_0 \in \mathbb{R}^{l_u \times l_{r,0}}$, and $Z_0 \in \mathbb{R}^{l_u \times l_n}$:

$$\begin{aligned}
H_0 L_0 &= L_0(A + BK_0C) && (49)\\
V_0 P &= L_0 B_p && (50)\\
W_0 N &= L_0 B K_0 D_\eta && (51)\\
H_0 \mathbf{1}_{l_{r,0}} + V_0 \mathbf{1}_{l_p} + W_0 \mathbf{1}_{l_\eta} &\leq \mathbf{1}_{l_{r,0}} && (52)\\
M_0 L_0 &= U K_0 C && (53)\\
Z_0 N &= U K_0 D_\eta && (54)\\
M_0 \mathbf{1}_{l_{r,0}} + Z_0 \mathbf{1}_{l_\eta} &\leq \mathbf{1}_{l_u} && (55)
\end{aligned}$$

- the inclusion (47) $\Leftrightarrow \exists$ a non-negative matrix $T_0 \in \mathbb{R}^{l_{r,0} \times l_s}$:

$$T_0 S = L_0 \tag{56}$$

$$T_0 \mathbf{1}_{l_s} \leq \mathbf{1}_{l_{r,0}} \tag{57}$$

- $\mathcal{L}_0$ compact (see Remark 10) $\Leftrightarrow \exists\, J_0 \in \mathbb{R}^{n \times l_{r,0}}$:

$$J_0 L_0 = I_n \tag{58}$$

Notice that the algebraic relation (49) presents two bi-linear terms involving the pair of matrix decision variables (H_0, L_0) in its left-hand side, and (L_0, K_0) in the right-hand side. This last bi-linearity also appears in (51). Likewise, the left hand side of inequality (53) has a bilinear product involving the pair (M_0, L_0). The remaining conditions are all linear with regard to the set of decision variables $\Gamma_0 = \{H_0, V_0, W_0, L_0, K_0, M_0, Z_0, T_0, J_0, \delta_0\}$. Thus, a solution for Step 1 in Algorithm 1 can be obtained from the following bi-linear optimization problem:

$$\begin{aligned} \underset{\Gamma_0}{\text{minimize}} \quad & \delta_0 \\ \text{subject to} \quad & (49)-(58), \\ & 0 < \delta_0 \leq 1, \\ & f_\ell(\cdot) \leq \varphi_\ell, \end{aligned} \tag{59}$$

where $f_\ell(\cdot) \leq \varphi_\ell$, for $\ell = 1, \ldots, \bar{\ell}$, are additional constraints used to reduce the decision variable space. These bounds are essential to deal with non-linear or non-convex optimization problems and promote an efficient search of the optimal solution. Please refer to the section 3.5 for a discussion about the implementation of (59) using the nonlinear KNITRO solver.

3.4.2 Family of one-step controllable sets $\mathcal{L}_i$ and K_i

The computation of the ROSC polyhedral sets is based on the following Proposition.

Proposition 5 *Consider $\mathcal{L}_0$ obtained from* (59)*. Then let the compact sets $\mathcal{L}_i$, for any $i = 1, \ldots, \bar{N}$, be defined by* (45)-(46)*. Then, $\mathcal{L}_i$ is ROSC to $\mathcal{L}_{i-1}$ by SoF, and $\mathcal{L}_i \supseteq \mathcal{L}_{i-1}$, if and only if there exist $K_i \in \mathbb{R}^{m \times p}$, $L_i \in \mathbb{R}^{l_{r,i} \times n}$ and non-negative matrices $H_i \in \mathbb{R}^{l_{r,(i-1)} \times r_i}$, $V_i \in \mathbb{R}^{l_{r,(i-1)} \times l_p}$,*

$W_i \in \mathbb{R}^{l_{r,(i-1)} \times l_\eta}$, $M_i \in \mathbb{R}^{l_u \times l_{r,i}}$, $Z_i \in \mathbb{R}^{l_u \times l_n}$, $T_i \in \mathbb{R}^{l_{r,i} \times l_{r,(i-1)}}$, *and* $J_i \in \mathbb{R}^{n \times l_{r,i}}$ *such that*

$$
\begin{aligned}
H_i L_i &= L_{i-1}(A + BK_iC) && (60)\\
V_i P &= L_{i-1} B_p && (61)\\
W_i N &= L_{i-1} BK_i D_\eta && (62)\\
H_i \mathbf{1}_{l_{r,i}} + V_i \mathbf{1}_{l_p} + W_i \mathbf{1}_{l_\eta} &\leq \mathbf{1}_{l_{r,(i-1)}} && (63)\\
M_i L_i &= UK_iC && (64)\\
Z_i N &= UK_iD_\eta && (65)\\
M_i \mathbf{1}_{l_{r,i}} + Z_i \mathbf{1}_{l_\eta} &\leq \mathbf{1}_{l_u} && (66)\\
T_i L_{i-1} &= L_i && (67)\\
T_i \mathbf{1}_{l_{r,(i-1)}} &\leq \mathbf{1}_{l_{r,i}} && (68)\\
J_i L_i &= I_n && (69)
\end{aligned}
$$

Proof: By definition, the set $\mathcal{L}_i$ is ROSC to $\mathcal{L}_{i-1}$ by SoF, with matrix K_i, if it satisfies (30)-(33). The conditions (30)-(31) can be equivalently described by

$$
\begin{aligned}
& L_{i-1}\begin{bmatrix} A_{K_i} & B_p & BK_iD_\eta \end{bmatrix}\begin{bmatrix} x_k \\ p_k \\ \eta_k \end{bmatrix} \leq \mathbf{1}_{l_{r,(i-1)}},\\
& \forall x_k, p_k \text{ and } \eta_k : diag(L_i, P, N)\begin{bmatrix} x_k \\ p_k \\ \eta_k \end{bmatrix} \leq \begin{bmatrix} \mathbf{1}_{l_{r,i}} \\ \mathbf{1}_{l_p} \\ \mathbf{1}_{l_\eta} \end{bmatrix},
\end{aligned}
\tag{70}
$$

where $A_{K_i} = (A + BK_iC)$ and $diag(L_i, P, N)$ stands for the block-diagonal matrix formed from the argument matrices.

Thus, by the Extended Farkas' Lemma, (70) is equivalent to the existence of a non-negative matrix $Q_i = \begin{bmatrix} H_i & V_i & W_i \end{bmatrix} \in \mathbb{R}^{l_{r,(i-1)} \times (l_{r,i}+l_p+l_\eta)}$ such that:

$$
\begin{aligned}
Q_i diag(L_i, P, N) &= L_{i-1}\begin{bmatrix} A_{K_i} & B_p & BK_iD_\eta \end{bmatrix}, && (71)\\
Q_i \begin{bmatrix} \mathbf{1}_{l_{r,i}} \\ \mathbf{1}_p \\ \mathbf{1}_\eta \end{bmatrix} &\leq \mathbf{1}_{l_{r,(i-1)}}, && (72)
\end{aligned}
$$

which corresponds to (60)-(63). Moreover, the condition (32), which is algebraically described by (42), can be re-written in the matrix form

$$
\begin{aligned}
& U\begin{bmatrix} K_iC & D_\eta \end{bmatrix}\begin{bmatrix} x_k \\ \eta_k \end{bmatrix} \leq \mathbf{1}_{l_u},\\
& \forall x_k \text{ and } \eta_k : diag(L_i, N)\begin{bmatrix} x_k \\ \eta_k \end{bmatrix} \leq \begin{bmatrix} \mathbf{1}_{l_{r,i}} \\ \mathbf{1}_{l_\eta} \end{bmatrix}.
\end{aligned}
\tag{73}
$$

By resorting to the extended Farka's Lemma and by following the same reasoning used for (71)-(72), (73) is equivalent to the existence of non negative matrices M_i and Z_i verifying (64)-(66). Furthermore, the inclusion $\mathcal{L}_{i-1} \subseteq \mathcal{L}_i$ (see (33)), which, in a matrix form, reads

$$L_i x_k \leq \mathbf{1}_{l_{r,i}}, \forall x_k : L_{i-1} x_k \leq \mathbf{1}_{l_{r,(i-1)}},$$

is equivalently described (using the extended Farka's Lemma) by the existence of a non-negative matrix T_i such that conditions (67) and (68) hold true. Finally, the condition (69) imposes that the set $\mathcal{L}_i$ is compact (see Remark 10). □

Remark 11 *In the above demonstration if we consider $i = 0$ and $\mathcal{L}_{i-1} = \mathcal{L}_0$, then it is possible to prove, see (MILANI, B. E. et al., 1996), that the algebraic relations* (49)-(58) *describe the RCI set $\mathcal{L}_0$. In particular,* (49)-(52) *means that the set $\mathcal{L}_0$ is robust positively invariant or, equivalently, Δ-invariant as defined in Chapter 2.*

Now, notice that the algebraic relations (60) and (64) present bi-linear terms involving the pairs of matrix decision variables (H_i, L_i) and (M_i, L_i). Furthermore, because both L_{i-1} and K_{i-1} are known in the current step i, the other *ROSC* and inclusion conditions are all linear with regard to the set of decision variables $\Gamma_i = \{H_i, V_i, W_i, M_i, Z_i, L_i, K_i, T_i, J_i, \delta_i\}$. In order to maximize the size of $\mathcal{L}_i$, we introduce the following auxiliary inequalities

$$\gamma_{t,i} L_i v_t \leq \mathbf{1}_{l_{r,i}}, t = 1, \ldots, \bar{t}. \tag{74}$$

where $\gamma_{t,i}$, for $t = 1, \ldots, \bar{t}$, are real positive scaling factors associated to a given set $\mathcal{V}_i$ of $\bar{t} > 0$ directions $v_t \in \mathbb{R}^n$, where

$$\mathcal{V}_i = \{\gamma_{t,i} v_t, t = 1, \ldots, \bar{t}\}. \tag{75}$$

Hence, the computation of the ROSC set $\mathcal{L}_i$ and associated SoF matrix K_i can be obtained from the following bi-linear optimization program

$$\begin{aligned} \underset{\Gamma_i, \gamma_{t,i}}{\text{maximize}} \quad & \mathcal{J}_i = \sum_{t=1}^{n} \gamma_{t,i} \\ \text{subject to} \quad & (60) - (69) \text{ and } (74), \\ & \delta_{i-1} < \delta_i \leq 1, \\ & f_\ell(\cdot) \leq \varphi_\ell. \end{aligned} \tag{76}$$

Remark 12 *Please note that the condition* (74) *imposes that $\mathcal{V}_i \subseteq \mathcal{L}_i$. Moreover, at each step i, the objective function $\mathcal{J}_i = \sum_{t=1}^{n} \gamma_t$ is used to maximize the size of $\mathcal{L}_i$ w.r.t. the set of directions in $\mathcal{V}_i$. Notice that the set $\mathcal{L}_i$ obtained from* (76) *depends on the used directions, which are designer's choices.*

Moreover, the criterion

$$\mathcal{J}_i - \mathcal{J}_{i-1} = \sum_{t=1}^{n} (\gamma_{t,i} - \gamma_{t,i-1}) \leq tol. \tag{77}$$

with tol a small tolerance value, can be used to numerically approximate the stopping condition (34) used by the ST-OF off-line *algorithm. In simpler terms, if at the iteration $i > 0$ the condition (77) is verified, then $\bar{N} = i - 1$.*

3.5 NUMERICAL EXAMPLE

In this section, some numerical results are presented to verify the proposed control strategy's effectiveness and compare it with two existing approaches. The simulations have been performed on Matlab 2019b, using a Windows 10 PC equipped with an AMD Ryzen 5 3600 6-Core Processor (3.59 GHz) and 16,0 GB of RAM.

In particular, we consider the LTI system (17), already used in the previous chapter, defined by the matrices

$$A = \begin{bmatrix} 1 & 1 \\ 0 & 1 \end{bmatrix}, B = \begin{bmatrix} 2 \\ 1 \end{bmatrix}, B_p = \begin{bmatrix} 1 \\ 1 \end{bmatrix}.$$

The state and control constraints, and the disturbance limits in (22) are shaped by the matrices

$$X = \begin{bmatrix} 0.8 & 0 \\ 0 & 1 \\ -1 & 0 \\ 0 & -1 \end{bmatrix}, U = \begin{bmatrix} 1.25 \\ -1 \end{bmatrix}, P = \begin{bmatrix} 10 \\ -10 \end{bmatrix}, N = \begin{bmatrix} 10 \\ -10 \end{bmatrix},$$

corresponding to $-1 \leq x_1 \leq 1.25$, $|x_2| \leq 1$, $-1 \leq u \leq 0.8$, $|p| \leq 0.1$, and $|\eta| \leq 0.1$, respectively. The matrices C and D_η related to output equation (18) will be defined in the sequel, depending if the used control law is ST-SF or ST-OF.

In the optimization problems (59) and (76), f_ℓ and φ_ℓ are tuned such that each element of the positive definite variables is bounded in the interval $[0,\ 100]$, each element of R, K is in $[-100,\ 100]$, and each element of J is in $[-1000,\ 1000]$. The optimizations (59) and (76) have been written in the AMPL language (FOURER et al., 2003) and solved with KNITRO (BYRD et al., 2006). Please note that by using KNITRO, we have obtained an optimal solution that can be considered halfway between a local and a global optimum. This is obtained by applying a local solver (Interior/CG algorithm) starting from multiple initial guesses properly covering the decision space.

3.5.1 State-feedback controller

In this subsection, we assume a scenario where the entire state vector can be measured with some bounded errors, i.e., $C = I_2$ and $D_\eta = \begin{bmatrix} 1 & 1 \end{bmatrix}^T$. Therefore, in this particular setup, the proposed strategy is a ST-SF controller (see Remark 9).

The ST-SF controller is offline designed considering $\bar{t} = 4$ auxiliary constraints (74), where the normalized vectors v_t point towards the vertices of the state constraints set $\mathcal{X}$.

Step i	K_i	$\mathcal{L}_i$ Area	$\mathcal{J}_i$
0	[-0.4805 -0.5000]	0.2584	1.2887
1	[-0.4967 -0.4966]	0.7330	2.6329
2	[-0.8407 -0.4966]	1.8310	3.4379
3	[-0.5032 -0.1955]	2.9355	4.4746
4	[-0.2088 -0.4665]	3.7965	5.0647
5	[-0.2250 -0.3861]	4.4456	5.8774
6	[-0.1772 -0.4914]	4.5000	6.0299

Table 9 – ST-OF, offline design for $r_i = 3$ and $\bar{t} = 4$.

Furthermore, the auxiliary polyhedral sets R_i in (44) are such that $r_i = 3, \forall\, i$. By following the offline steps indicated in Algorithm 1, $\bar{N} = 6$ pairs $(K_i, \mathcal{L}_i)$ have been computed, see Table 9. Moreover, in the Table 9, it is possible to note that the cost function $\mathcal{J}_i$ and area of the polyhedral sets, namely "$\mathcal{L}_i$ area," monotonically increase with i while the $\|K_i\|_\infty$ decreases. In Fig. 14, the obtained ROSC sets $\mathcal{L}_i$ are plotted, showing that their union covers the entire admissible state constraint regions $\mathcal{X}$. Moreover, in the same figure, we have shown (using a black dashed dot (-.) line) the plant's state trajectory evolution applying the proposed controller (using the switching rule (36)) starting from an initial condition $x_0 = [1.25, -1]^T \in \mathcal{L}_6$ (i.e., $i_0 = 6$). The obtained results show that in 5-step the state enters the terminal RPI region, i.e. $x_5 \in \mathcal{L}_0$, where it remains confined despite the presence of process and measurement bounded noises. Such a result is compatible with the theoretical worst-case convergence time equals to $i_0 = 6$ (see Proposition 4).

3.5.2 State-feedback: comparison

Here, the ST-SF controller performance are compared with the dual-mode state-feedback controller proposed in Angeli et al. (2008). To provide a fair comparison, here we assume the absence of measurement noise ($\eta_k = 0, \forall\, k$ as assumed in Angeli et al. (2008)). Moreover for Angeli et al. (2008), exact polyhedral robust one-step controllable sets are computed (BORRELLI et al., 2017). Furthermore, the same terminal RPI set $\mathcal{L}_0$ is used in the offline computations of both strategies, and the online simulation has been repeated 1000 times considering different noise realizations and different initial states x_0 belonging to the two outermost ROSC sets.

The obtained results are summarized in Table 10. First, it is possible to note that a slightly smaller number of ROSC sets is computed in (ANGELI et al., 2008) to cover $\mathcal{X}$. The latter finds justification in the fact that for (ANGELI et al., 2008) we have computed, at each step, the biggest controllable sets, while in the proposed approach, we impose the further constraint that $\mathcal{L}_i$ is an admissible ROSC set if and only if each $x \in \mathcal{L}_i$ is one-step controllable to $\mathcal{L}_{i-1}$ under the same admissible control gain K_i. This also justifies why in our solution, the convergence of x_k to $\mathcal{L}_0$, requires, on average, a slightly bigger number of steps (5 using (35), 3.90 using (36), and 3.04 in (ANGELI et al., 2008)). This can also

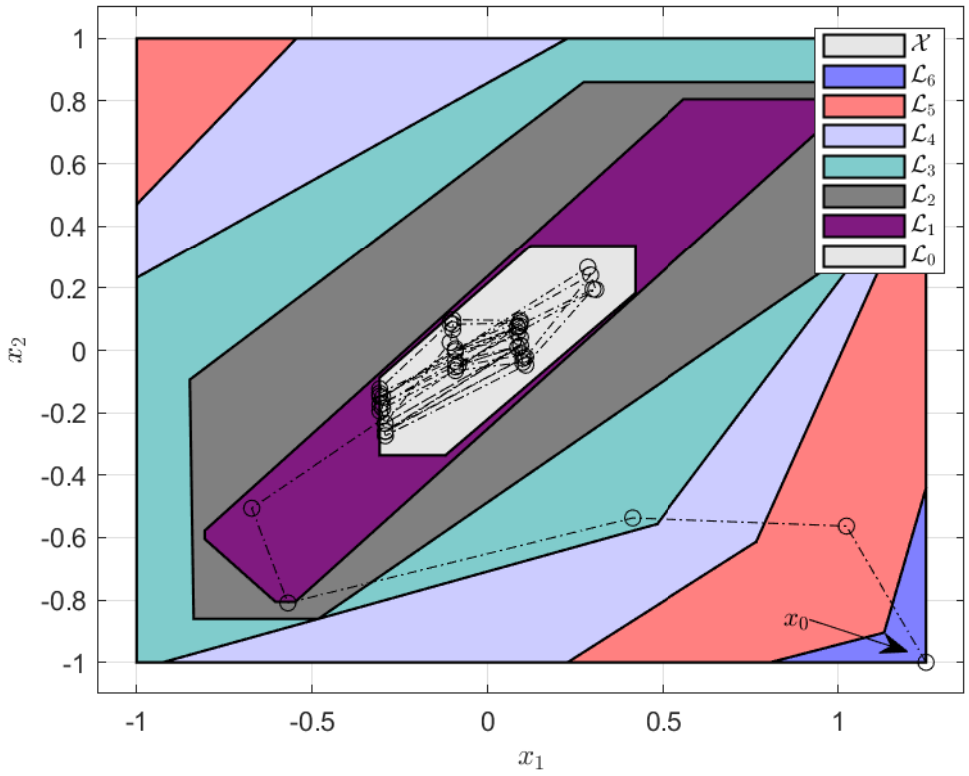

Figure 14 – ST-SF: ROSC sets and state trajectory evolution from $x_0 = [1.25, -1]^T$.

	Avg. CPU time [s] until $x_k \in \mathcal{L}_0$	$\bar{N}$	Avg. steps to $\mathcal{L}_0$
Alg. 1 with (35)	5.9770e-07	6	5.00
Alg. 1 with (36)	2.8134e-05	6	3.90
(ANGELI et al., 2008)	0.05s	5	3.04

Table 10 – State feedback control: proposed solution vs (ANGELI et al., 2008).

be noted in Fig. 15, where the state trajectory for a single initial condition is reported. On the other hand, the proposed solution outperforms (ANGELI et al., 2008) in terms of the average computation time needed to online compute the control action. The latter is justified by the fact that contrary to (ANGELI et al., 2008), the proposed approach offline computes also the controller gain K_i, so making the strategy better suited for strict real-time control system contexts or where limited computational capabilities are available. Last but not least, differently from our approach, the solution in (ANGELI et al., 2008) cannot be used if the entire state vector cannot be measured.

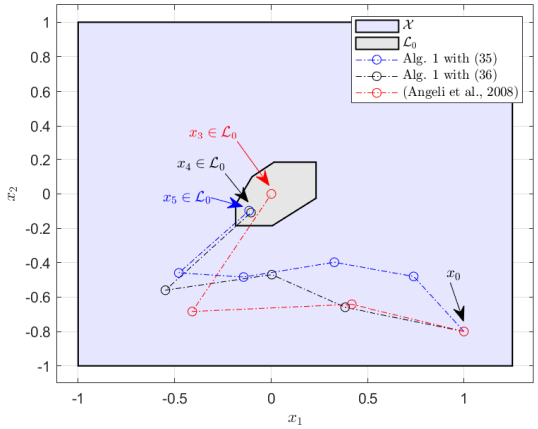

Figure 15 – State trajectory for $x_0 = [1, -0.8]^T$, under state-feedback control, and until the RCI region $\mathcal{L}_0$ is reached: proposed solution vs (ANGELI et al., 2008).

3.5.3 Output feedback controller

In this subsection, we assume that only a noisy version of the first state x_1 can be measured. In particular, $C = \begin{bmatrix} 1 & 0 \end{bmatrix}$ and $D_\eta = 1$. In Table 11, the results of the offline computation of the ROSC sets are reported for two different choices of the design parameters $(\bar{t}, r_i)$. In the first, we have used $(\bar{t} = 4, r_i = 3)$ (as in the state-feedback case) while, in the second $(\bar{t} = 8, r_i = 4)$, four more additional normalized vectors v_i, each one of them orthogonal to one face of $\mathcal{X}$, and one more face in $\mathcal{R}_i$, have been added. From the obtained results, it is possible to note that a bigger Domain of Atraction (DoA) (i.e., the maximum area of $\mathcal{L}_i$) is obtained for $(8, 4)$. This result finds justification in the fact that a bigger r_i, implies ROSC sets with more degrees of freedom, and, as a consequence, that bigger approximations of the admissible robust one-step controllable set can be in principle found. Moreover, in both setups, the stopping condition (77) is reached ($\bar{N} = 8$ for $(4, 3)$ and $\bar{N} = 6$ for $(8, 4)$) when the ROSC sets do not entirely cover $\mathcal{X}$, see, e.g., the DoA obtained for $(8, 4)$ in Fig. 16. Finally, the black dashed dot (-.) line in Fig. 16, representing the state-trajectory under ST-SOF (for $x_0 = [1.25, -1]^T \in \mathcal{L}_8$), confirms that the proposed output controller can robustly steer, is a finite number of steps (by design ≤ 8), the state vector inside the RPI region $\mathcal{L}_0$.

3.5.4 ST-OF - Comparison

Here, we contrast our approach with the output feedback controller proposed in De Almeida and Dorea (2020). [1]

The solution in De Almeida and Dorea (2020), besides an *off-line* design phase, requires the *on-line* computation of a static output control action $u_k = f(y_k)$ at each sampling-time by solving an LP problem. Thus, using the approach described in Section

[1] We acknowledge the help of the authors, especially in the code implementation

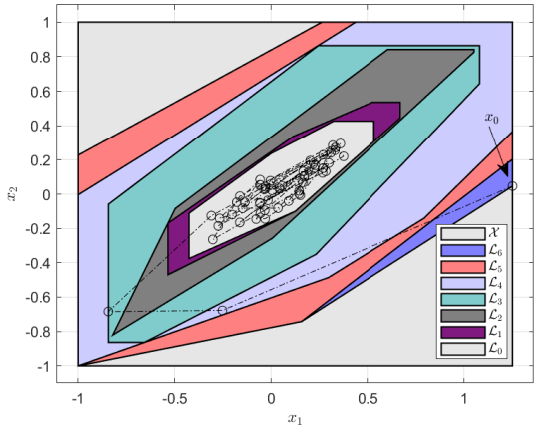

Figure 16 – ST-OF: DoA for $(\bar{t} = 8,\ r = 4,)$, and state trajectory for $x_0 = [1.25,\ 0.047]^T \in \mathcal{L}_6$.

$(\bar{t},\ r)$	Step i	K_i	$\mathcal{L}_i$ Area	$\mathcal{J}_i$
(4,3)	0	[-0.7500]	0.2933	1.4556
	1	[-0.7713]	0.3231	1.5591
	2	[-0.8232]	0.4678	2.0250
	3	[-0.8575]	0.9319	3.0014
	4	[-0.8156]	1.7325	3.6051
	5	[-0.7139]	2.4063	4.2004
	6	[-0.6241]	2.9448	4.4577
	7	[-0.6241]	3.0124	4.4670
	8	[-0.6241]	3.0415	4.4676
(8,4)	0	[-0.7500]	0.3120	2.3466
	1	[-0.7803]	0.4054	2.7227
	2	[-0.8686]	0.7949	4.1941
	3	[-0.8476]	1.7372	5.9305
	4	[-0.6979]	2.5962	7.3990
	5	[-0.6111]	3.0652	8.0587
	6	[-0.6111]	3.1510	8.2741

Table 11 – ST-OF, offline design.

III of De Almeida and Dorea (2020), we find the OFCI-set $\mathcal{L}_{AD} = \{x : L_{AD}x \leq 1\}$ with complexity $r_{AD} = 7$ and Area = 2.4837, painted with green color in Figure 17.

The sets $\mathcal{L}_6$ and $\mathcal{L}_0$, from Table 11 with $r_i = 4$ and $\bar{t} = 8$, are illustrated in blue and gray in Figure 17, showing that the $\mathcal{L}_6$ is 26.87% bigger than the one obtained by De Almeida and Dorea (2020) and illustrating our ultimate-bounded set $\mathcal{L}_0$.

3.6 CONCLUSION

In this chapter, a novel output feedback controller for constrained linear systems subject to bounded process and measurement noises has been presented. The proposed solution exploits the extended Farkas' lemma and controllability and set invariance argu-

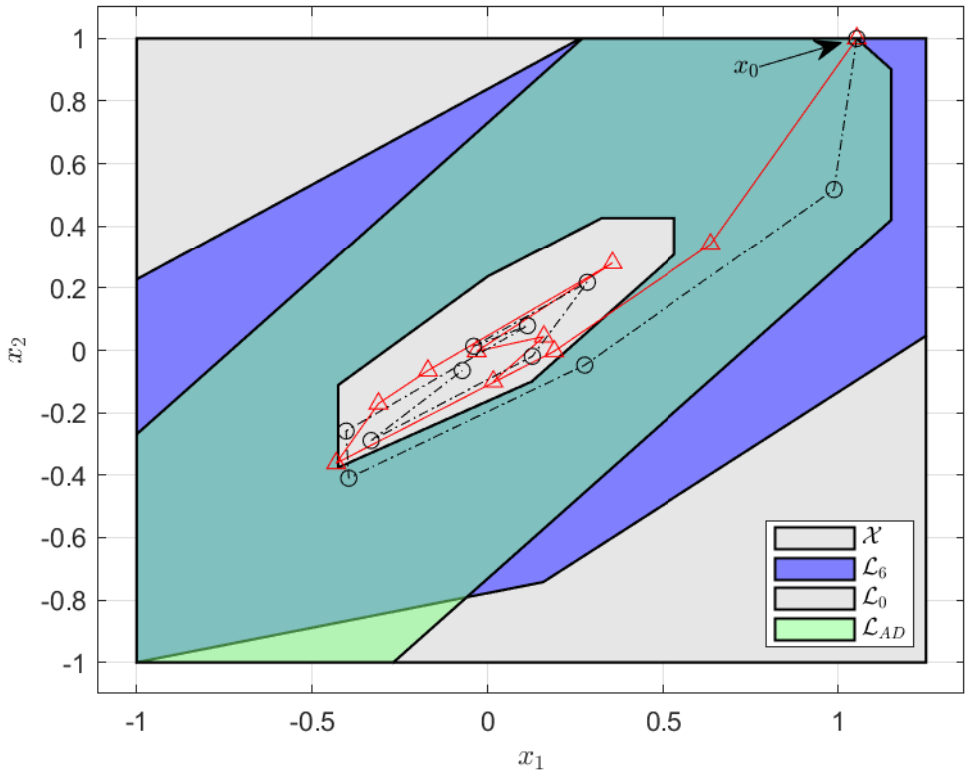

Figure 17 – DoA and state trajectory: ST-OF vs De Almeida and Dorea (2020).

ments to offline design, by means of bilinear optimizations, a family of robust switching static output feedback controllers and associated domain of attraction. Such information are online leveraged to efficiently compute admissible and robust control actions. The properties of the proposed strategy have been formally proved and verified through numerical comparisons with two alternative schemes.

4 INCREMENTAL OUTPUT FEEDBACK DESIGN APPROACH FOR LPV SYSTEMS WITH RATE CONTROL CONSTRAINTS

In this chapter, the proposed solution to an LPV-constrained stabilization problem subject to control-rate limits is built up on the description of the LPV control system in the extended state space composed of the system's state and control variables, also used in Blanchini and Miani (2015) and Da Silva et al. (2008), in which the control variations act as the control inputs; see also Remark 3. From this extended LPV formulation, we use the known necessary and sufficient algebraic conditions for positive-invariance and contractivity of polyhedral sets (BLANCHINI; MIANI, 2015) to propose a design procedure based on a bilinear optimization problem.

It is remarkable that the proposed design approach avoids the product among the parameter-varying matrices that appear in Dórea et al. (2020), allowing the simultaneous computation of the closed-loop positively-invariant set and an LPV output-feedback control law, and deals with non-symmetrical constraints. Also, more control degrees of freedom appear because the control law feeds back not only the plant outputs but also the control variables. Furthermore, the considered objective function optimizes the size of the associated polyhedral set in given directions. Once more, KNITRO is the chosen solver to tackle the present bilinearities.

This chapter is divided into four sections, the first one presenting the problem we want to solve. Section 4.2 tackles the incremental output feedback design approach for discrete-time parameter-varying systems with amplitude and rate control constraints, following the results published in Ernesto et al. (2021). Next, we present an alternative formulation where the state and control constraints directly help construct the positive invariant sets, as proposed in Ernesto et al. (2022). Finally, we present some conclusions about the chapter.

4.1 PROBLEM PRESENTATION

Consider the plant represented by a linear parameter-varying (LPV) discrete-time system, given by

$$x_{k+1} = A(\alpha_k)x_k + B(\alpha_k)u_k \tag{78a}$$

$$y_k = Cx_k \tag{78b}$$

where $k \in \mathbb{N}$, $x_k \in \mathbb{R}^n$ is the state vector, $u_k \in \mathbb{R}^m$ is the control input, and $y_k \in \mathbb{R}^p$ is the measured output, $C \in \mathbb{R}^{p\times n}$ and

$$\begin{bmatrix} A(\alpha_k) & B(\alpha_k) \end{bmatrix} = \sum_{i=1}^{N} \alpha_{i,k} \begin{bmatrix} A_i & B_i \end{bmatrix}, \tag{79}$$

with $A_i \in \mathbb{R}^{n\times n}$ and $B_i \in \mathbb{R}^{n\times m}$, for $i = 1,\ldots,N$. The varying parameters $\alpha_{i,k} \in \mathcal{S} = \{\alpha_k \in \mathbb{R} : \alpha_{i,k} \geq 0, \sum_{i=1}^{s} \alpha_{i,k} = 1\}$, are supposed to be measured or computed in real-time.

The plant is subject to state constraints, control amplitude limits, and bounds of the control-rate variation $\delta u_k = u_k - u_{k-1}$, represented, respectively, by the closed polyhedral sets

$$\mathcal{X} = \{x_k : Xx_k \leq \mathbf{1}_{l_x}\},\ X \in \mathbb{R}^{l_x\times n}, \tag{80a}$$

$$\mathcal{U} = \{u_k : Uu_k \leq \mathbf{1}_{l_u}\},\ U \in \mathbb{R}^{l_u\times m}, \tag{80b}$$

$$\mathcal{D} = \{\delta u_k : D\delta u_k \leq \mathbf{1}_{l_u}\},\ D \in \mathbb{R}^{l_d\times m}. \tag{80c}$$

The primary control objective is to guarantee local (regional) asymptotic closed-loop stability while respecting the constraints given above. To this end, we consider an incremental LPV output-feedback control law,

$$u_{k+1} = u_k + \delta u_k,\ \text{with } \delta u_k := f(y_k, u_k, \alpha_k) \tag{81}$$

and such that the control variation obeys

$$\delta u_k = \begin{bmatrix} K(\alpha_k) & \bar{K}(\alpha_k)\end{bmatrix}\begin{bmatrix} y_k \\ u_k\end{bmatrix} \tag{82a}$$

$$= \sum_{i=1}^{N} \alpha_{i,k}\begin{bmatrix} K_i & \bar{K}_i\end{bmatrix}\begin{bmatrix} y_k \\ u_k\end{bmatrix}, \tag{82b}$$

where $K_i \in \mathbb{R}^{m\times p}$ and $\bar{K}_i \in \mathbb{R}^{m\times m}$.

From the feedback of the plant (78) by the incremental feedback control law (81) with the control variation (82), we obtain an LPV closed-loop system that reads

$$\begin{bmatrix} x_{k+1} \\ u_{k+1}\end{bmatrix} = \underbrace{\begin{bmatrix} A(\alpha_k) & B(\alpha_k) \\ K(\alpha_k) & I_m + \bar{K}(\alpha_k)\end{bmatrix}}_{A^{cl}(\alpha_k)}\begin{bmatrix} x_k \\ u_k\end{bmatrix}, \tag{83}$$

where, by construction,

$$A^{cl}(\alpha_k) = \sum_{i=1}^{N} \alpha_{i,k} A_i^{cl} = \sum_{i=1}^{N} \alpha_{i,k}\begin{bmatrix} A_i & B_i \\ K_i & I_m + \bar{K}_i\end{bmatrix}. \tag{84}$$

Thus, let us define the closed-loop state-vector

$$\xi_k = \begin{bmatrix} x_k^T & u_k^T\end{bmatrix}^T \in \mathbb{R}^{n_{cl}},\ n_{cl} = n + m.$$

To deal with the state constraints and input amplitude limits in the closed-loop state-space, from (80a) and (80b), we define the following augmented set

$$\mathcal{X}^{cl} = \left\{\xi_k : X^{cl}\xi_k \leq \mathbf{1}_{l_{cl}}\right\},\ X^{cl} = \begin{bmatrix} X & 0 \\ 0 & U\end{bmatrix} \in \mathbb{R}^{l_{cl}\times n_{cl}}. \tag{85}$$

Furthermore, to guarantee the satisfaction of the bounds of the control-rate variation, the following condition obtained from (80c) and (82) has to be fulfilled for every $\alpha_k \in \mathcal{S}$:

$$\mathcal{D}^{cl}(\alpha_k) = \left\{ \xi_k : D \begin{bmatrix} K(\alpha_k)C & \bar{K}(\alpha_k) \end{bmatrix} \xi_k \leq \mathbf{1}_{l_d} \right\}. \tag{86}$$

More specifically, we are interested in solving the following constrained control problem.

Problem 2 Given the plant (78), compute control gains $K_i(\alpha_k)$ and $\bar{K}_i(\alpha_k)$ in (82), and determine a set $\mathcal{L} \in \mathbb{R}^{n_{cl}}$ such that for any initial condition $\xi_0 \in \mathcal{L}$ the corresponding trajectory of the closed-loop system (83) converges asymptotically to the origin without leaving $\mathcal{X}^{cl}$ in (85), and fulfilling $\mathcal{D}^{cl}(\alpha_k)$ in (86).

Possible solutions to Problem 2 might be based on imposing the positive-invariance and contractivity to a compact convex (C)-set $\mathcal{L} \in \mathbb{R}^{n_{cl}}$ such that $\mathcal{L} \subseteq (\mathcal{X}^{cl} \cap \mathcal{D}^{cl}(\alpha_k))$. Notice that, by definition, any C-set $\mathcal{L} \in \mathbb{R}^{n_{cl}}$ is a positive invariant set of system (83), if every trajectory starting at $\mathcal{L}$ remains in $\mathcal{L}$ for every $t \geq 0$ and for any $\alpha_k \in \mathcal{S}$. In addition, if the origin is contained within, the set $\mathcal{L}$ is contractive if $\tau\mathcal{L}$ is also positive invariant for any value $\tau \in \mathbb{R}^+$ in the interval $[0\ ,\ 1)$. Therefore, because the considered convex polyhedral set $\mathcal{L} \subseteq (\mathcal{X}^{cl} \cap \mathcal{D}^{cl}(\alpha_k))$ is compact and contains the origin inside, its positive-invariance with contraction guarantees local asymptotic stability to the origin for all trajectories of system (83) that start at $\mathcal{L}$. Thus, we also pursue the control objective of obtaining this set *as large as possible*, for instance, following the guidelines introduced later. Finally, the considered approach fulfills the control constraints by avoiding saturation, thus guaranteeing the LPV dynamical behavior regionally inside the positive invariant and contractive set $\mathcal{L}$.

Remark 13 The LPV plant model (78) can be viewed as N linear dynamical systems, each one represented from a pair (A_i, B_i), that are combined through the varying-parameters in α_k. Such a model allows representing different parameter-varying phenomena and incorporating the system's nonlinear dynamics that depend on the measured output variable y_k, trough the so-called Fuzzy/*Quasi*-LPV representation. In this case we have $\alpha_k = \alpha(y_k)$, which allows to implement the proposed parameter-varying control-law. Furthermore, the set of state constraints, $\mathcal{X}$, can be used to represent the *region of validity* for Fuzzy/*Quasi*-LPV representation (see (KLUG et al., 2015b)).

Remark 14 Linear time-invariant (LTI) discrete-time systems can be viewed as the particular case where $N = 1$ in the LPV model (78). Thus, for plants represented by LTI models, the proposed control-law has fixed gain matrices K and $\bar{K}$.

4.2 INCREMENTAL OUTPUT FEEDBACK DESIGN APPROACH FOR LPV SYSTEMS WITH RATE CONTROL CONSTRAINTS

In this section, the first possible solution to the Problem 2 is discussed, in which we aim to impose the closed-loop positive-invariance and contractivity to a compact polyhedral set $\mathcal{L} \in \mathbb{R}^{n_{cl}}$,

$$\mathcal{L} = \{\xi_k : L\xi_k \leq \mathbf{1}_{l_r}\}, \tag{87}$$

where $L \in \mathbb{R}^{l_r \times n_{cl}}$, $l_r > n_{cl}$ is the *set complexity*, and $rank(L) = n_{cl}$. By definition, the origin of $\mathbb{R}^{n_{cl}}$ belongs to the interior of $\mathcal{L}$. Notice that $\mathcal{L}$ may have some redundant constraints. Thus, the *set complexity* l_r defines a bound for the maximum number of faces of the polyhedron.

4.2.1 Algebraic Conditions

Now, we state the necessary and sufficient algebraic conditions that allow solving Problem 2 and determining a contractive positive-invariant polyhedron $\mathcal{L}$, with prespecified *complexity*.

Theorem 1 For a given plant represented by an LPV-system (78)-(79), with associated constraints (80), Problem 2 admits a solution formed by control gains K_i and $\bar{K}_i$ in (82), and a positive invariant and contractive polyhedral set $\mathcal{L}$ in (87), with contraction factor $\lambda \in [0\,,\,1)$ and *complexity* $l_r > n_{cl}$, if and only if there exist matrices $L_x \in \mathbb{R}^{l_r \times n}$, $L_u \in \mathbb{R}^{l_r \times m}$ and $J \in \mathbb{R}^{n_{cl} \times l_r}$, and nonnegative matrices $H_i \in \mathbb{R}^{l_r \times l_r}$, $M \in \mathbb{R}^{l_{cl} \times l_r}$ and $Q_i \in \mathbb{R}^{l_d} \times l_r$ such that the following conditions are verified, for all $i = 1, \ldots, N$,

$$H_i \begin{bmatrix} L_x & L_u \end{bmatrix} = \begin{bmatrix} L_x & L_u \end{bmatrix} \begin{bmatrix} A_i & B_i \\ K_i C & I_m + \bar{K}_i \end{bmatrix}, \tag{88a}$$

$$H_i \mathbf{1}_{l_r} \leq \lambda \mathbf{1}_{l_r}, \tag{88b}$$

$$M \begin{bmatrix} L_x & L_u \end{bmatrix} = \begin{bmatrix} X & 0 \\ 0 & U \end{bmatrix}, \tag{89a}$$

$$M \mathbf{1}_{l_r} \leq \mathbf{1}_{l_{cl}}, \tag{89b}$$

$$Q_i \begin{bmatrix} L_x & L_u \end{bmatrix} = D \begin{bmatrix} K_i C & \bar{K}_i \end{bmatrix}, \tag{90a}$$

$$Q_i \mathbf{1}_{l_r} \leq \mathbf{1}_{l_d}, \tag{90b}$$

$$J \begin{bmatrix} L_x & L_u \end{bmatrix} = I_{n_{cl}}. \tag{91}$$

Proof: In conditions (88)-(91), consider $L = \begin{bmatrix} L_x & L_u \end{bmatrix}$, with corresponding set $\mathcal{L}$ in (87). Thus:

- the existence of non-negative matrix H_i and gain matrices K_i and $\bar{K}_i$, verifying the N equalities (88a) for the vertices of $A(\alpha_k)$, and such that N inequalities (88b) hold true for $0 \leq \lambda < 1$, is necessary and sufficient for $\mathcal{L}$ be a positive invariant set, with contraction factor λ, of the parameter varying system (83) (see Basílio EA Milani et al. (1996) and Blanchini and Miani (2015));

- from the Extended Farkas' Lemma (see Hennet (1995) and Blanchini and Miani (2015)), the existence of a non-negative matrix M verifying (89) is equivalent to the set inclusion $\mathcal{L} \subseteq \mathcal{X}^{cl}$;

- By convexity, (90) is equivalent to

$$Q(\alpha_k)\begin{bmatrix} L_x & L_u \end{bmatrix} = D\begin{bmatrix} K_1(\alpha_k)C & K_1(\alpha_k) \end{bmatrix}, \tag{92a}$$

$$Q(\alpha_k)\mathbf{1}_{l_r} \leq \mathbf{1}_{l_d}, \tag{92b}$$

  where $Q(\alpha_k) = \sum_{i=1}^{N} \alpha_{k,i} Q_i$ is a non-negative matrix for all $\alpha_k \in \mathcal{S}$. Thus, using again the Extended Farkas' Lemma, this is equivalent to the fulfillment of $\mathcal{L} \subseteq \mathcal{D}(\alpha_k)$; and

- the existence of J such that (91) holds, is equivalent to $rank(L) = n_{cl}$ since, by hypothesis, $l_r > n_{cl}$, meaning that J is the pseudo-inverse matrix of L. □

4.2.2 Bilinear Programming Design Approach

The proposed solution to Problem 2, given by Theorem 1, carries some products among pairs of matrix variables, such as $H_i L_x$, $H_i L_u$, LK_i and $L_u K_{1i}$ in (88a), as well as other similar bilinear products in (89a)-(91). These products can be appropriately considered as design constraints, and adapted nonlinear optimization techniques can be used to solve Problem 2 (see Brião et al. (2018) and França et al. (2021)).

The proposed optimization strategy is to enlarge the size of the set of initial admissible conditions $\mathcal{L}$ along with some directions in $\mathbb{R}^{n_{cl}}$ while minimizing the rate of contractivity. For this purpose, the set of directions is defined by

$$\mathcal{V} = \{\gamma_j \upsilon_j, j = 1, \ldots, \bar{j}\},$$

where $\upsilon_j \in \mathbb{R}^{n_{cl}}$ are given vectors and $0 < \gamma_t \in \mathbb{R}^{l_{cl}}$ are scaling factors to be optimized, such that the inclusion $\mathcal{V} \subseteq \mathcal{L}$ is satisfied or, equivalently:

$$\begin{bmatrix} L_x & L_u \end{bmatrix} \gamma_j \upsilon_j \leq 1\,,\ j = 1, \ldots, \bar{j}. \tag{93a}$$

Possible design choices for the set $\mathcal{V}$ are, for instance, a set of directions defined from the vertices of $\mathcal{X}^{cl}$, or a set of normalized directions, possibly equally spaced in the state-space, covering a significant number of directions for the optimization process.

Moreover, consider that the following design parameters are chosen *a priori*: *i)* allowed complexity (*i.e* maximum number of faces) for the invariant sets, by choosing $l_r > n_{cl}$; and *ii)* $\bar{t}$ directions v_t used to enlarge $\mathcal{L}$. Thus, we propose the following bilinear optimization problem to find solutions to the design Problem 2:

$$\begin{aligned} &\underset{\Gamma(\cdot)}{\text{maximize}}\ \Phi(\gamma_j) = \sum_{j=1}^{\bar{j}} \gamma_j \\ &\text{subject to } (88) - (91) \\ &0 \leq \lambda < 1 \\ &f_\ell(\cdot) \leq \varphi_\ell, \quad \ell = 1, \ldots, \bar{\ell}, \end{aligned} \tag{94}$$

with $\Gamma(\cdot) = (H_i, L_x, L_u, K_i, \bar{K}_i, M, Q_i, J, J_u, \gamma_j, \lambda)$, where:

i) the proposed objective function $\Phi(\gamma_j)$ allows the maximization of the set $\mathcal{L}$ through the scaling factors γ_j associated to the directions in $\mathcal{V}$, by considering $\phi(\gamma_j) = \sum_{j=1}^{\bar{j}} \gamma_j$; notice that the optimization program (94) can provide different solutions to Problem 2 depending on the designer choices of $\mathcal{V}$ and l_r.

ii) the additional constraints, represented by $f_\ell(\cdot) \leq \varphi_\ell$, may be imposed on the decision variables for different purposes, including the numerical ones. To reduce the search space, thus promoting a more efficient search for solutions to the considered problem, we impose upper and lower bounds on the elements of the decision variables. These bounds are an essential strategy used in mathematical programming to deal with bilinear optimization problems. See Remark 4 in Chapter 2, also in Briao et al. (2021)

4.2.3 Numerical Examples

The examples below were solved using the KNITRO solver (BYRD et al., 2006), with the Interior/CG (barrier) algorithm, multistart option, and the other solver's default settings. Also, the following lower and upper bound pairs were assigned to each element of matrices or vectors:

$$\begin{aligned} J, J_u: &\quad [-10^3, 10^3] \\ H_i, M, Q_i: &\quad [0, 10^2] \\ K_i, K_{1i}, L_x, L_u, : &\quad [-10, 10] \\ \gamma_j: &\quad [0, 10] \end{aligned}$$

Example 1: Consider the following first-order discrete-time LTI system, obtained by the ZoH discretization, with sample time $ts = 0.05$, of the continuous-time system used in Blanchini and Miani (2015),

$$x(k+1) = 1.0513x(k) + 0.0513u(k), \tag{95}$$

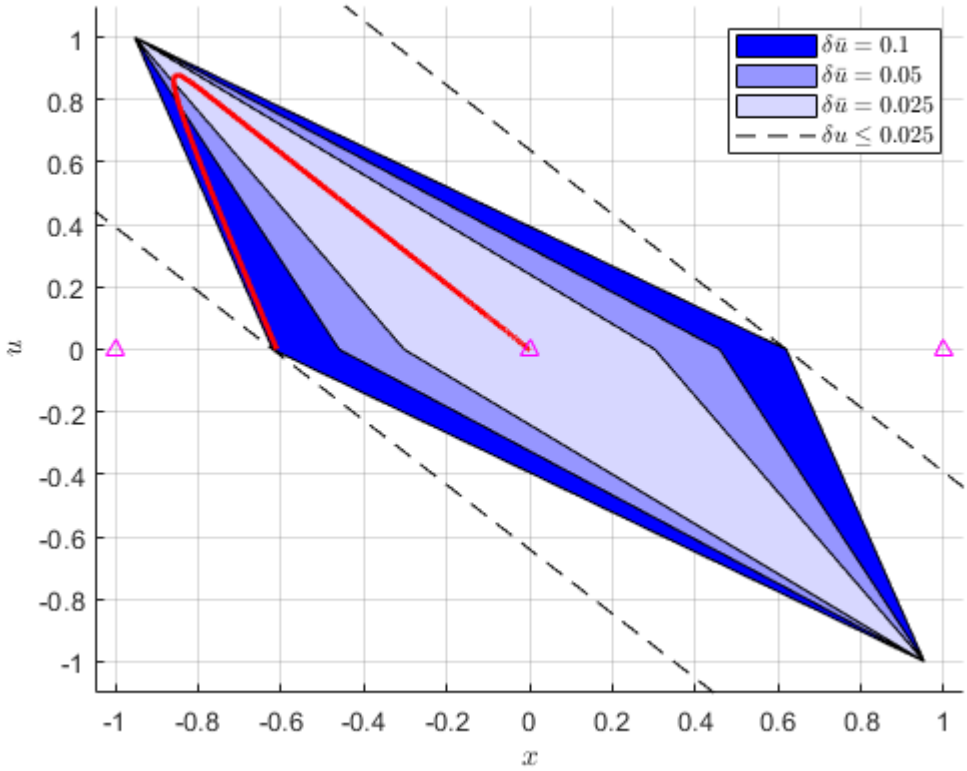

Figure 18 – Example 1: Discrete Sytem, $l_r = 4$

constrained by $|x_k| \leq 1$, $|u_k| \leq 1$ and $|\delta u| \leq \delta\bar{u}$, which imply the following matrices in (80):

$$X^T = \begin{bmatrix} 1 & -1 \end{bmatrix}, U^T = \begin{bmatrix} 1 & -1 \end{bmatrix}, D^T = \begin{bmatrix} 1/(\delta\bar{u}) & 1/(-\delta\bar{u}) \end{bmatrix}.$$

For the above LTI system, the control variation, (82), reads $\delta u_k = Kx_k + \bar{K}u_k$, where K and $\bar{K}$ are fixed scalar gains to be synthesized. To this end, we choose a big enough coefficient of contractivity, $\lambda = 0.9999 < 1$, the set complexity $l_r = 4$, and the directions $\upsilon_1^T = \begin{bmatrix} 1 & 0 \end{bmatrix}$ and $\upsilon_2^T = -\upsilon_1^T$, which allow maximizing the section of $\mathcal{L}$ on the plant state-space (in this case, a straight segment on the axis x_k). Thus, by considering three different bounds $\delta\bar{u}$ [1], and running the optimization problem (94), we obtained the results that are summarized by Figure 18 and Table 12.

In Figure 18, we draw in blue color the three obtained sets $\mathcal{L}$, whose respective areas and associated control gains are reported in Table 12. It is worth mentioning that in the three cases, the given areas closely approach the lengths of the segments on the x axis. Thus, we can conclude that the more significant the allowed control variation bound, the more important the set of initial conditions x_0 and u_0. Considering $u_0 = 0$, the allowable initial states are the mentioned segment, maximized from the directions υ_1 and υ_2.

[1] the values are equivalent to $\delta\bar{u} = 2, 1$ and 0.5 used in Blanchini and Miani (2015)

Table 12 – Example 1: Control gains and Area of obtained polyhedra

$\delta\bar{u}$	$[K\ K_1]$	Area
0.1	[-0.16127 -0.15627]	1.2402
0.05	[-0.10883 -0.10627]	0.9189
0.025	[-0.08261 -0.08127]	0.6052

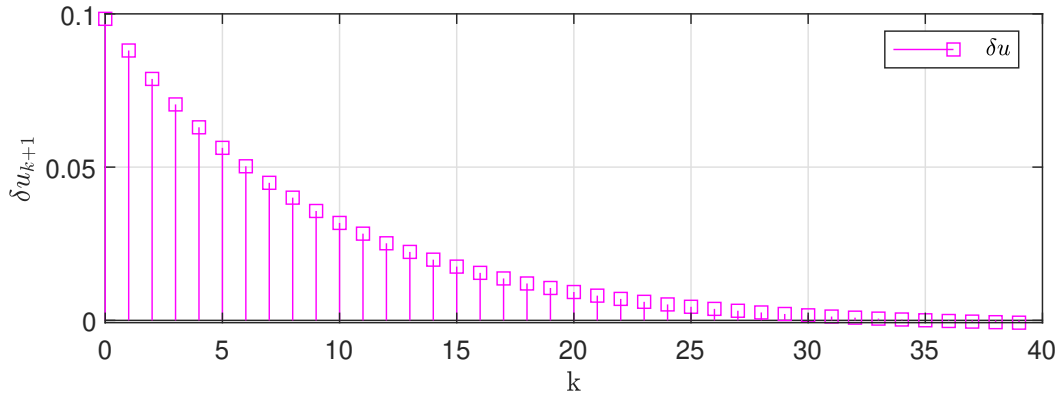

Figure 19 – Example 1: control rate - δu

Furthermore, in Figure 18 the dashed black lines represent the limits of the set $\mathcal{D}^{cl}$ (86), for $\delta\bar{u} = 0.1$, showing that the respective positive-invariant and contractive polyhedron $\mathcal{L}$ cope with the imposed inclusion conditions. Finally, the asymptotically stable trajectory depicted in red, which initiates in $x_{cl} = [-0.610]$, implies the control variation shown in Figure 19, which also verify the associated constraints without saturation, as expected.

Example 2: Now we consider the parameter varying system built from the continuous system in Blanchini and Miani (2015)

$$\dot{x}(t) = (1 + \rho(t)x(t) + (1 + \rho(t)u(t) \tag{96}$$

by considering the varying parameter $\rho(t) \in [-0.05, 0.05]$ and $\rho(t) \in [-0.1, 0.1]$. Using the sampling-time $T_s = 0.05$, we obtain the discrete-time plant model under the form (78) for the two different intervals, as shown in Table 13. Hence, they are subject to the same state and control constraints as in Example 1 and $\delta\bar{u} = 0.05$.

To design the associate parameter varying control laws, we considered the same settings as in the previous example. By running the optimization problem (94), we obtained the results that are summarized by Figure 20 and Table 14.

As in the Example 1 the areas closely match to the lengths of the segments on the x axis. It is also possible to notice a reduction in the polyhedron area as the parameter variance increases, from LPV model I to LPV model II, as shown in Table 14.

Example 3: Consider the 2nd-order discrete-time TS-fuzzy system, borrowed from

Table 13 – LPV plant models for Example 2

LPV model	Variation	A_i	B_i
I	$\pm$5%	$A_1 = \begin{bmatrix} 1.0486 \end{bmatrix}$ $A_2 = \begin{bmatrix} 1.0486 \end{bmatrix}$ $A_3 = \begin{bmatrix} 1.0539 \end{bmatrix}$ $A_4 = \begin{bmatrix} 1.0539 \end{bmatrix}$	$B_1 = \begin{bmatrix} 0.0486 \end{bmatrix}$ $B_2 = \begin{bmatrix} 0.0538 \end{bmatrix}$ $B_3 = \begin{bmatrix} 0.0488 \end{bmatrix}$ $B_4 = \begin{bmatrix} 0.0539 \end{bmatrix}$
II	$\pm$10%	$A_1 = \begin{bmatrix} 1.0460 \end{bmatrix}$ $A_2 = \begin{bmatrix} 1.0460 \end{bmatrix}$ $A_3 = \begin{bmatrix} 1.0565 \end{bmatrix}$ $A_4 = \begin{bmatrix} 1.0565 \end{bmatrix}$	$B_1 = \begin{bmatrix} 0.0460 \end{bmatrix}$ $B_2 = \begin{bmatrix} 0.0511 \end{bmatrix}$ $B_3 = \begin{bmatrix} 0.0463 \end{bmatrix}$ $B_4 = \begin{bmatrix} 0.0565 \end{bmatrix}$

Table 14 – Example 2 - Control gains and areas

System	i	$[K_i\ K_i]$	Area
(95)		[-0.10883 -0.10627]	0.9189
LPV I	1	[-0.11657 -0.11055]	0.8126
	2	[-0.11707 -0.11987]	
	3	[-0.12306 -0.10890]	
	4	[-0.12306 -0.11823]	
LPV II	1	[-0.12552 -0.11493]	0.7186
	2	[-0.12752 -0.13341]	
	3	[-0.13916 -0.11154]	
	4	[-0.13916 -0.13133]	

Guerra and Vermeiren (2004),

$$x_{k+1} = A(\alpha(y_k))x_k + B(\alpha(y_k))u_k \tag{97a}$$

$$y_k = \begin{bmatrix} 1 & 0 \end{bmatrix} x_k \tag{97b}$$

where $\alpha(y_k) = \begin{bmatrix} \alpha_1(y_k) \\ 1 + \alpha_1(y_k) \end{bmatrix}$, with $\alpha_1(y_k) =$, and

$$A_1 = \begin{bmatrix} 1 & -1 \\ -1 & -0.5 \end{bmatrix}, B_1 \begin{bmatrix} 6 \\ 2 \end{bmatrix}, A_2 = \begin{bmatrix} 1 & 1 \\ -1 & -0.5 \end{bmatrix}, B_2 = \begin{bmatrix} 4 \\ -2 \end{bmatrix}.$$

According to Remark 13, this quasi-LPV system exactly represents the nonlinear system (10) of Guerra and Vermeiren (2004) if $|x_{1k}| \leq 1$, which defines the set state-constraints $\mathcal{X}$, with $X^T = \begin{bmatrix} 1 & 0 & -1 & 0 \\ 0 & 0 & 0 & 0 \end{bmatrix}$. By also considering non-symmetric control constraints, $0.2 \leq u \leq 1$, and $|\delta u| \leq 0.2$, the matrices $U^T = \begin{bmatrix} 1 & -5 \end{bmatrix}$ and $D = \begin{bmatrix} 5 & -5 \end{bmatrix}$ give the remaining constraint sets in (89), $\mathcal{U}$ and $\mathcal{D}$.

In the sequel, we consider a state-feedback (SF) control law, which suppose that both states x_{1k} and x_{2k} are measured,

$$\delta u_k^{SF} = K(\alpha(y_k))x_k + \bar{K}(\alpha(y_k))u_k, \tag{98}$$

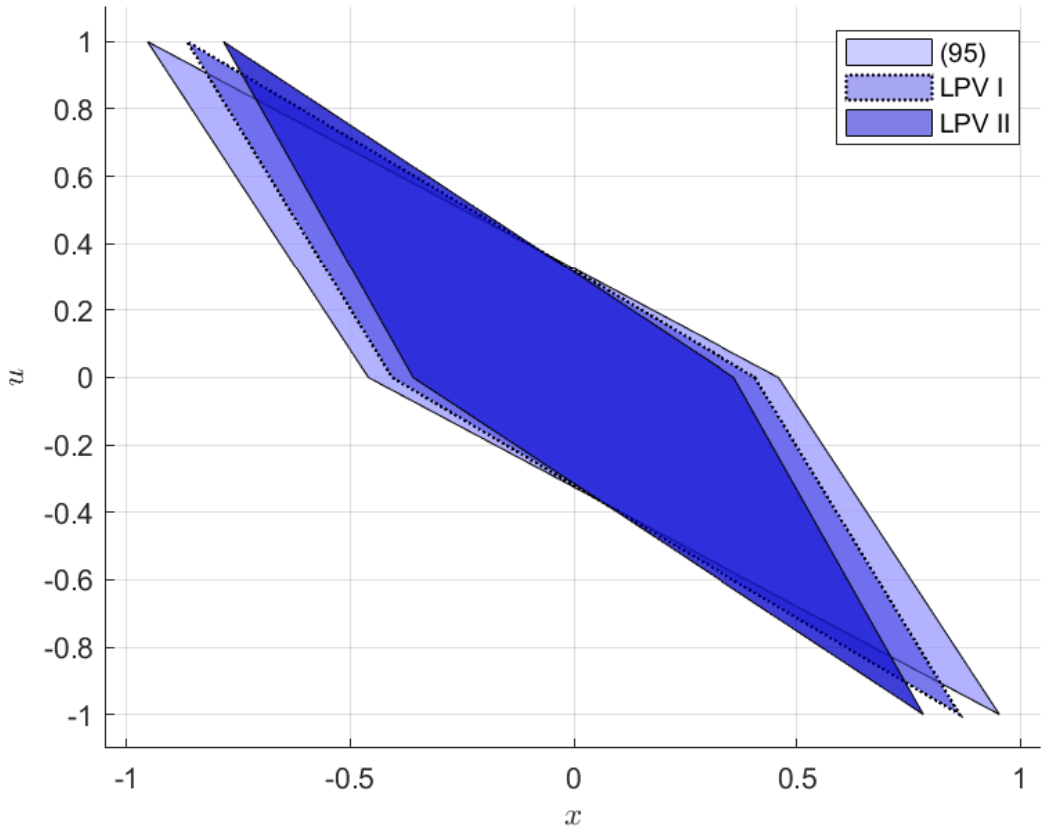

Figure 20 – Example 2 - Parameter Varying System, $r = 4$

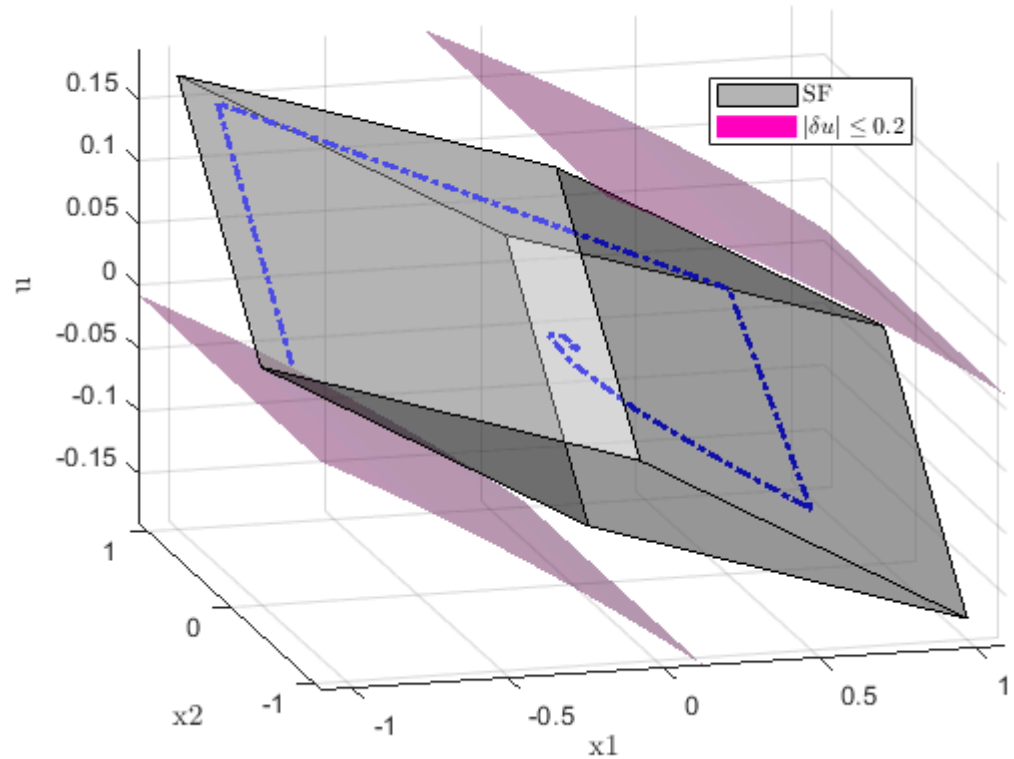

Figure 21 – Example 3: State Feedback

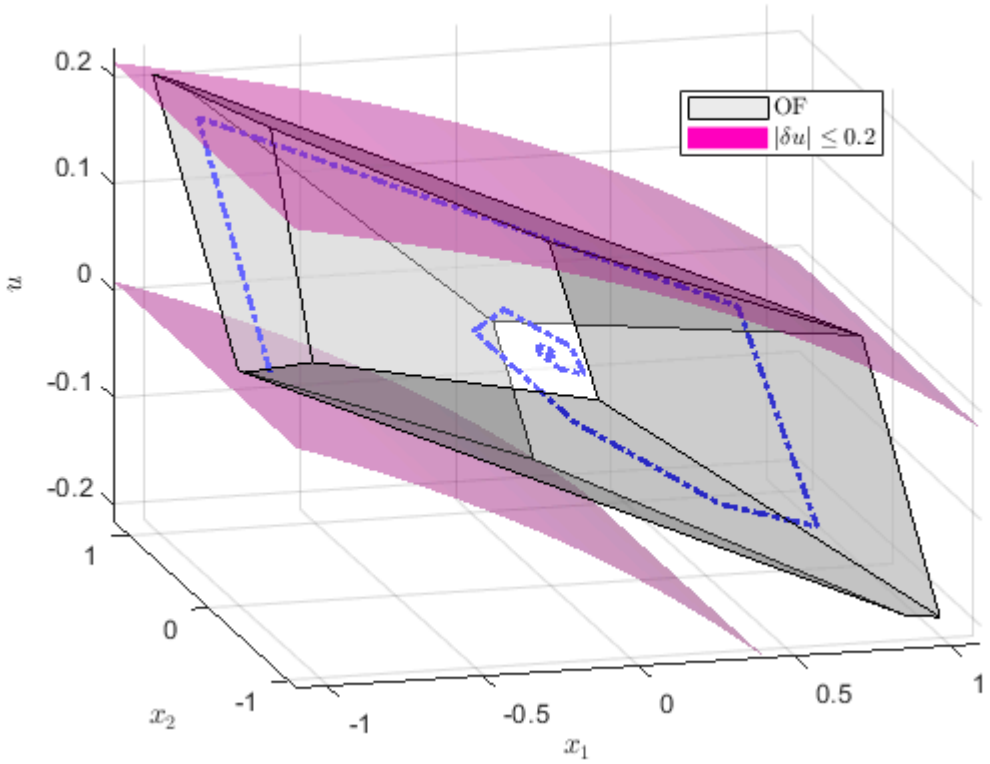

Figure 22 – Example 3: Static Output Feedback

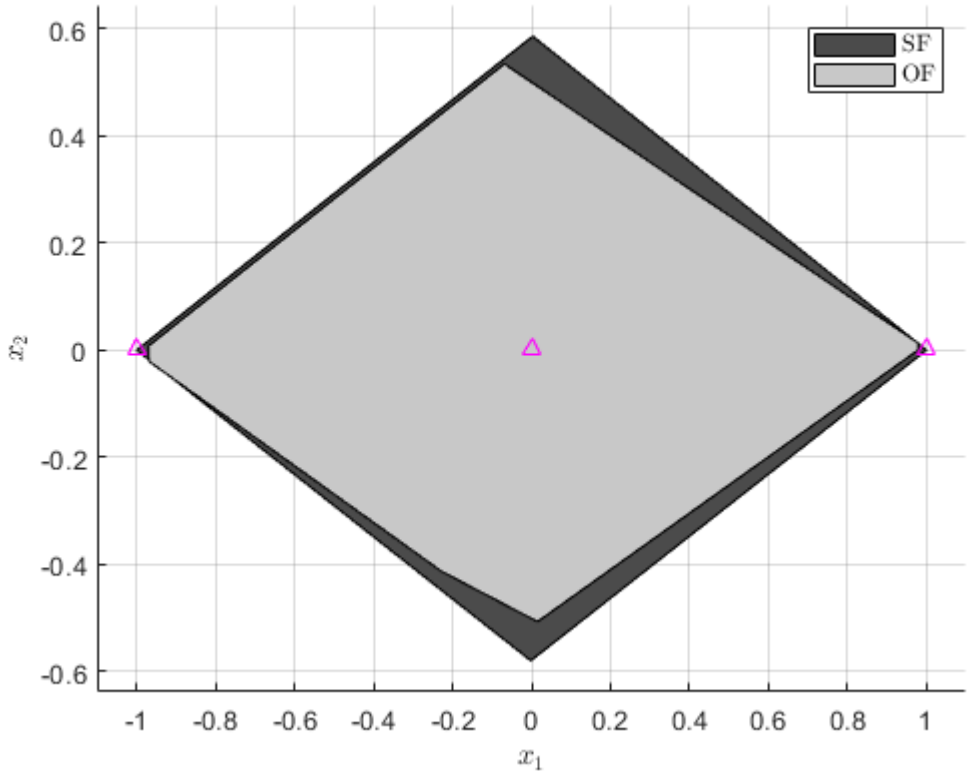

Figure 23 – Example 3: $u = 0$

Table 15 – Example 3

Control	i	$[K_i\ \bar{K}_i]$	Area	Volume
SF	1	[-0.17276 -0.02160 -1.01583]	1.1659	0.2018
	2	[-0.17276 -0.08657 -1.35999]		
OF	1	[-0.19582 -1.02778]	1.0481	0.1880
	2	[-0.19678 -1.91152]		

and an output-feedback (OF) control law, by considering that only the output $y_k = x_{1k}$ is measured,

$$\delta u_k^{OF} = K(\alpha(y_k))y_k + \bar{K}(\alpha(y_k))u_k, \tag{99}$$

The first column of Table 15 shows the control gains, computed using (94), using $l_r = 6$ for SF-design, and $l_r = 9$ for the OF-design. In both cases, we set $\lambda = 0.99999$. The other two table's columns show the volumes of the corresponding polyhedrons, and the areas of their sections on the plane-x_k. These sections, correspond to the set of admissible state initial conditions for $u_0 = 0$.

Table 16 – Example 3: Polyhedral Sets $\mathcal{L}$

Control	$\mathcal{L}$
SF	$\begin{bmatrix} 1.0000 & 0.9130 & 6.2704 \\ 1.0000 & 1.7014 & -9.8481 \\ -1.0000 & 1.7118 & -9.9084 \\ -1.0000 & -0.8993 & -6.3460 \\ 1.0000 & -1.7274 & 9.9990 \\ -1.0000 & -1.7214 & 9.9639 \end{bmatrix}$
OF	$\begin{bmatrix} 1.0216 & -1.9410 & 10.0000 \\ -0.9892 & -1.0894 & 5.7001 \\ -1.0173 & 1.7404 & -9.1087 \\ 1.0216 & 0.0208 & 9.6312 \\ -1.0313 & -0.0465 & -9.5469 \\ -0.7723 & -1.9944 & 10.0000 \\ 0.9946 & 1.9995 & -1.1876 \\ -0.9917 & -1.8733 & -0.4979 \\ 0.9784 & 1.9257 & -10.0000 \end{bmatrix}$

The two obtained positively-invariant and contractive polyhedrons are illustrated in Figures 21 and 22,the corresponding sets $\mathcal{L}$ is presented in Table 16 and the corresponding slices, obtained for $u_0 = 0$, are depicted in Figure 23. In the first two figures, we also show the surfaces that delimit the sets $\mathcal{D}(\alpha y_k)$, (86), which are depicted in magenta color. In the third figure, the sign Δ aims at representing the vectors v_1 and v_V, chosen to optimize the size in the direction of x_1, which is the constrained state. It can be observed that, for this example, the size of the slice obtained for OF-design is close to that of the SF-design.

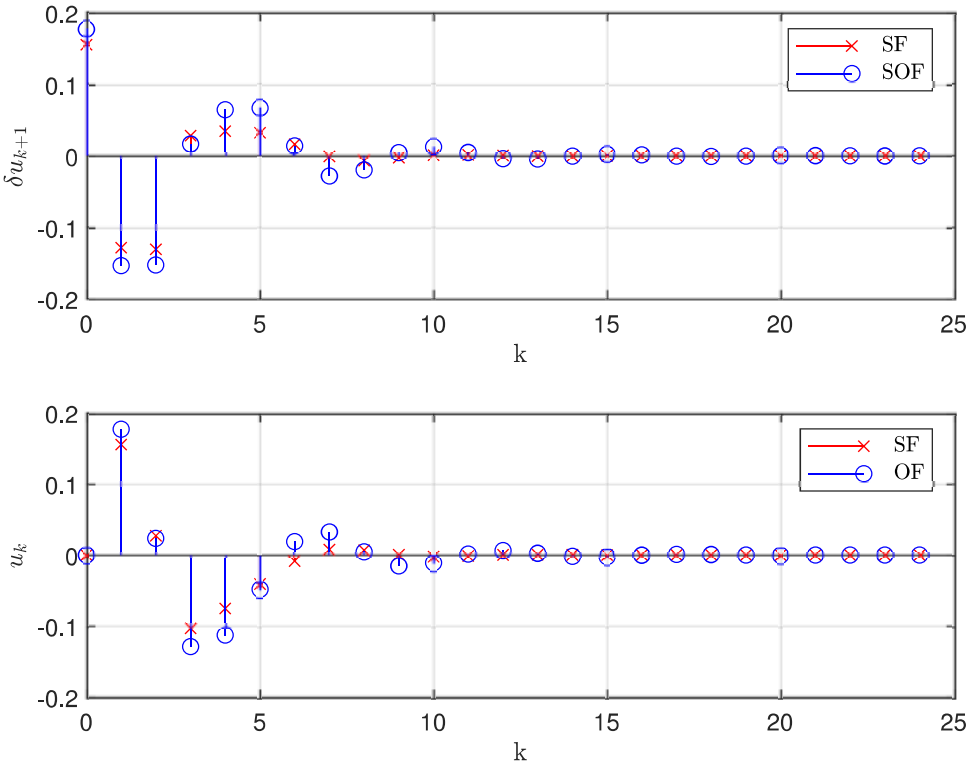

Figure 24 – Example 3: Control Signal - u and control rate - δu

Finally, the trajectories represented in dashed blue-line in Figures 21, 22 initiate at [–0.900], and remain inside the positive invariant sets. They imply the control variations and control trajectories shown in Figure 24, which respect associated constraints, as expected.

4.3 ALTERNATIVE IMPLEMENTATION TO AN INCREMENTAL OUTPUT-FEEDBACK DESIGN APPROACH

This section discusses an alternative implementation to solve the Problem 2 presented in Section 4.1, in which the state and control constraints help build the positive invariant sets. Following this context, we describe the alternative in which we impose the closed-loop positive-invariance and contractivity to a possibly compact polyhedral set $\mathcal{L}$,

$$\mathcal{L} = \{\xi_k : L\xi_k \leq \mathbf{1}_{l_r}\}, \tag{100}$$

where, by construction

$$L = \begin{bmatrix} R_x & R_u \\ \beta_x X & 0 \\ 0 & \beta_u U \end{bmatrix} \in \mathbb{R}^{l_r \times n_{cl}}, \tag{101}$$

with $l_r = (r + l_x + l_u) > n_{cl}$ being the *set complexity*, $rank(L) = n_{cl}$, and with the (scalar) scaling factors $\beta_x \geq 1$ and $\beta_u \geq 1$. With such a structured polyhedral invariant set, we

guarantee, in particular, the fulfillment of the state and control amplitude constraints as assured by the following lemma.

Lemma 2 *The set $\mathcal{L}$, defined by* (100) *and* (101)*, verifies the inclusion $\mathcal{L} \subseteq \mathcal{X}^{cl}$.*

Proof: The set $\mathcal{L}$ is the intersection of the closed polyhedral set $\mathcal{R}$,

$$\mathcal{R} = \{\xi_k \in \mathbb{R} : \begin{bmatrix} R_x & R_u \end{bmatrix} \xi_k \leq \mathbf{1}_r\}, \tag{102}$$

with $R_x \in \mathbb{R}^{r\times n}$ and $R_u \in \mathbb{R}^{r\times m}$, and the scaled augmented state constraints set $\beta\mathcal{X}^{cl}$

$$\beta\mathcal{X}^{cl} = \{\xi_k \in \mathbb{R} : \begin{bmatrix} \beta_x X & 0 \\ 0 & \beta_u U \end{bmatrix} \xi_k \leq \mathbf{1}_{l_x+l_u}\}, \tag{103}$$

that, by construction, implies $\beta\mathcal{X}^{cl} \subseteq \mathcal{X}^{cl}$. As a consequence, $\mathcal{L} \subseteq \mathcal{X}^{cl}$. □

Remark 15 *Observe that the polyhedral set defined by equation* (87)*, is constructed similarly to* (102)*, emphasizing that the addition of the scaled augmented state constraints* (103) *is the main difference between the proposed polyhedral set and the one from the mentioned section.*

By definition, the origin of $\mathbb{R}^{n_{cl}}$ belongs to the interior of $\mathcal{L}$. Notice that $\mathcal{L}$ may have some redundant constraints; thus, the *set complexity* l_r defines a bound for the maximum number of faces of the polyhedron.

4.3.1 Algebraic Conditions

Now, we state the algebraic conditions that allow solving Problem 2 under the saturation avoidance approach (TARBOURIECH et al., 2011) and determining a contractive positive-invariant polyhedron $\mathcal{L}$, with pre-specified *complexity*.

Theorem 2 For a plant represented by the LPV-system (78)-(79), with associated constraints (80), Problem 2 admits a solution formed by control gains K_i and $\bar{K}_i$ in (82), and a positive invariant and contractive polyhedral set $\mathcal{L}$ in (100), with the structured L in (101), contraction factor $\lambda \in [0\ ,\ 1)$ and *complexity* $l_r > n_{cl}$, if there exist matrices $R_x \in \mathbb{R}^{r\times n}$, $R_u \in \mathbb{R}^{r\times m}$ and $J \in \mathbb{R}^{n_{cl}\times l_r}$, nonnegative matrices $H_i \in \mathbb{R}^{l_r\times l_r}$ and $Q_i \in \mathbb{R}^{l_d\times l_r}$, and scalars $\beta_x \geq 1$ and $\beta_u \geq 1$ such that $rank(L) = n_{cl}$, and the following conditions are verified, for all $i = 1, \ldots, N$,

$$H_i \begin{bmatrix} R_x & R_u \\ \beta_x X & 0 \\ 0 & \beta_u U \end{bmatrix} = \begin{bmatrix} R_x & R_u \\ \beta_x X & 0 \\ 0 & \beta_u U \end{bmatrix} \begin{bmatrix} A_i & B_i \\ K_i C & I_m + \bar{K}_i \end{bmatrix}, \tag{104a}$$

$$H_i \mathbf{1}_{l_r} \leq \lambda \mathbf{1}_{l_r}, \tag{104b}$$

$$Q_i \begin{bmatrix} R_x & R_u \\ \beta_x X & 0 \\ 0 & \beta_u U \end{bmatrix} = D \begin{bmatrix} K_i C & \bar{K}_i \end{bmatrix}, \tag{105a}$$

$$Q_i \mathbf{1}_{l_r} \leq \mathbf{1}_{l_d}, \tag{105b}$$

$$J \begin{bmatrix} R_x & R_u \\ \beta_x X & 0 \\ 0 & \beta_u U \end{bmatrix} = I_{n_{cl}}. \tag{106}$$

Proof: In conditions (104)-(106), consider L as in (101), with corresponding set $\mathcal{L}$ in (100). Thus:

- the existence of nonnegative matrices H_i and gain matrices K_i and $\bar{K}_i$, verifying the N equalities (104a) for the vertices of $A^{cl}(\alpha_k)$, and such that N inequalities (104b) hold true for $0 \leq \lambda < 1$, are necessary and sufficient for $\mathcal{L}$ be a positive invariant set, with contraction factor λ, of the parameter varying system (83) (see Basílio EA Milani et al. (1996) and Blanchini and Miani (2015));

- Lemma 2 guarantees that $\mathcal{L} \subseteq \mathcal{X}^{cl}$ and, hence, the respect of the control and state constraints;

- Just like we did for (90), (105) is by convexity equivalent to

$$Q(\alpha_k) L = D \begin{bmatrix} K(\alpha_k) C & K_1(\alpha_k) \end{bmatrix}, \tag{107a}$$

$$Q(\alpha_k) \mathbf{1}_{l_r} \leq \mathbf{1}_{l_d}, \tag{107b}$$

  where $Q(\alpha_k) = \sum_{i=1}^{N} \alpha_{k,i} Q_i$ is a nonnegative matrix for all $\alpha_k \in \mathcal{S}$. Thus, from the Extended Farkas' Lemma, this is equivalent to $\mathcal{L} \subseteq \mathcal{D}(\alpha_k)$, thus guaranteeing the control-rate constraints are fulfilled; and

- the existence of J such that (106) holds, is equivalent to $rank(L) > n_{cl}$ since, by hypothesis, $l_r > n_{cl}$, meaning that J is the pseudo-inverse matrix of L. □

Remark 16 *In the state feedback (SF) case, when $C = I_n$, the initial state conditions x_0 corresponds to the initial output conditions y_0, where $x_0 = y_0$. To assure that both x_0 and u_0 are within the set $\mathcal{L}$, the following convex optimization program is capable of determining the initial condition u_0 for given initial state conditions x_0:*

$$\begin{aligned} &\underset{u_0}{\text{minimize}}\ \Omega(u_0) = \|u_0\|_{1,\infty} \\ &\text{subject to} \begin{bmatrix} R_u \\ 0 \\ \beta_u U \end{bmatrix} u_0 \leq \mathbf{1}_{l_r} - \begin{bmatrix} R_x \\ \beta_x X \\ 0 \end{bmatrix} x_0 \end{aligned} \tag{108}$$

Notice that in the output-feedback (OF) case, when $p < n$, it is difficult to determine an initial state x_0 from a given initial output signal y_0. Therefore, we can only consider $u_0 = 0$ as a possible initial condition in this case.

Remark 17 *The main difference between the Theorem 2 and the Theorem 1 in Section 4.2 is that in the latter the polyhedron $\mathcal{L}$ in* (100) *is not structured but takes the generic form in* (102)*, i.e., $\mathcal{L} = \mathcal{R}$, with $l_r = r$, by definition. Thus, in Section 4.2, the following additional algebraic conditions are added to* (104) - (106) *to describe the inclusion $\mathcal{L} \subseteq \mathcal{X}^{cl}$:*

$$\exists T \geq 0; \quad TL = X^{cl} \tag{109a}$$

$$T\mathbf{1}_{l_r} \leq \mathbf{1}_{l_{cl}} \tag{109b}$$

4.3.2 Bilinear Programming Design Approach

The proposed solution to Problem 2, given by Theorem 2, carry some products among matrix variables, more specifically among the elements of H_i, R_x, R_u, β_x, β_u, K_i, $\bar{K}_i$, Q_i, D, and, J in (104)-(106). As emphasized in previous chapters, these products can be appropriately considered as design constraints, and adapted nonlinear optimization techniques can be used to solve Problem 2.

The proposed optimization strategy is to enlarge the size of the set of initial admissible conditions $\mathcal{L}$ along with some directions in $\mathbb{R}^{n_{cl}}$. For this purpose, the set of directions is defined by

$$\mathcal{V} = \{\gamma_j \upsilon_j, j = 1, \ldots, \bar{j}\},$$

where $\upsilon_j \in \mathbb{R}^{n_{cl}}$ are given vectors and $0 < \gamma_t \in \mathbb{R}^{l_{cl}}$ are scaling factors to be optimized, such that the inclusion $\mathcal{V} \subseteq \mathcal{L}$ is satisfied or, equivalently

$$L\gamma_j \upsilon_j \leq 1\,, \; j = 1, \ldots, \bar{j}. \tag{110a}$$

Possible design choices for the set $\mathcal{V}$ are, for instance, a set of directions defined from the vertices of $\mathcal{X}^{cl}$, or a set of normalized directions, possibly equally spaced in the state-space, covering a significant number of directions for the optimization process.

Moreover, consider that the following design parameters are chosen *a priori*: *i)* allowed complexity (*i.e* maximum number of faces) for the invariant sets, by choosing $l_r > n_{cl}$; and *ii)* $\bar{j}$ directions v_j used to enlarge $\mathcal{L}$. Thus, we propose the following bilinear optimization problem to find solutions to the design Problem 2:

$$\begin{aligned} &\underset{\Gamma(\cdot)}{\text{maximize}}\ \Phi(\gamma_j) = \sum_{j=1}^{\bar{j}} \gamma_j \\ &\text{subject to (104)} - \text{(106)} \\ &0 \leq \lambda < 1 \\ &f_\ell(\cdot) \leq \varphi_\ell, \quad \ell = 1, \ldots, \bar{\ell}, \end{aligned} \tag{111}$$

Table 17 – Comparisons with in Section 4.2

Number of	Section 4.2	New
Equalities	$(N(r + l_d) + (l_x + l_u + n_{cl})) \times n_{cl}$	$(N(r + l_x + l_u + l_d) + n_{cl}) \times n_{cl}$
Inequalities	$N(r + l_d) + (l_x + l_u + n_{cl})$	$N(r + l_x + l_u + l_d) + n_{cl}$
Variables	$(N(r + l_d) + (l_x + l_u + n_{cl})) \times r$	$(N(r + l_x + l_u + l_d) + n_{cl}) \times (r + l_x + l_u)$
Bilinearities	$N(3r + 2m) + r$	$N(2(r + l_x + l_u) + 2m) + (r + l_x + l_u)$

with $\Gamma(\cdot) = (H_i, R_x, R_u, \beta_x, \beta_u, K_i, \bar{K}_i, Q_i, D, J, \gamma_j, \lambda)$, where:

Both remarks i) and ii) in the optimization problem (94) are also valid for the present optimization problem (111).

Remark 18 *From Remark 17, we can implement the design optimization problem proposed in Section 4.2 following* (111)*, by considering $\mathcal{L}$ under the form in* (102), (109) *as optimization constraints, and T in the decision variables set Γ. Table 17 allows a comparison between the two proposals in terms of the number of variables, equations, and inequalities. It also includes the number of bilinearities present in both cases. Notice that, if we consider the same value of l_r, the present optimization approach allows a higher set complexity, $l_r = r + l_x + l_u$, than the one presented in Section 4.2, $l_r = r$. In particular, that implies more extensive computations due to the higher number of variables and optimization constraints the employed solver must manage.*

4.3.3 Numerical Example

The example below was solved using the KNITRO solver (BYRD et al., 2006), with the Interior/CG (barrier) algorithm, multi-start option, and the other solver's default settings. To make the result comparisons as fair as possible, we use the same settings to implement both techniques, the one presented in Section 4.2 and the one proposed in this subsection. Also, the following lower and upper bound pairs were assigned to each element of matrices or vectors:

$$\begin{aligned} J, J_u: &\quad [-10^2, 10^2] \\ H_i, Q_i: &\quad [0, 10^2] \\ K_i, K_{1i}, R_x, R_u, : &\quad [-10^2, 10^2] \\ \gamma_j: &\quad [0, 10] \end{aligned}$$

Example: Consider the 2nd-order discrete-time TS-fuzzy system, borrowed from Guerra and Vermeiren (2004), as in (78) - (79) whith $A_1 = \begin{bmatrix} 1 & -1 \\ -1 & -0.5 \end{bmatrix}$, $B_1 \begin{bmatrix} 6 \\ 2 \end{bmatrix}$, $A_2 = \begin{bmatrix} 1 & 1 \\ -1 & -0.5 \end{bmatrix}$ and $B_2 = \begin{bmatrix} 4 \\ -2 \end{bmatrix}$.

As in Section 4.2, this quasi-LPV system exactly represents the nonlinear system (10) of Guerra and Vermeiren (2004), with $|x_{1k}| \leq 1$, and considering non-symmetric control constraints, $0.2 \leq u \leq 1$, and $|\delta u| \leq 0.2$.

In this example, we implemented the technique presented in Section 4.2 and the one proposed in this section using a set of eight directions equally spaced in the state space (x_1 and x_2), starting at [1 0]. A more in-depth discussion on how to choose the set of directions to maximize can be found in Chapter 2, also in Briao et al. (2021).

4.3.4 State-Feedback Controller

First, we consider a state-feedback (SF) control law, which supposes that both states x_{1k} and x_{2k} are measured,

$$\delta u_k^{SF} = K(\alpha(y_k))x_k + \bar{K}(\alpha(y_k))u_k. \tag{112}$$

Table 18 – SF - Results

	i	$[K_i \; K_i]$	Area
Section 4.2	1	[–0.1702 0.0849 –1.6383]	1.3278
	2	[–0.1702 –0.0851 –1.3423]	
New results	1	[–0.1669 –0.0064 –1.1062]	1.3919
	2	[–0.1654 –0.1340 –1.1190]	

In Table 18, we have summarized the results for the SF control law. Our objective in this example is to maximize the area of initial conditions in x_1 and x_2 for $u = 0$. Therefore, the last column shows the area of such polyhedrons, and the third column shows the control gains using $r = 6$ in both cases. Notice that for the new results, we have an increase of 4.8% in the area. Figure 25 depicts these polyhedrons areas for a visual comparison, in blue we have the results obtained using the technique from Section 4.2 and in green the results obtained using the techinique proposed in this section. However, for the results using the implementation from Section 4.2, we had a computational time of 65s, while for the new results, we got a computational time of 103s.

In the state-feedback control case, Remark 16 allows us to find initial conditions for $u \in \mathcal{L}$. This means we can also use initial conditions for $u \neq 0$. Therefore, in Figure 26 we have the projections of the resulting polyhedrons depicting the real area of initial state conditions considering all the possible initial conditions for u. In blue, we have the results from Section 4.2 with an area of 2.6619, and in green, we have the newly obtained results with an area of 2.8667, showing an increase of 7.7%.

In Figure 27, we have the resulting polyhedron using the implementation from Section 4.2, and in Figure 28, we have the polyhedron obtained through the implementation suggested in this section, in **black** inside the polyhedron is the state's trajectory initiating

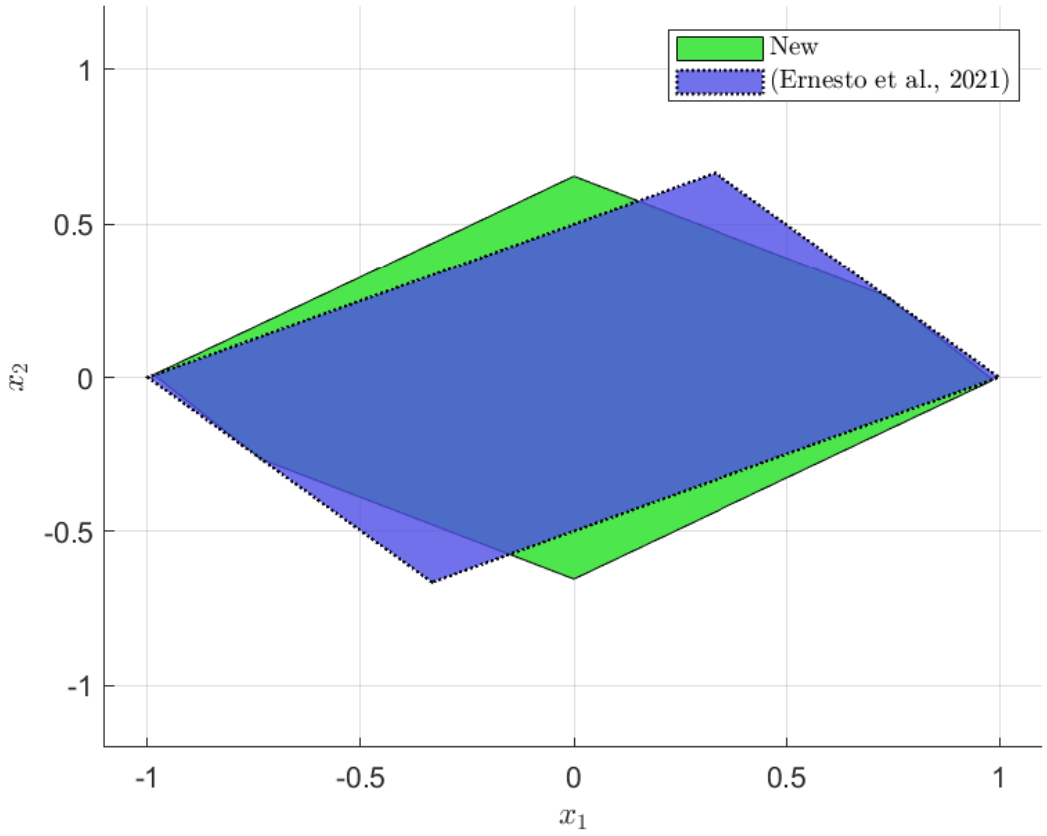

Figure 25 – SF - Polyhedrons area for $u = 0$

at [–1 1.1]. Finally, in the color magenta we show the control variation restriction in both Figures 27 and 28.

4.3.5 Output-Feedback Controller

Now, the output-feedback (OF) control law is obtained by considering that only the output $y_k = x_{1k}$ is measured,

$$\delta u_k^{OF} = K(\alpha(y_k))y_k + \bar{K}(\alpha(y_k))u_k. \tag{113}$$

Table 19 – OF - Results

	i	$[K_i \; K_i]$	Area
Section 4.2	1	[–0.1745 –2.0389]	1.1752
	2	[–0.1669 –1.9276]	
New results	1	[–0.1669 –1.1667]	1.3513
	2	[–0.1745 –2.0389]	

We have summarized the results for the OF control law in Table 19. We obtained these results using the same settings as the ones previously stated, the only exception being a new value for $r = 9$.

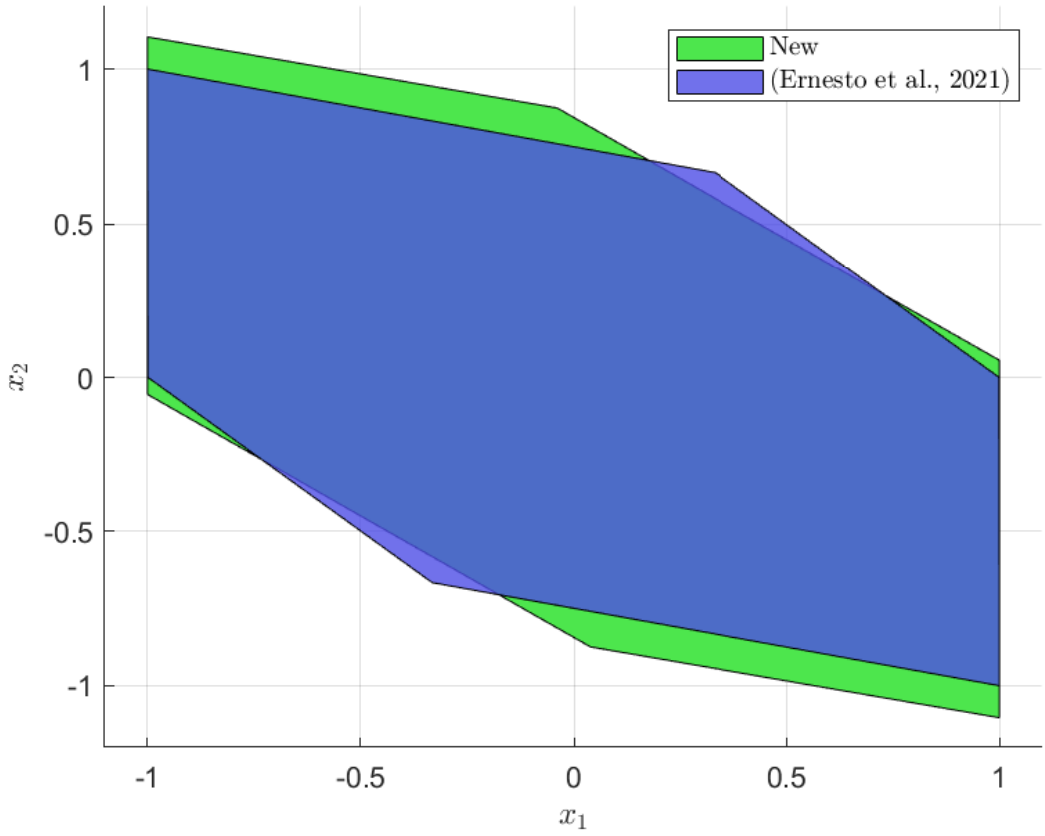

Figure 26 – SF - Polyhedrons projections

The area in the last column refers to the set of admissible state initial conditions when $u = 0$, where we can notice an increase of 15% from the results obtained using the technique from Section 4.2. In Figure 29, we have in green the new results obtained, in light green is the projection of the polyhedron and in blue the results obtained in Section 4.2, for a visual comparison, and in **black** is the state's trajectory initiating at [–1 0]. For this control law, we cannot accurately identify the state x_2 initial conditions, for a given output signal y_k. Therefore, we cannot refer to Remark 16 to use non-null initial control signals.

4.4 CONCLUSION

In this chapter, algebraic conditions for a polyhedral set to be positively invariant for an LPV system subject to state, control, and control-rate constraints have been translated into two bilinear programming problems. Such an optimization control approach delivers a stabilizing control law that feeds back both the plant and control outputs and a positive-invariant polyhedron that determines the region of local closed-loop stability. The second bilinear optimization problem is an alternative implementation, proposing a different structure to $\mathcal{L}$.

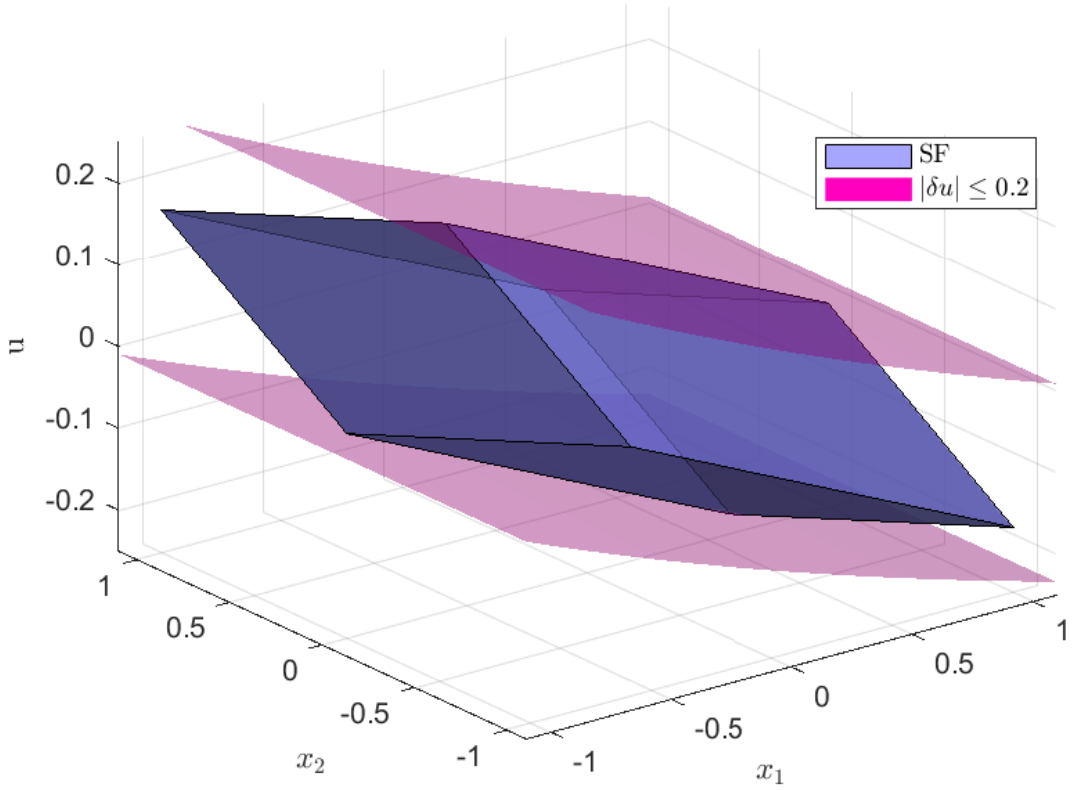

Figure 27 – SF - Polyhedron using the technique from Section 4.2

The nonlinear solver KNITRO was used to solve the proposed bilinear program design. The numerical experiments obtained reliable solutions, showing the proposal's potential in dealing with LPV systems with asymmetrical state, control, and control rate constraints. However, the approach presented in Section 4.3 added more variables and constraints to be handled by the solver.

Finally, in Section 4.3, which deals with the alternative approach, we show that it is possible to use appropriate initial values for the control variables for a given initial output signal in the state feedback case. However, such a possibility also applies in the original approach presented in Section 4.2.

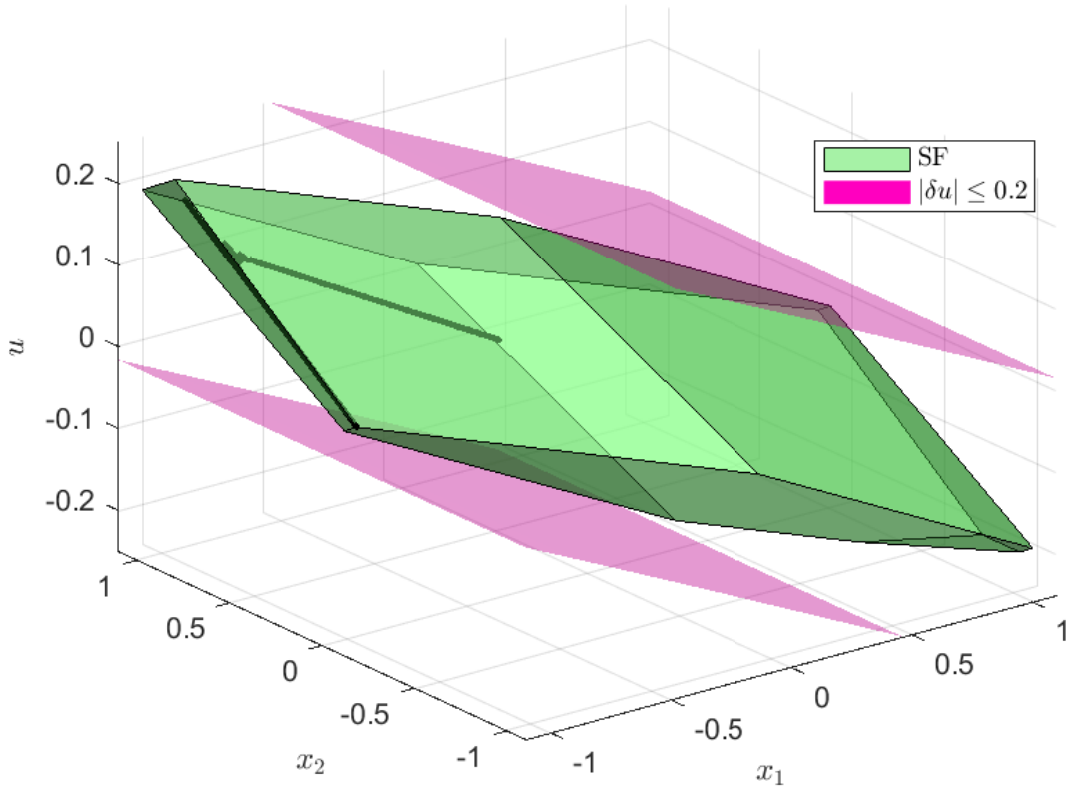

Figure 28 – SF - Polyhedron using the new technique

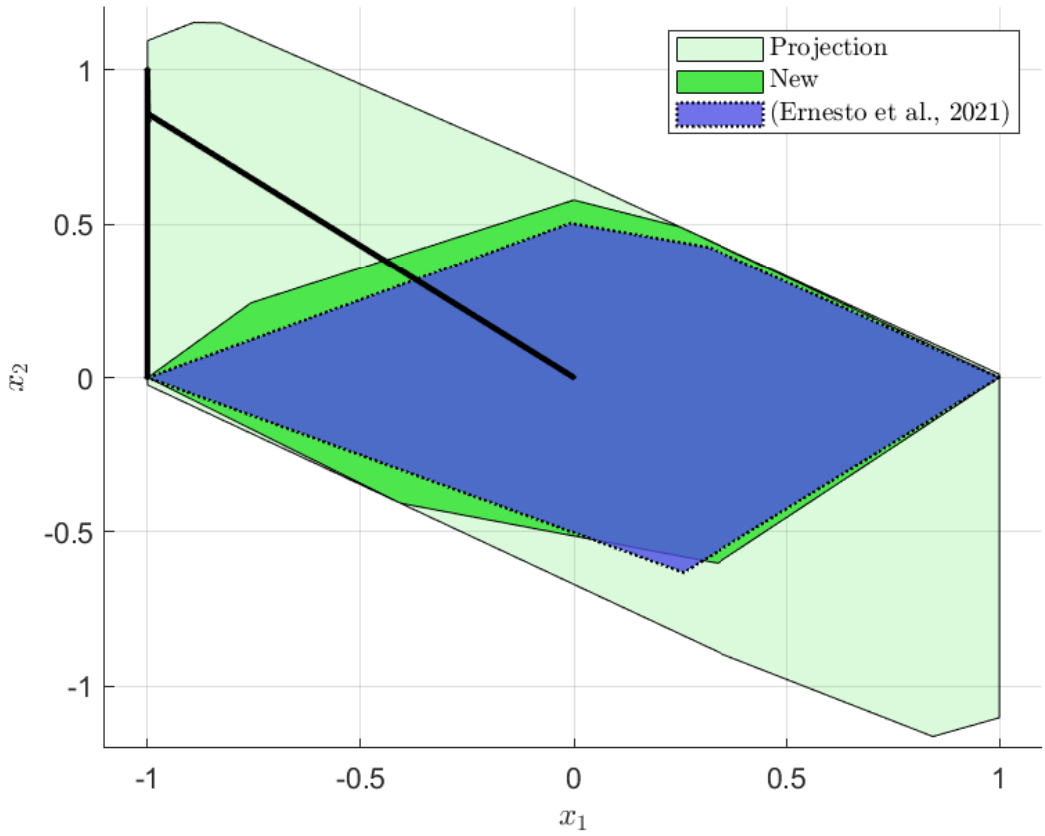

Figure 29 – OF - Polyhedrons area for $u = 0$

5 CONSTRAINED OUTPUT FEEDBACK DESIGN FOR LPV SYSTEMS SUBJECT TO DISTURBANCES

In this chapter, we present an extension of the results of Chapter 4, to deal with constrained linear parameter-varying systems subject to bounded persistent disturbances. Thus, the proposed solution, which also considers state and control constraints and limited control rate variations, is built upon the description of the LPV control system in the extended state space composed of the system's state and control variables, in which the control variations act as the control inputs.

However, to deal with the persistent disturbance and fulfill the imposed constraints, similarly to Chapter 2, we use the Robust Positive Invariance (RPI) property for polyhedral sets to build a large RPI polyhedron of admissible initial augmented states and a small polyhedron around the origin where the corresponding trajectories will be ultimately bounded. This application of the RPI property enhances the robustness of the system, making it more applicable in real-world scenarios.

Moreover, aiming to obtain more degrees of freedom in the controller design, we consider an additional memory-less output feedback gain to the incremental control law. This study shows, in particular, that such a memoryless term keeps the closed-loop system represented as a classical polytopic LPV system. Thus, the proposed numerical solution can be built up from the vertex matrices of the closed-loop polytopic model, as in the previous chapter. However, the memoryless term cannot be set in some particular cases that are commented on and exemplified in the present chapter, showing a drawback of the present proposal, which points out the use of an addition parameter-varying control gain instead.

The chapter is organized as follows: First, we present the target system, its constraints and disturbances, and the incremental control problem. Followed by section 5.2, where we tackle the incremental output feedback design approach by utilizing the robust positive invariance and sets inclusions concepts. Then, we illustrate the results with two examples: a theoretical double integrator and a real coupled tank system. Finally, we present some conclusions about the chapter.

5.1 PROBLEM PRESENTATION

Consider the plant represented by a linear parameter-varying (LPV) discrete-time system given by

$$x_{k+1} = A(\alpha_k)x_k + B(\alpha_k)u_k + B_p(\alpha_k)p_k \tag{114a}$$

$$y_k = Cx_k + D_\eta \eta_k \tag{114b}$$

where $x_k \in \mathbb{R}^{n_x}$ is the state space vector, $u_k \in \mathbb{R}^{n_u}$ is the control input, $y_k \in \mathbb{R}^{n_y}$ the measured output vector, and $p_k \in \mathbb{R}^{n_p}$ *and* $\eta_k \in \mathbb{R}^{n_\eta}$ are exogenous and bounded

process and measurement disturbance vectors, respectively.

The system's matrices are such that $C \in \mathbb{R}^{n_y \times n_x}$, $D_\eta \in \mathbb{R}^{n_y \times n_\eta}$, and

$$\begin{bmatrix} A(\alpha_k) & B(\alpha_k) & B_p(\alpha_k) \end{bmatrix} = \sum_{i=1}^{M} \alpha_{i,k} \begin{bmatrix} A_i & B_i & B_{pi} \end{bmatrix}, \tag{115}$$

with $A_i \in \mathbb{R}^{n_x \times n_x}$, $B_i \in \mathbb{R}^{n_x \times n_u}$ and $B_{pi} \in \mathbb{R}^{n_x \times n_p}$, for $i = 1, \ldots, M$, where the parameter-varying vector $\alpha_k \in \mathcal{S} = \{\alpha_k \in \mathbb{R}^M : \alpha_{i,k} \geq 0, \sum_{i=1}^{M} \alpha_{i,k} = 1\}$.

Moreover, the system is subject to state, control amplitude, and control rate variation constraints,

$$x_k \in \mathcal{X}, \quad u_k \in \mathcal{U}, \quad \delta u_k \in \mathcal{U}_d, \quad \forall k \geq 0,$$

where, by definition,

$$\delta u_k = u_{k+1} - u_k, \tag{116}$$

and the bounded disturbances are considered persistent, with

$$p_k \in \mathcal{P}, \quad \eta_k \in \mathcal{N}, \quad \forall k \geq 0.$$

Such state, control input and rate variation constraints are represented by the closed polyhedral sets

$$\mathcal{X} = \{x_k : Xx_k \leq \mathbf{1}_{l_x}\}, \quad X \in \mathbb{R}^{l_x \times n_x}, \tag{117a}$$

$$\mathcal{U} = \{u_k : Uu_k \leq \mathbf{1}_{l_u}\}, \quad U \in \mathbb{R}^{l_u \times n_u}, \tag{117b}$$

$$\mathcal{U}_d = \{\delta u_k : U_d \delta u_k \leq \mathbf{1}_{l_d}\}, \quad U_d \in \mathbb{R}^{l_d \times n_u}, \tag{117c}$$

and the exogenous disturbances bounds by

$$\mathcal{P} = \{p_k : Pp_k \leq \mathbf{1}_{l_p}\}, \quad P \in \mathbb{R}^{l_p \times n_p}, \tag{118a}$$

$$\mathcal{N} = \{\eta_k : N\eta_k \leq \mathbf{1}_{l_n}\}, \quad N \in \mathbb{R}^{l_n \times n_\eta}. \tag{118b}$$

In the above constrained control set-up, the desired objective is: *to compute an incremental output feedback control law, possibly dependent of the varying parameters,*

$$u_{k+1} = u_k + \delta u_k, \text{ with } \delta u_k := f(y_k, u_k, y_{k+1}, \alpha_k), \tag{119}$$

and an admissible set of initial conditions for the corresponding closed-loop system, denoted $\mathcal{L}$, such that for any closed-loop initial state belonging to $\mathcal{L}$, any persistent disturbances sequences $p_k \in \mathcal{P}$ and $\eta_k \in \mathcal{N}$, and for any varying parameter $\alpha_k \in \mathcal{S}$, the corresponding closed-loop state trajectory fulfils the state, control amplitude, and the control rate variation constraints, (117a)- (117c)*, and is ultimately bounded in a small set $\mathcal{L}_0$ around the origin.*

To pursue the above constrained control objective, which, in particular, considers rate-control limits and an incremental output-like feedback control law, we shall re-formulate the problem by defining the augmented state as in the last chapter,

$$\xi_k = \begin{bmatrix} x_k' & u_k' \end{bmatrix}' \in \mathbb{R}^{n_\xi},\ n_\xi = n_x + n_u, \tag{120}$$

and an output vector as follows:

$$\upsilon_k = \begin{bmatrix} y_k' & u_k' & y_{k+1}' \end{bmatrix}' \in \mathbb{R}^{n_\upsilon},\ n_\upsilon = 2n_y + n_u. \tag{121}$$

Thus, we can define the following augmented LPV system from (114) such that the control variation vector δu_k and the augmented output vector υ_k, appear as *virtual* control input and output signals, respectively:

$$\xi_{k+1} = \mathbb{A}(\alpha_k)\xi_k + \mathbb{B}\delta u_k + \mathbb{B}_p(\alpha_k)p_k \tag{122a}$$

$$\upsilon_k = \mathbb{C}\begin{bmatrix} \xi_k \\ y_{k+1} \end{bmatrix} + \mathbb{D}_\eta \eta_k \tag{122b}$$

where, by construction, $\begin{bmatrix} \mathbb{A}(\alpha_k) & \mathbb{B}_p(\alpha_k) \end{bmatrix} = \sum_{i=1}^{M} \alpha_{k,i} \left[\begin{bmatrix} A_i & B_i \\ 0 & I \end{bmatrix} \quad \begin{bmatrix} B_{p,i} \\ 0 \end{bmatrix} \right]$, $\mathbb{B} = \begin{bmatrix} 0 \\ I \end{bmatrix}$, and $\mathbb{C} = \begin{bmatrix} C & 0 & 0 \\ 0 & I & 0 \\ 0 & 0 & I \end{bmatrix}$ and $\mathbb{D}_\eta = \begin{bmatrix} D_\eta \\ 0 \\ 0 \end{bmatrix}$.

Thus, we can consider the following parameter-varying control increment input vector, which is the *virtual* output feedback control input for the augmented system (122),

$$\delta u_k = \mathbb{K}(\alpha_k)\upsilon_k = \begin{bmatrix} K(\alpha_k) & \bar{K}(\alpha_k) & K_1 \end{bmatrix} \begin{bmatrix} y_k \\ u_k \\ y_{k+1} \end{bmatrix}, \tag{123}$$

where, by definition, $\mathbb{K}(\alpha_k) = \sum_{i=1}^{M} \alpha_{ki} \begin{bmatrix} K_i & \bar{K}_i & K_1 \end{bmatrix}$, with $K_i \in \mathbb{R}^{n_u \times n_y}$, $\bar{K}_i \in \mathbb{R}^{n_u \times n_u}$, $\forall i = 1, \ldots, M$, and $K_1 \in \mathbb{R}^{n_u \times n_y}$.

It is worth mentioning, that the control gain matrix K_1 is, by definition, independent of the varying parameter α_k. As in the last chapter, such a choice will allow us to deal with an LPV closed-loop system with a polytopic representation. Moreover, whenever $K_1 \neq 0$, such a gain matrix will represent an additional degree of freedom with respect to the simpler increment input (81)-(82), which may still consider $K_1 = 0$ as a valid solution.

Remark 19 *Notice, from* (123)*, that the actual parameter-varying incremental control input,* (119)*, to be applied to the plant* (114) *at each new discrete-time instant k, reads*

$$u_k = \left(I + \bar{K}(\alpha_{k-1})\right) u_{k-1} + K(\alpha_{k-1})y_{k-1} + K_1 y_k. \tag{124}$$

In particular, in the initial instant $k = 0$, y_0 is directly transfered to u_0, if $K_1 \neq 0$.

From (122) and (123), we have the closed-loop system can be represented by

$$\xi_{k+1} = \mathbb{A}^{cl}(\alpha_k)\xi_k + \mathbb{B}_d^{cl}(\alpha_k)d_k, \tag{125}$$

where

$$\left[\mathbb{A}^{cl}(\alpha_k) \quad \mathbb{B}_d^{cl}(\alpha_k)\right] = \sum_{i=1}^{M}\alpha_{k,i}\left[\mathbb{A}_i^{cl} \quad \mathbb{B}_{d,i}^{cl}\right], \text{ with } \mathbb{A}_i^{cl} = \begin{bmatrix} A_i & B_i \\ (K_iC + K_1CA_i) & (I + \bar{K}_i + K_1CB_i) \end{bmatrix},$$

$$\mathbb{B}_{d,i}^{cl} = \begin{bmatrix} B_{p,i} & 0 & 0 \\ K_1CB_{p,i} & K_iD_\eta & K_1D_\eta \end{bmatrix}, \text{ and } d_k = \begin{bmatrix} p_k' & \eta_k' & \eta_{k+1}' \end{bmatrix}' \in \mathbb{R}^{n_d}, n_d = 2n_p + n_\eta.$$

Notice that, both sequences η_{k+1} and η_k are, by definition, bounded within the same set $\mathcal{N}$, (118b). Thus, from (117) and (118), the closed-loop system (125) is subject to the control rate constraints represented by $\mathcal{U}_d$, as well as to the augmented state constraints represented by

$$\Xi = \{\xi_k : \mathbb{X}\xi_k \leq \mathbf{1}_{l_\xi}\}, \ \Xi = \begin{bmatrix} X & 0 \\ 0 & U \end{bmatrix} \in \mathbb{R}^{l_\xi \times n_\xi}, \tag{126}$$

where $l_\xi = l_x + l_u$, and the augmented persistent disturbance bounds

$$\Delta = \{d_k : \mathbb{D}d_k \leq \mathbf{1}_{l_\Delta}\}, \ \mathbb{D} = \begin{bmatrix} P & 0 & 0 \\ 0 & N & 0 \\ 0 & 0 & N \end{bmatrix} \in \mathbb{R}^{l_\Delta \times n_d} \tag{127}$$

where $l_\Delta = l_p + 2l_\eta$.

Now, we introduce the concept of contractive Robust Positively Invariant (RPI) set (also called Δ-invariant), with a UB-set, extending to the parameter-varying augmented system (125) the Definition 1 in Chapter 2 (BRIAO et al., 2021, p. 9746).

Definition 7 *A set $\mathcal{L} \in \mathbb{R}^{n_\xi}$ is a contractive robust positive invariant (RPI-) set of the system* (125)*, with ultimately bounded (UB-)set $\mathcal{L}_0 \subseteq \mathcal{L}$, if for any initial condition $\xi_0 = \begin{bmatrix} x_0' & u_0' \end{bmatrix}' \in \mathcal{L}$ and subject to any disturbance sequence $d_k = \begin{bmatrix} p_k' & \eta_k' & \eta_{k+1}' \end{bmatrix}' \in \Delta$, the corresponding state trajectory remains inside $\mathcal{L}$, converge to $\mathcal{L}^0$ in a finite number of steps, and remains ultimately bounded within $\mathcal{L}^0$, for all $\alpha_k \in S$.*

Hence, the control problem tackled in this chapter can be formulated within the augmented state framework, utilizing the above concept of RPI-set, as follows.

Problem 3 *Find stabilizing control increment input gains $K(\alpha)$, $\bar{K}(\alpha)$ and K_1 in* (123)*, a* large *contractive RPI set $\mathcal{L} \subseteq \Xi$, a* small *UB-set $\mathcal{L}^0 \subseteq \mathcal{L}$, such that, for any initial condition $\xi_0 \in \mathcal{L}$, $d_k \in \Delta$, and for all $\alpha_k \in \mathcal{S}$, the state and control constraints,* (117a) *and* (117b)*, and the control rate variation constraint* (117c) *are fulfilled.*

5.2 PROPOSED SOLUTION

To tackle *Problem 3*, we first define the polyhedral sets:

$$\mathcal{L} = \{\xi_k : \mathbb{L}\xi_k \leq \mathbf{1}_{l_r}\}, \tag{128a}$$

$$\mathcal{L}^0 = \{\xi_k : \mathbb{L}\xi_k \leq \rho\mathbf{1}_{l_r}\} \tag{128b}$$

with $\mathbb{L} \in \mathbb{R}^{l_r \times n_\xi}$, $l_r > n_\xi$, $rank(\mathbb{L}) = n_\xi$, and $0 < \rho \leq 1$, which guarantees $\mathcal{L}^0 \subseteq \mathcal{L}$. Note that $\mathcal{L}^0$ is a homotetic set of $\mathcal{L}$ with scale factor given by ρ. Moreover, the matrix $\mathbb{L} = \begin{bmatrix} L_x & L_u \end{bmatrix}$ is composed by $L_x \in \mathbb{R}^{l_r \times n_x}$ and $L_u \in \mathbb{R}^{l_r \times n_u}$. As in previous chapters, l_r defines the *set complexity* for both $\mathcal{L}$ and $\mathcal{L}^0$.

Next, we propose the algebraic conditions that allow solving Problem 3.

Proposition 6 *For a plant represented by the LPV-system* (114)-(115)*, with associated constraints* (117)*, and disturbance bounds* (118)*, Problem 3 admits a solution* $\left(\mathbb{K}(\alpha_k), \mathcal{L}, \mathcal{L}^0\right)$ *if, for some real scalars* $\lambda \in [0\,,\,1)$ *and* $\rho \in [0\,,\,1]$*, and a given* complexity $l_r > n_\xi$*, there exist matrices* $\mathbb{L} = \begin{bmatrix} L_x & L_u \end{bmatrix} \in \mathbb{R}^{l_r \times n_\xi}$ *and* $J \in \mathbb{R}^{n_\xi \times l_r}$*, nonnegative matrices* $H_i \in \mathbb{R}^{l_r \times l_r}$*,* $V_i \in \mathbb{R}^{l_r \times n_p}$*,* $Z_i \in \mathbb{R}^{l_r \times n_\eta}$*,* $Z_1 \in \mathbb{R}^{l_r \times n_\eta}$*,* $G \in \mathbb{R}^{l_\xi \times l_r}$*,* $Q_i \in \mathbb{R}^{l_d \times l_r}$*,* $T_i \in \mathbb{R}^{l_d \times n_p}$*,* $W_i \in \mathbb{R}^{l_d \times n_\eta}$ *and* $W_1 \in \mathbb{R}^{l_d \times n_\eta}$ *such that the following conditions are verified, for all* $i = 1, \ldots, N$*,*

$$\begin{bmatrix} L_x & L_u \end{bmatrix} \begin{bmatrix} A_i & B_i \\ (K_i C + K_1 C A_i) & (I + \bar{K}_i + K_1 C B_i) \end{bmatrix} = H_i \begin{bmatrix} L_x & L_u \end{bmatrix} \tag{129a}$$

$$\begin{bmatrix} L_x & L_u \end{bmatrix} \begin{bmatrix} B_{p,i} & 0 & 0 \\ K_1 C B_{p,i} & K_i D_\eta & K_1 D_\eta \end{bmatrix} = \begin{bmatrix} V_i & Z_i & Z_1 \end{bmatrix} \begin{bmatrix} P & 0 & 0 \\ 0 & N & 0 \\ 0 & 0 & N \end{bmatrix} \tag{129b}$$

$$H_i\mathbf{1}_{l_r} + V_i\mathbf{1}_{l_p} + Z_i\mathbf{1}_{l_\eta} + Z_1\mathbf{1}_{l_\eta} \leq \lambda\mathbf{1}_{l_r} \tag{129c}$$

$$H_i\rho\mathbf{1}_{l_r} + V_i\mathbf{1}_{l_p} + Z_i\mathbf{1}_{l_\eta} + Z_1\mathbf{1}_{l_\eta} \leq (1-\epsilon)\rho\mathbf{1}_{l_r} \tag{129d}$$

$$\begin{bmatrix} X & 0 \\ 0 & U \end{bmatrix} = G \begin{bmatrix} L_x & L_u \end{bmatrix} \tag{130a}$$

$$G\mathbf{1}_{l_r} \leq \mathbf{1}_{l_\xi} \tag{130b}$$

$$U_d \begin{bmatrix} K_i C + K_1 C A_i & \bar{K}_i + K_1 C B_i \end{bmatrix} = Q_i \begin{bmatrix} L_x & L_u \end{bmatrix} \tag{131a}$$

$$U_d \begin{bmatrix} K_1 C B_{p,i} & K_i D_\eta & K_1 D_\eta \end{bmatrix} = \begin{bmatrix} T_i & W_i & W_1 \end{bmatrix} \begin{bmatrix} P & 0 & 0 \\ 0 & N & 0 \\ 0 & 0 & N \end{bmatrix} \tag{131b}$$

$$Q_i\mathbf{1}_{l_r} + T_i\mathbf{1}_{l_p} + W_i\mathbf{1}_{l_\eta} + W_1\mathbf{1}_{l_\eta} \leq \mathbf{1}_{l_d} \tag{131c}$$

$$J \begin{bmatrix} L_x & L_u \end{bmatrix} = I_{n_\xi} \tag{132}$$

Proof: By leveraging the previous chapters' proofs, in special in the proof of Proposition 1, in Chapter 2, and Theorems 1 and 2, in Chapter 4, we firstly recall the existence of J such that (132) holds, is equivalent to $rank(\mathbb{L}) = n_\xi$ since, by hypothesis, $l_r > n_\xi$, meaning that J is the pseudo-inverse matrix of $\mathbb{L}$. Second, the remaining proof is divided into three parts:

1st Part - RPI of $\mathcal{L}$, with contractivity and UB-set $\mathcal{L}^0$: Firstly, by considering the notation associated to the augmented closed-loop system representation, (125), and by resorting to convexity arguments, the algebraic relations (129a)-(129d) admits the infinite dimensional description, i.e. $\forall \alpha_k \in S$, given by

$$H(\alpha_k)\mathbb{L} = \mathbb{L}\mathbb{A}^{cl}(\alpha_k), \tag{133a}$$

$$\mathbb{V}(\alpha_k)\mathbb{D} = \mathbb{L}\mathbb{B}_d^{cl}(\alpha_k), \tag{133b}$$

$$H(\alpha_k)\mathbf{1}_{l_r} + \mathbb{V}(\alpha_k)\mathbf{1}_{l_\Delta} \leq \lambda \mathbf{1}_{l_r}, \tag{133c}$$

$$H(\alpha_k)\rho\mathbf{1}_{l_r} + \mathbb{V}(\alpha_k)\mathbf{1}_{l_\Delta} \leq (1-\epsilon)\rho\mathbf{1}_{l_r} \tag{133d}$$

where, by construction, $H(\alpha_k) = \sum_{i=1}^{N} \alpha_{k,i} H_i$ and $\mathbb{V}(\alpha_k) = \sum_{i=1}^{N} \alpha_{k,i} \begin{bmatrix} V_i & Z_i & Z_1 \end{bmatrix}$ are non-negative matrices.

Moreover, by resorting to the EFL, relations (133a)-(133c) imply the following one-step admissibility condition, which is valid for any $\alpha_k \in \mathcal{S}$ and $\forall k \geq 0$, thus proving that $\mathcal{L}$ is an RPI-set, with contraction factor λ,

$$\mathbb{L}\xi_{k+1} = L \begin{bmatrix} \mathbb{A}^{cl}(\alpha_k) & \mathbb{B}_d^{cl}(\alpha_k) \end{bmatrix} \begin{bmatrix} \xi_k \\ d_k \end{bmatrix} \leq \lambda \mathbf{1}_{l_r}, \ \forall \begin{bmatrix} \mathbb{L} & \mathbf{0} \\ \mathbf{0} & \mathbb{D} \end{bmatrix} \begin{bmatrix} \xi_k \\ d_k \end{bmatrix} \leq \begin{bmatrix} \mathbf{1}_{l_r} \\ \mathbf{1}_{l_\pi} \end{bmatrix}.$$

Next, by using similar arguments as above, the relations (133a), (133b) and (133d) guarantees that $\mathcal{L}^0$ is also an RPI polyhedron, with guaranteed contractive factor $(1-\epsilon)$. Hence, any trajectory that reaches or emanates from $\mathcal{L}^0 \subseteq \mathcal{L}$ remains ultimately bounded inside in it for any $d_k \in \Delta$, which shows that $\mathcal{L}^0$ is a UB-set associated to the RPI $\mathcal{L}^0$.

2nd Part - Constraints admissibility: We first recall that (130) guarantees $\mathcal{L} \subseteq \Xi$, which means that any closed-loop trajectory initiating inside $\mathcal{L}$ respect the state and control constraints, $\mathcal{X}$ and $\mathcal{U}$.

Next, as in the first part of this proof, from (131b)-(131c), one obtains the following infinite dimensional relations, which are also valid $\forall \alpha_k \in S$,

$$U_d \overbrace{\begin{bmatrix} K(\alpha_k)C + K_1 CA(\alpha_k) & \bar{K}(\alpha_k) + K_1 CB(\alpha_k) \end{bmatrix}}^{\mathbb{F}(\alpha_k)} = \mathbb{Q}(\alpha_k)\mathbb{L} \tag{134a}$$

$$U_d \overbrace{\begin{bmatrix} K_1 CB_p(\alpha_k) & K(\alpha_k)D_\eta & K_1 D_\eta \end{bmatrix}}^{\mathbb{G}(\alpha_k)} = \mathbb{T}(\alpha_k)\mathbb{D} \tag{134b}$$

$$\mathbb{Q}(\alpha_k)\mathbf{1}_{l_r} + \mathbb{T}(\alpha_k)\mathbf{1}_{l_{p+2\eta}} \leq \mathbf{1}_{l_d}, \tag{134c}$$

where, by construction, $\mathbb{Q}(\alpha_k) = \sum_{i=1}^{N} \alpha_{k,i} Q_i$ and $\mathbb{T}(\alpha_k) = \sum_{i=1}^{N} \alpha_{k,i} \begin{bmatrix} T_i & W_i & W_1 \end{bmatrix}$ are non-negative matrices.

Once more, by resorting to the EFL, relations (134a)-(134c) guarantee that the following condition holds true $\forall \alpha_k \in \mathcal{S}$ and $\forall k \geq 0$:

$$U_d \delta u_k = U_d \begin{bmatrix} \mathbb{F}(\alpha_k) & \mathbb{G}(\alpha_k) \end{bmatrix} \begin{bmatrix} \xi_k \\ d_k \end{bmatrix} \leq \mathbf{1}_{l_d}, \ \ \forall \xi_k \text{ and } \eta_k : \begin{bmatrix} \mathbb{L} & 0 \\ 0 & \mathbb{D} \end{bmatrix} \begin{bmatrix} \xi_k \\ d_k \end{bmatrix} \leq \begin{bmatrix} \mathbf{1}_l \\ \mathbf{1}_{l_\eta} \end{bmatrix},$$

which means that the control rate variation constraint is verified for any trajectory starting from the RPI-set $\mathcal{L}$ and for any admissible disturbances $p_k \in \mathcal{P}$ and $\eta_k \in \mathcal{N}$.

3rd Part - Finite-time convergence:

It remains to show the finite-time convergence of the trajectories starting from $\mathcal{L}$ to $\mathcal{L}_0$. To this end, notice that $\eta\mathcal{L}_0 = \{\xi_k : L\xi_k \leq \eta\boldsymbol{\rho}\}$, with $1 \leq \eta \leq \bar{\rho}^{-1}$, is also a RPI set of the system (114) and shares the guaranteed contractivity coefficient $\tilde{\lambda} = (1-\epsilon) < 1$ of $\mathcal{L}_0$; Thus, as in the proof of Proposition 1 in Chapter 2, see also (DE ALMEIDA; DOREA, 2020), we assume that $\xi_0 \in \eta_0\mathcal{L}_0$ and $\xi_k \in (\tilde{\lambda}^k\eta_0)\mathcal{L}_0 \subseteq \mathcal{L}_0$, $\forall d_k \in \Delta$ with $k > 0$. It can be observed that $\xi_k \in \mathcal{L}_0$ when $\tilde{\lambda}^k\eta_0 \leq 1 \Rightarrow \tilde{\lambda}^k \leq \eta_0^{-1}$, and solving it for k, we can conclude that for $k \geq \tilde{k} = -\log_{\tilde{\lambda}} \eta_0 \Rightarrow \xi_k \in \mathcal{L}_0$. The number of steps $\tilde{k}$ should be seen as a reference value because the trajectory may reach the set $\mathcal{L}_0$ in a number of steps k less than $\tilde{k}$. □

It is worth noting that if the LPV system (114) is not subject to the control rate-variation constraint (117c), Proposition 6 can be easily adapted to find admissible solutions for an instance of Problem 3 that considers only the state and control constraints (117a) and (124). For that, it suffices to remove the control-rate variation conditions (131a)-(131c) from the proposed relations (129a) to (132).

Moreover, to apply the above Proposition to the LPV systems unaffected by disturbances considered in the previous Chapter, it suffices to remove the conditions (129b) and (131b) and setting V_i, Z_i, Z_1, T_i, W_i and W_1 as zero in (129c), (129d) and (131c). In addition, by considering $K_1 = 0$, we retrieve exactly the local asymptotic stabilization conditions proposed by Theorem 1 of Chapter 4.

5.3 BILINEAR OPTIMIZATION DESIGN

Notice that the algebraic relations in (129a) present bi-linear terms involving the pair of matrix decision variables (H_i, L_x, L_u) in its left-hand side, and (L_x, L_u, K_i, $\bar{K}_i$, and K_1) in the right-hand side. Likewise, the left-hand side of the conditions (130a) and (132), and the right-hand side of (131a) have bilinear products involving the matrices (G, L_x, L_u), (J, L_x, L_u) and (Q_i, L_x, L_u), respectively. The remaining conditions are all linear with

regard to the set of decision variables $\Gamma = \{ H_i, V_i, Z_i, Z_1, G, Q_i, T_i, W_i, W_1, L_x, L_u, K_i, K_1, \bar{K}_i, J, \lambda, \rho\}$.

Furthermore, in order to maximize the size of $\mathcal{L}$, we introduce the following auxiliary inequalities

$$\gamma_t \mathbb{L} \psi_t \leq \mathbf{1}_{l_r}, t = 1, \ldots, \bar{t}. \tag{135}$$

where γ_t, for $t = 1, \ldots, \bar{t}$, are real positive scaling factors associated to a given set Ψ of $\bar{t} > 0$ directions $\psi_t \in \mathbb{R}^{n_\xi}$, where

$$\Psi = \{\gamma_t \psi_t, t = 1, \ldots, \bar{t}\}. \tag{136}$$

with $\psi_t = \begin{bmatrix} \psi'_{x,t} & \psi'_{u,t} \end{bmatrix}'$, $\psi_{x,t} \in \mathbb{R}^{n_x}$ and $\psi_{u,t} \in \mathbb{R}^{n_u}$, resulting in the following bi-linear optimization problem:

$$\begin{aligned} \underset{\Gamma, \gamma_t}{\text{maximize}} \quad & \mathcal{J} = \sum_{t=1}^{\bar{t}} \gamma_t - \alpha\rho \\ \text{subject to} \quad & (129a) - (135), \\ & 0 < \rho \leq 1, \\ & f_\ell(\cdot) \leq \varphi_\ell, \end{aligned} \tag{137}$$

where:

i) like the optimization problem (15) the proposed weighted objective function $\mathcal{J}(\gamma_t, \rho)$ allows to trade off the maximization of the external set $\mathcal{L}$ through the scaling factors associated to the directions in Ψ, by considering $\mathcal{J}(\gamma_t) = \Sigma_{t=1}^{\bar{t}} \gamma_t$, and the relative size of an internal set $\mathcal{L}^0$, represented by ρ; notice that, for different choices of the weighting parameter α, the optimization program (137) can provide different solutions to Problem 3, which may also depend on the designer choices of Ψ and l_r.

ii) the additional constraints, represented by $f_\ell(\cdot) \leq \varphi_\ell$, may be imposed on the decision variables for different purposes, including the numerical ones, discussed in Chapter 2.

iii) Optionally, $\psi_{u,t}$ can also be considered as a supplementary decision variable in (137). In such case, $\psi_{u,t}$ appears as additional degrees of freedom to allow for the maximization of the projection of the positive invariant sets $\mathcal{L}$ and $\mathcal{L}_0$ in the system state-subspace $\mathbb{R}^2$. Otherwise, it is possible to maximize the outer RPI set by choosing the set of directions a priori.

5.4 EXAMPLES

The examples below were solved using the KNITRO solver (BYRD et al., 2006), with the Interior/CG (barrier) algorithm, multi-start option, and the other solver's default settings. The following additional constraints were considered :

α	$\mathcal{L}$ Volume	$\mathcal{L}$ Projection Area	ρ	$\begin{bmatrix} K & \bar{K} & K_1 \end{bmatrix}$
1	3.0736	4.5000	0.9931	$\begin{bmatrix} 0.5000 & -0.5000 & -0.6680 \end{bmatrix}$
5	2.9757	4.5000	0.9080	$\begin{bmatrix} 0.4839 & -0.5000 & -0.6656 \end{bmatrix}$
10	2.5674	4.3576	0.6464	$\begin{bmatrix} 0.4856 & -0.5222 & -0.7733 \end{bmatrix}$
20	2.3301	4.1579	0.6130	$\begin{bmatrix} 0.4959 & -0.5000 & -0.7867 \end{bmatrix}$

Table 20 – LTI results

$$\begin{aligned} H_i, V_1, Z_i, Z_1, G, Q_i, T_i, W_i, W_1 : &\ [0, 10^2] \\ K_i, \bar{K}_i, K_1, L_x, L_u : &\ [-10^2, 10^2] \\ J : &\ [-10^3, 10^3] \\ \gamma_t : &\ [0, 10^2]. \end{aligned}$$

5.4.1 Example 1

Consider the system (114) and constraints (117) represented by the following matrices,

$$A = \begin{bmatrix} 1 & 1 \\ 0 & 1 \end{bmatrix},\ B = \begin{bmatrix} b \\ 1 \end{bmatrix}\ B_p = \begin{bmatrix} 1 \\ 1 \end{bmatrix},\ C = \begin{bmatrix} 1 & 0 \end{bmatrix},\ \text{and } D_\eta = \begin{bmatrix} 1 \end{bmatrix}$$

with the persistent disturbances defined from $P' = \begin{bmatrix} 10 & -10 \end{bmatrix}'$ and $N' = [\ 10 \quad -10\ ]'$, meaning that $|p_k| \leq 0.1$ and $|\eta_k| \leq 0.1$. The state and control constraints are defined from $X' = \begin{bmatrix} 0.8 & 0 & -1 & 0 \\ 0 & 1 & 0 & -1 \end{bmatrix}'$ and $U' = \begin{bmatrix} 1 & -1.25 \end{bmatrix}'$, meaning $-1 \leq x_1 \leq 1.25$, $|x_2| \leq 1$ and $-0.8 \leq u \leq 1$.

5.4.1.1 LTI system

We are able to consider the same example from Chapter 2, Section 2.4.1.3, by assuming $b = 2$, choosing the maximum number of faces $l_r = 9$, and the same sixteen directions equally spaced in the system state-subspace $\mathbb{R}^2$, here denoted $\psi_{x,t}$. Notice that in Section 2.4.1.3, the chosen directions promote the enlargement of the sets in the system state-subspace $\mathbb{R}^2$ because we were only considering $x_c = 0$ as a valid initial condition. However, for the present example, by leveraging all possible values of initial conditions within $\mathcal{L}$, we consider $-1 \leq \psi_{u,t} \leq 1$ as part of the decision variables in order to maximize the projection of the RPI set, $\mathcal{L}$, in the system state-subspace $\mathbb{R}^2$ through the chosen $\psi_{x,t}$ directions.

In Table 20, we summarize the results for different values of the weighting factor α, showing the resulting $\mathcal{L}$ polyhedron volume, the projection areas, the associated ρ values, and the associated control gains. Notice that the areas and volumes decrease with the increase of α, just as expected since bigger α's indicate a bigger incentive in building a smaller inner set, identifiable by the values of ρ, instead of bigger outer sets.

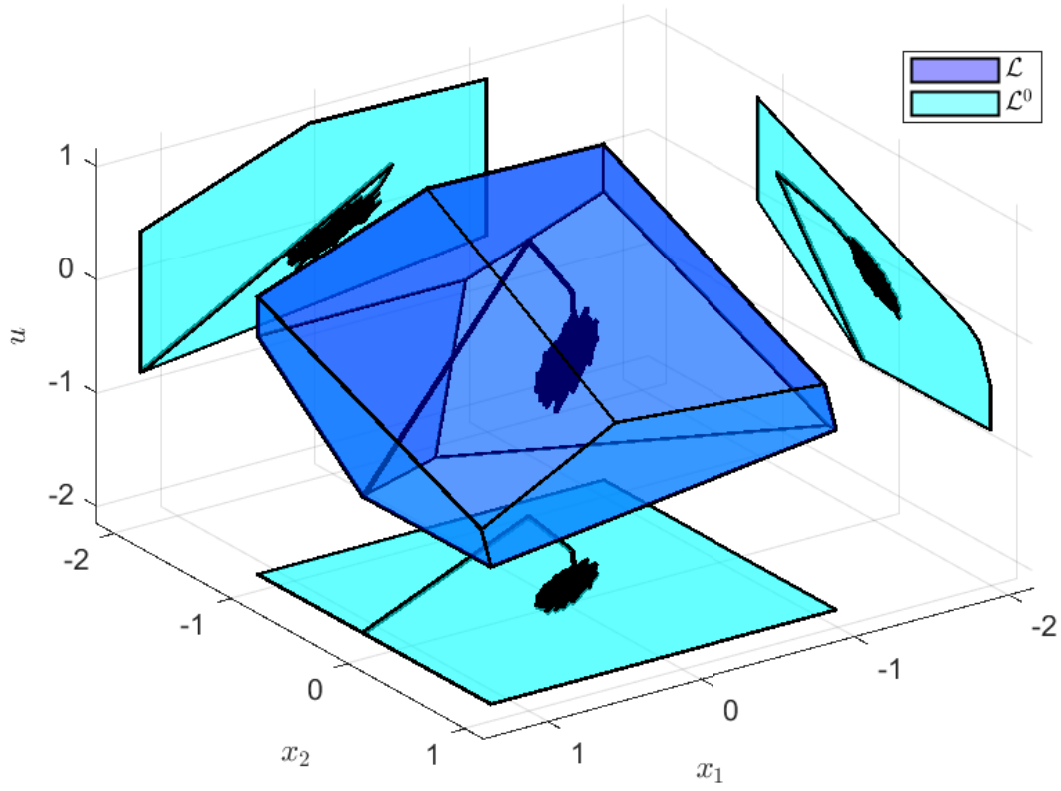

Figure 30 – LTI, with $\alpha = 1$

α	$\mathcal{L}$ Volume	$\mathcal{L}$ Projection Area	ρ	$\begin{bmatrix} K_i & \bar{K}_i & K_1 \end{bmatrix}$
1	2.1846	4.2366	0.9970	$\begin{bmatrix} 0.4018 & -0.5383 & -0.6372 \end{bmatrix}$ $\begin{bmatrix} 0.4018 & -0.4412 & -0.6372 \end{bmatrix}$
5	2.7570	4.1934	0.8558	$\begin{bmatrix} 0.4580 & -0.4978 & -0.6538 \end{bmatrix}$ $\begin{bmatrix} 0.4580 & -0.4444 & -0.6538 \end{bmatrix}$
10	2.4217	4.4656	0.6710	$\begin{bmatrix} 0.4431 & -0.5420 & -0.7376 \end{bmatrix}$ $\begin{bmatrix} 0.4661 & -0.4377 & -0.7376 \end{bmatrix}$
20	1.9943	3.9331	0.5949	$\begin{bmatrix} 0.4571 & -0.5348 & -0.7769 \end{bmatrix}$ $\begin{bmatrix} 0.4706 & -0.4222 & -0.7769 \end{bmatrix}$

Table 21 – LPV α results

Furthermore, Figures 30 and 31, illustrate the sets $\mathcal{L}$ and $\mathcal{L}_0$ obtained for $\alpha = 1$ and 10 and their projections, we also show in **black** the system trajectories evolution over time. Highlighting that, for an initial condition and randomly generated disturbances within the bounds previously stated, the trajectories go to the region around the origin where it stays indefinitely.

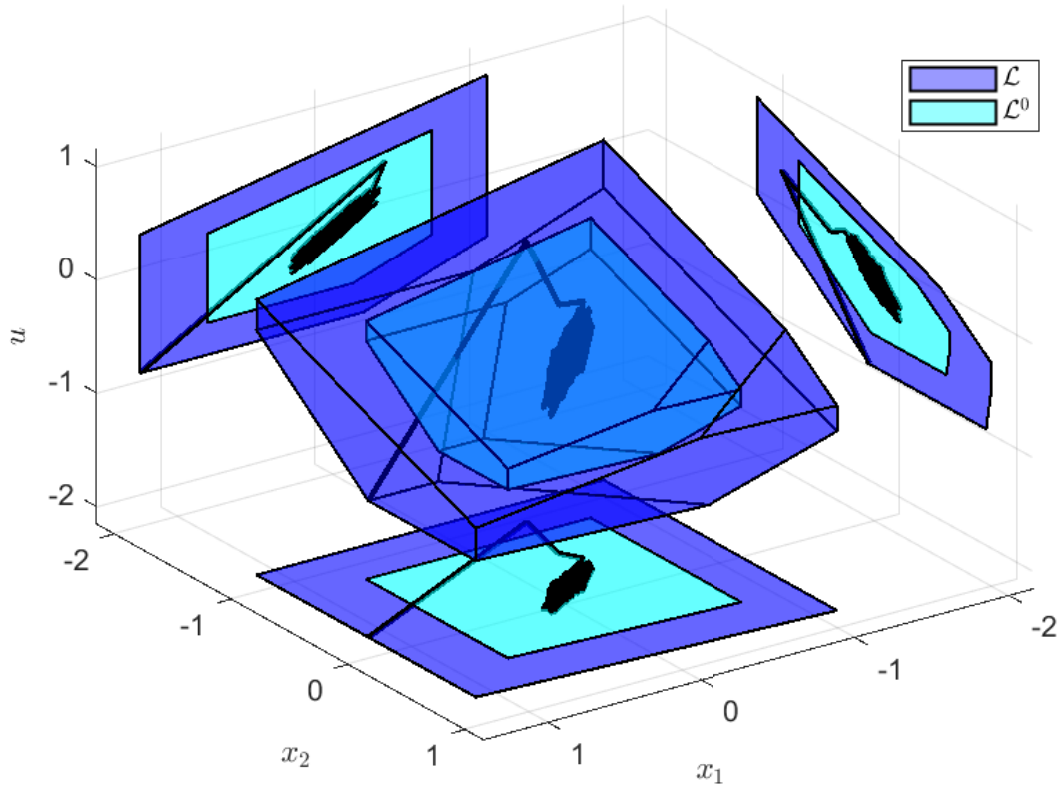

Figure 31 – LTI, with $\alpha = 10$

δu_k bounds	$\mathcal{L}$ Volume	$\mathcal{L}$ Projection Area	ρ	$\begin{bmatrix} K_i & \bar{K}_i & K_1 \end{bmatrix}$
without	2.4217	4.4656	0.6710	$\begin{bmatrix} 0.4431 & -0.5420 & -0.7376 \end{bmatrix}$ $\begin{bmatrix} 0.4661 & -0.4377 & -0.7376 \end{bmatrix}$
[–0.9 , 0.6]	1.3584	4.4679	0.8864	$\begin{bmatrix} 0.4033 & -0.5366 & -0.6016 \end{bmatrix}$ $\begin{bmatrix} 0.4033 & -0.4317 & -0.6016 \end{bmatrix}$
[–0.7 , 0.5]	1.1997	4.4028	0.9980	$\begin{bmatrix} 0.3743 & -0.5575 & -0.5551 \end{bmatrix}$ $\begin{bmatrix} 0.3734 & -0.4533 & -0.5551 \end{bmatrix}$
[–0.5 , 0.4]	0.3195	1.8801	0.9961	$\begin{bmatrix} 0.0000 & -1.0324 & -0.4231 \end{bmatrix}$ $\begin{bmatrix} 0.0000 & -0.9849 & -0.4231 \end{bmatrix}$

Table 22 – Resulting Polyhedrons Areas and Volumes

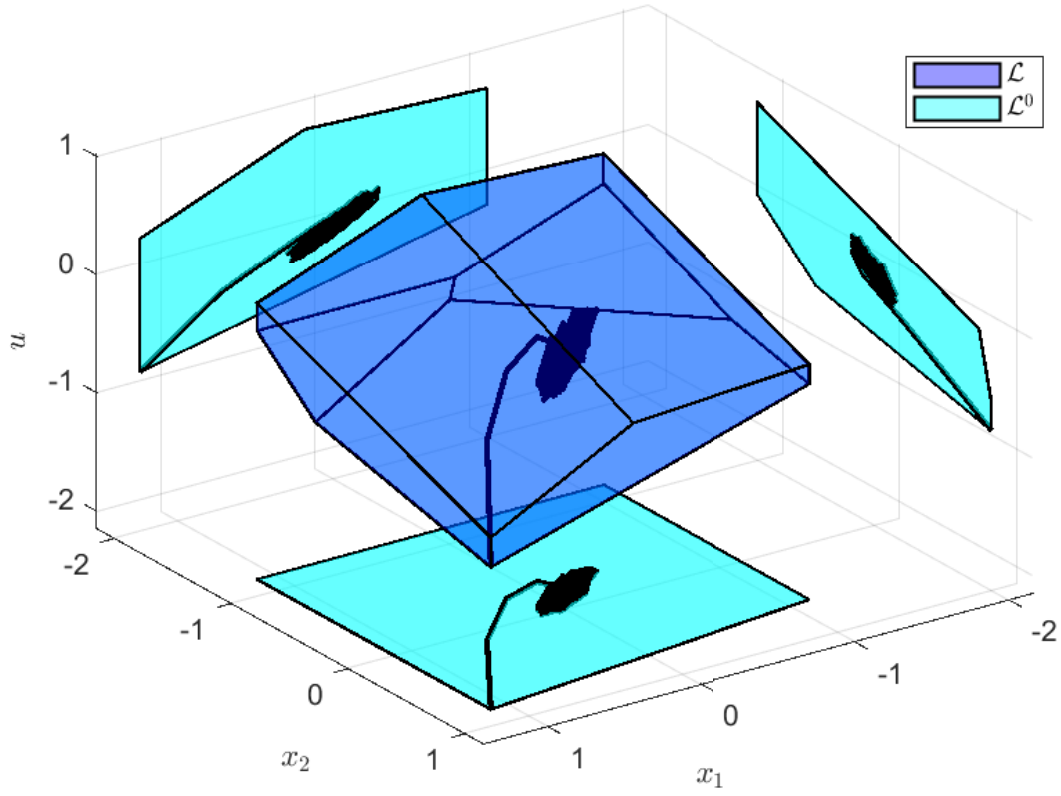

Figure 32 – LPV, with $\alpha = 1$

5.4.1.2 LPV

Next, we consider the input matrix to be parameter varying, $B(\alpha_k) = \begin{bmatrix} b & 1 \end{bmatrix}'$, by admitting $2 \leq b \leq 2.25$, using the same ψ_t directions and the set complexity $l_r = 9$, and as previously, the system is not subject to control variation constraints.

In Table 21, we show the $\mathcal{L}$ volumes, the area of projection in the state's subspace, the values of ρ, and the control gains $\mathbb{K}_i = \begin{bmatrix} K_i & \bar{K}_i & K_1 \end{bmatrix}$, for $i = 1, 2$, obtained for different values of α in the objective function $\mathcal{J}$ of the optimization problem (137). Notice the numerical behavior is similar to the previous LTI example, where the areas and volumes decrease with the increase of α, although $\alpha = 10$ has given an unexpected value for the $\mathcal{L}$ projection area. However, ρ still decreases steadily. Figures 32 and 33 illustrate two of those results, showing $\mathcal{L}$ and $\mathcal{L}^0$ in blue, the states trajectories in **black** and their projections.

Now, in Table 22 we show, for different ranges of control rate variation constraints and $\alpha = 10$, the $\mathcal{L}$ volumes, their projection areas, the associated ρ values, and the associated control gains. The results showcase the degrading of the volumes and areas effect as the constraints increase, which is especially observed when compared with the example without restrictions to the control variation constraints. Next, in Figures 34,

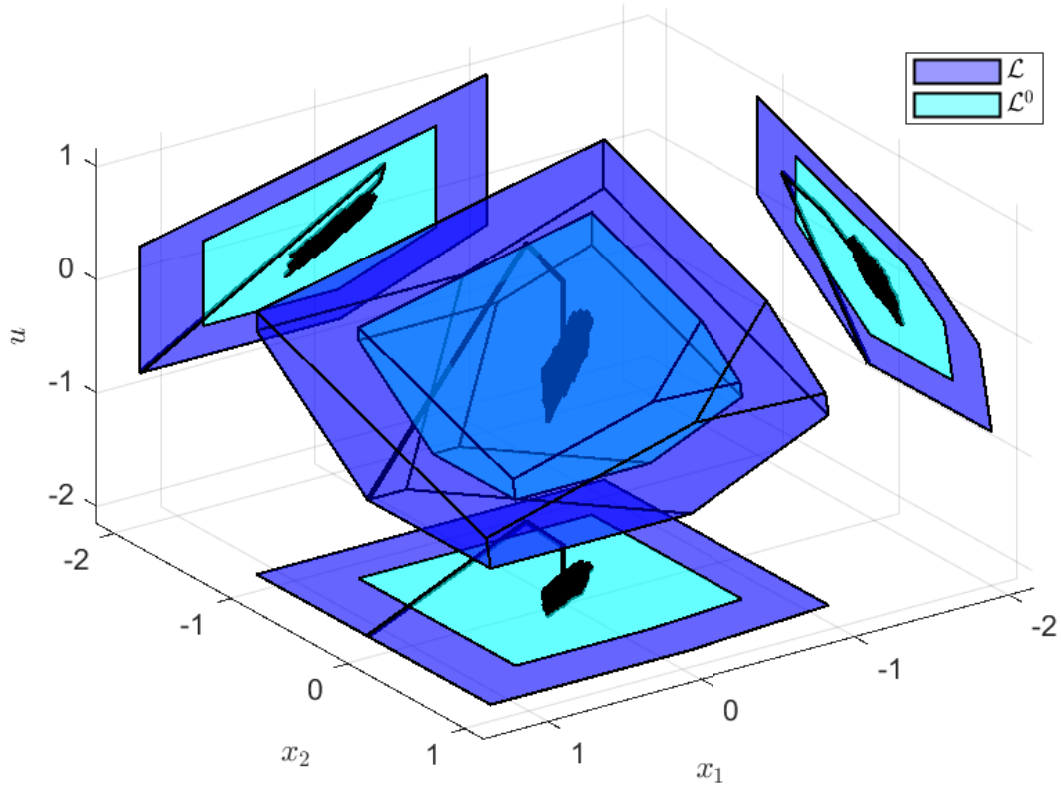

Figure 33 – LPV, with $\alpha = 10$

35, 36 and 37 we illustrate the sets $\mathcal{L}$ and $\mathcal{L}_0$ obtained and their projections, to visually exemplify the polyhedron size degradation with the increase of the control variation constraint. Finally, in Figures 38 and 39, we show the evolution of the control and control rate-variation over time to highlight that the trajectory respects the given constraints for the trajectory originally depicted in Figure 35. Notice that the initial conditions were chosen close to the limits of the control constraints.

5.4.2 Coupled Tank

In this section, we apply the proposed technique to a model of the coupled tank system depicted in Figure 40 manufactured by Quanser®, which is installed at Concordia University laboratory [1]. Consider the following set of parameters and variables for the coupled tank model:

- D_{ti} is the diameter of the tank i;
- D_{ofi} is the outflow orifice diameter of the tank i;

[1] Part of the work related to the Coupled Tank example has been developed during a semester research project supervised by prof. Dr. Walter Lucia, in Concordia University, Montreal, Canada

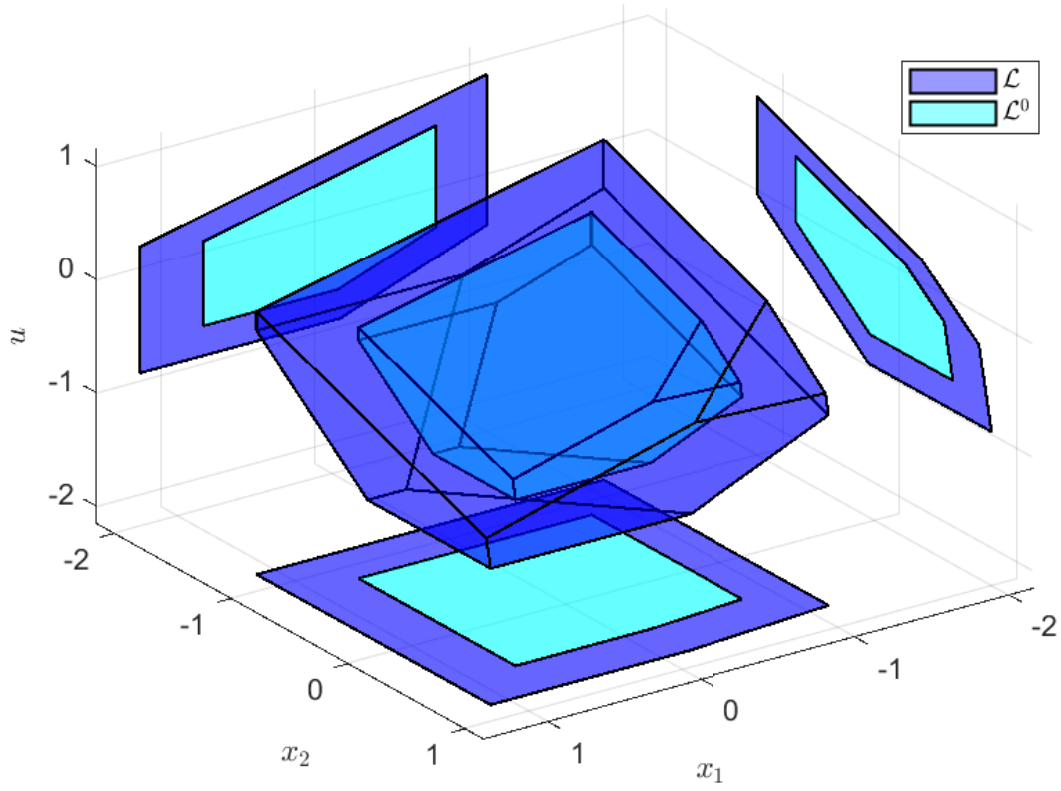

Figure 34 – LPV, without bounds to δ_u

- L_i is the level of the tank i;
- g is the gravitational acceleration;
- K_m is the pump gain;
- V_p is the voltage applied to the pump;

The rate of change of mass in the tank is equal to mass flow in minus mass flow out, resulting in:

$$\dot{L}_1 = -\frac{D_{of1}}{D_{t1}}\sqrt{2gL_1} + \frac{K_m(V_p)}{D_{t1}}V_p \tag{138}$$

$$\dot{L}_2 = -\frac{D_{of2}}{D_{t2}}\sqrt{2gL_2} + \frac{D_{of1}}{D_{t2}}\sqrt{2gL_1} \tag{139}$$

Notice that the pump gain depends on the voltage applied to the pump, therefore we obtained its values experimentally and approximated its behavior to the polynomial of 8^{th} order:

$$\begin{aligned} K_m(V_P) = {} & 6.3743e^{-7}V_p{}^8 - 3.7055e^{-5}V_p{}^7 + 9.2181e^{-4}V_p{}^6 - 0.0128V_p{}^5 \\ & +0.1090V_p{}^4 - 0.5833V_p{}^3 + 1.9261V_p{}^2 - 3.5006V_p{}^1 + 3.3407 \end{aligned}$$

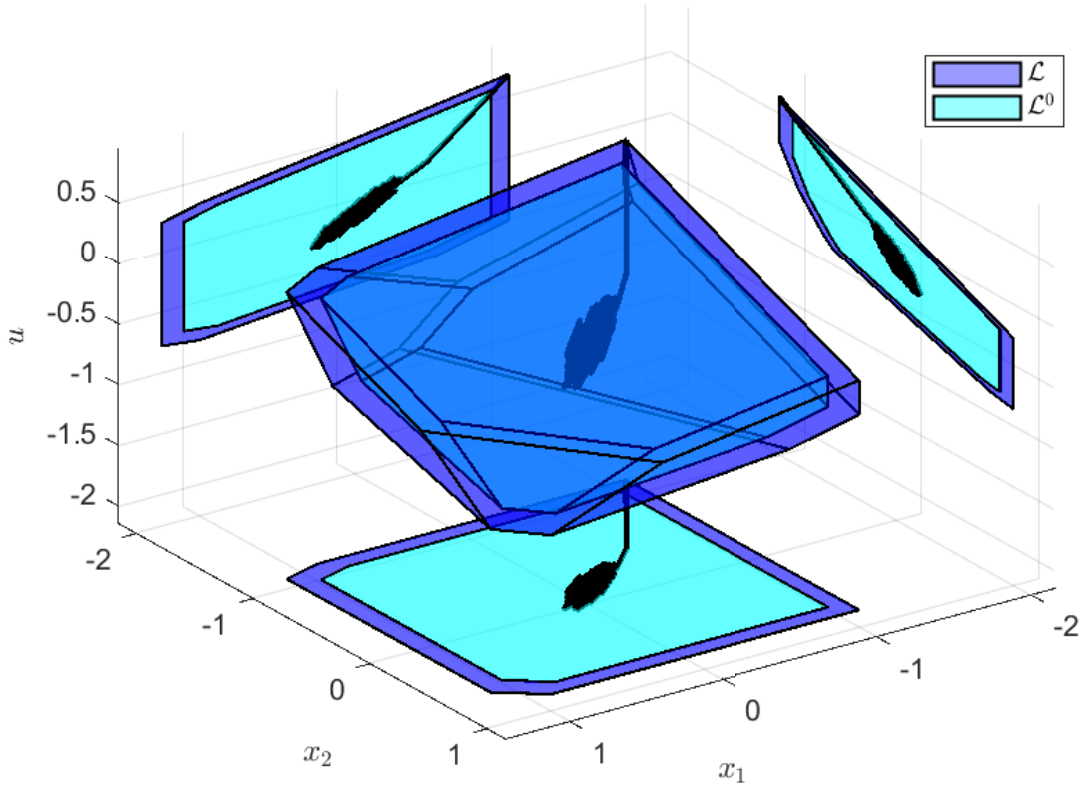

Figure 35 – LPV, with $-0.9 \leq \delta u \leq 0.6$

Furthermore, the nonlinear model is discretized and described as a T-S fuzzy system, where $\hat{x}_1 = L_1$, $\hat{x}_2 = L_2$, and $\hat{u} = V_p$. For more details about the fuzzification and discretization to obtain the fuzzy-TS model described above, the reader is referred to Appendix A. Additionally, to showcase the potential of the proposed technique, the system is shifted to the equilibrium point defined by $\hat{x}_{eq} = [15.25\ 14.87]'$ and $\hat{u}_{eq} = 8.1$, obtained experimentally. Therefore, the shifted states are defined as $x = \hat{x} - \hat{x}_{eq}$ and the shifted control variable $u = \hat{u} - \hat{u}_{eq}$, resulting in the system in the form of (114) with vertex matrices

$$A_1 = \begin{bmatrix} 0.8925256 & 0.0000000 \\ 0.1014803 & 0.8925256 \end{bmatrix}, A_2 = \begin{bmatrix} 0.8925256 & 0.0000000 \\ 0.0991277 & 0.8514655 \end{bmatrix}$$

$$A_3 = \begin{bmatrix} 0.8514655 & 0.0000000 \\ 0.1401877 & 0.8925256 \end{bmatrix}, A_4 = \begin{bmatrix} 0.8514655 & 0.0000000 \\ 0.1369125 & 0.8514655 \end{bmatrix}$$

$$A_5 = \begin{bmatrix} 0.8925256 & 0.0000000 \\ 0.1014803 & 0.8925256 \end{bmatrix}, A_6 = \begin{bmatrix} 0.8925256 & 0.0000000 \\ 0.0991277 & 0.8514655 \end{bmatrix}$$

$$A_7 = \begin{bmatrix} 0.8514655 & 0.0000000 \\ 0.1369125 & 0.8514655 \end{bmatrix}, A_8 = \begin{bmatrix} 0.8514655 & 0.0000000 \\ 0.1401877 & 0.8925256 \end{bmatrix}$$

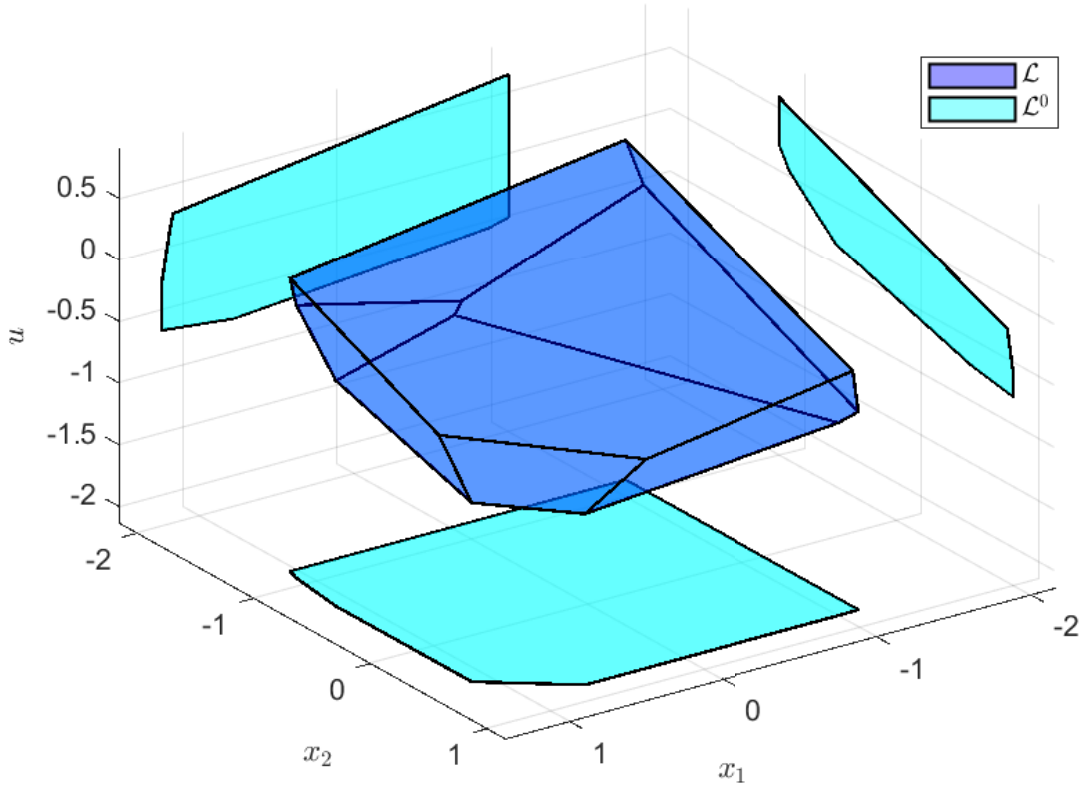

Figure 36 – LPV, with $-0.7 \leq \delta u \leq 0.5$

$$B_1 = \begin{bmatrix} 0.1364234 \\ 0.0076087 \end{bmatrix}, B_2 = \begin{bmatrix} 0.1364234 \\ 0.0074918 \end{bmatrix}, B_3 = \begin{bmatrix} 0.1333202 \\ 0.0105950 \end{bmatrix}, B_4 = \begin{bmatrix} 0.1333202 \\ 0.0104316 \end{bmatrix},$$
$$B_5 = \begin{bmatrix} 0.2250484 \\ 0.0125516 \end{bmatrix}, B_6 = \begin{bmatrix} 0.2250484 \\ 0.0123587 \end{bmatrix}, B_7 = \begin{bmatrix} 0.2199292 \\ 0.0172082 \end{bmatrix}, B_8 = \begin{bmatrix} 0.2199292 \\ 0.0174779 \end{bmatrix}.$$

Additionally, to encompass possible values of unmodeled control input uncertainty, we considered $B_{p,i} = B_i$, for $i = 1...8$, with disturbance bounds within $-0.1 \leq p_k \leq 0.1$, meaning that we are robust to an input disturbance of $\pm 10\%$ of the control input u. Moreover, we considered the state feedback case, with the matrices $C = \begin{bmatrix} 1 & 0 \\ 0 & 1 \end{bmatrix} = I_2$ and $D_\eta = 0$. The systems constraints are $-5 \leq x \leq 5$ for both states, $-4 \leq u \leq 4$, and $-0.5 \leq \delta u \leq 0.5$, from which it is possible to define matrices $X' = \begin{bmatrix} -0.2 & 0.2 & 0 & 0 \\ 0 & 0 & -0.2 & 0 \end{bmatrix}'$, $U' = \begin{bmatrix} -0.25 & 0.25 \end{bmatrix}'$, $U'_d = \begin{bmatrix} -2 & 2 \end{bmatrix}'$, and the disturbance matrix $P' = \begin{bmatrix} -10 & 10 \end{bmatrix}'$. Notice, in particular, that the state constraints correspond to the bounds considered in the fuzzification process, meaning that the corresponding sets $\mathcal{X}$ and $\mathcal{U}$ of state and control amplitude constraints defines the validity for the considered Fuzzy T-S model (KLUG, 2015).

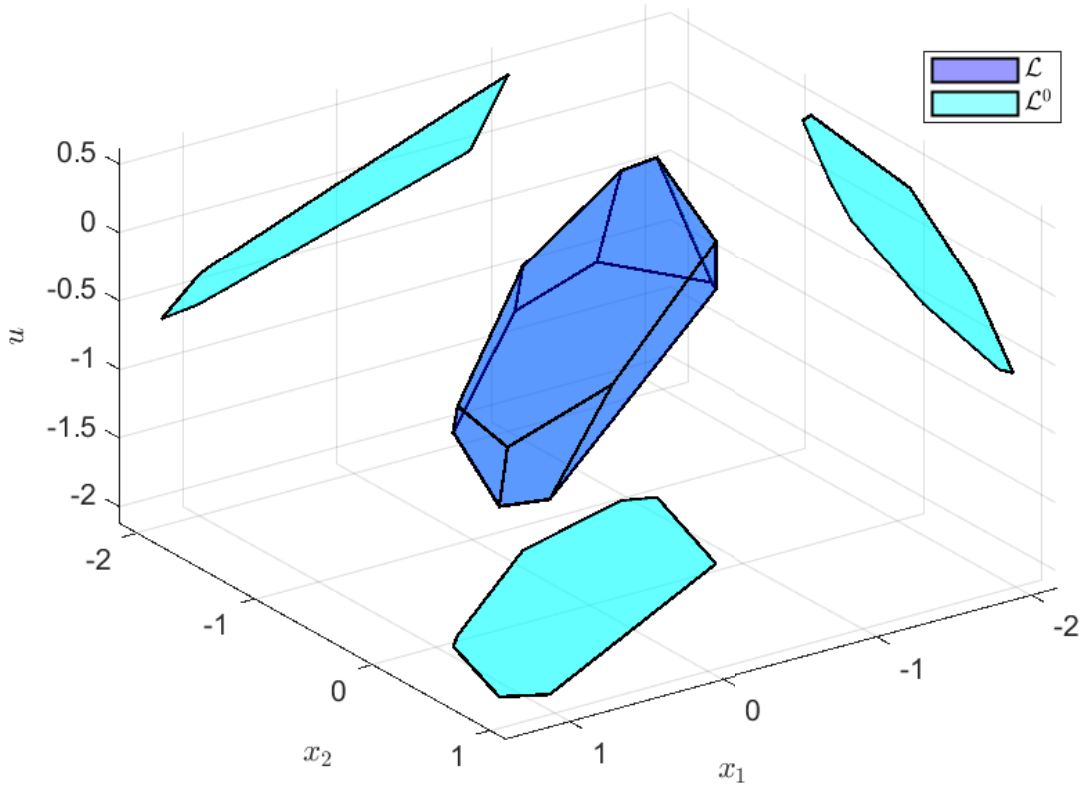

Figure 37 – LPV, with $-0.5 \leq \delta u \leq 0.4$

The obtained control gains from the optimization problem (137), for $\alpha = 1$ are shown in Table 23. The associated RPI sets $\mathcal{L}$ and $\mathcal{L}_0$ are obtained from the computed scalar $\rho = 0.9183835$ and matrix

$$L = \begin{bmatrix} -0.0562469 & -0.1580882 & -0.0049959 \\ -0.0745239 & -0.1346181 & -0.0500129 \\ 0.0000000 & -0.2000000 & 0.0000000 \\ 0.0000000 & 0.0000000 & 0.2500000 \\ 0.0000000 & 0.0000000 & -0.2500000 \\ -0.1236379 & -0.0028597 & -0.1872333 \\ 0.0000000 & 0.2000000 & 0.0000000 \\ 0.0745239 & 0.1346181 & 0.0500129 \\ 0.0562469 & 0.1580882 & 0.0049959 \\ -0.2000000 & 0.0000000 & 0.0000000 \\ 0.2000000 & 0.0000000 & 0.0000000 \\ 0.1236379 & 0.0028597 & 0.1872333 \end{bmatrix}.$$

The resulting polyhedron has a projection area in $\mathbb{R}^2$ that covers 99.6994% of the state constraints $\mathcal{X}$, and a volume that covers 92.0450% of its augmented state

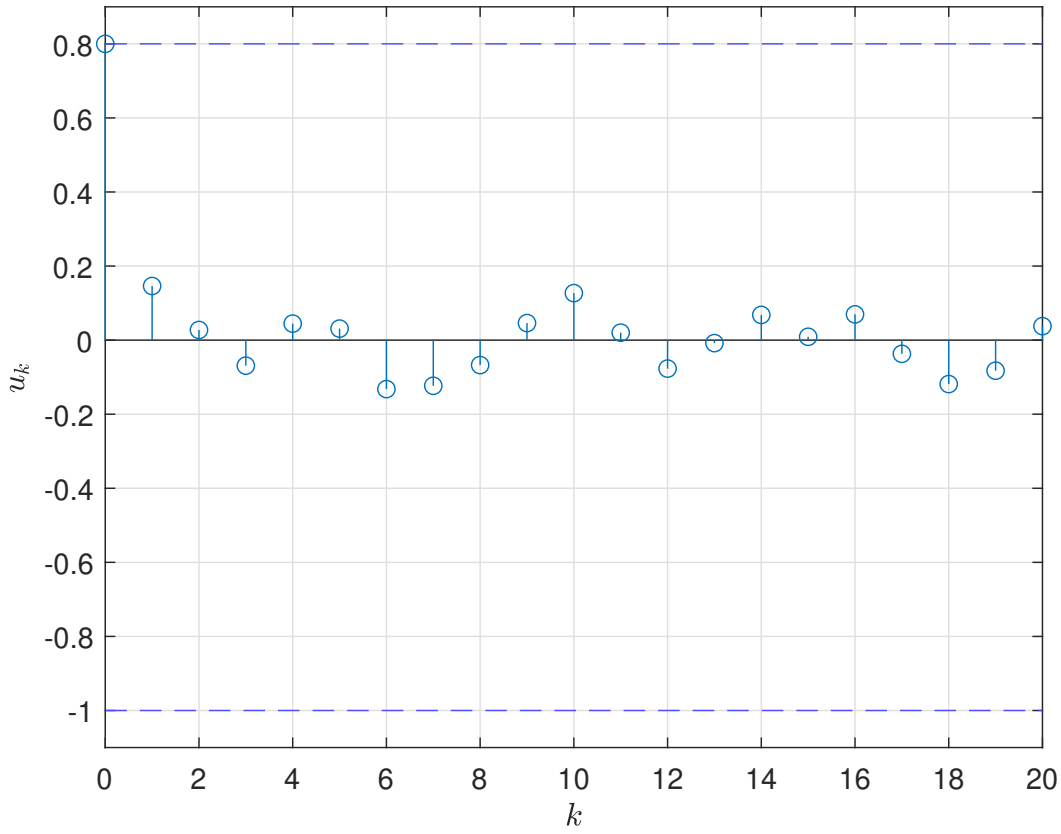

Figure 38 – u_k evolution overtime

Vertices	K	$\bar{K}$	K_1
1	-0.0120810 -0.0015856	-0.0966010	0.0000000 0.0000000
2	-0.0073129 -0.0006120	-0.0972860	0.0000000 0.0000000
3	-0.0270717 -0.0036004	-0.0902390	0.0000000 0.0000000
4	-0.0079336 -0.0012842	-0.0939634	0.0000000 0.0000000
5	-0.0346602 -0.0007838	-0.1069854	0.0000000 0.0000000
6	-0.0232805 -0.0002278	-0.1127929	0.0000000 0.0000000
7	-0.0154042 -0.0004950	-0.1089970	0.0000000 0.0000000
8	-0.0590504 -0.0088570	-0.0858816	0.0000000 0.0000000

Table 23 – Control gains

constraints Ξ, showcasing the vast coverage of possible initial conditions that leads to an ultimately bounded stable trajectory.

Finally, in Figures 41 and 42, we show the positive invariant polyhedrons in blue and trajectory evolutions over time in black, as well their projections, highlighting the system stability for different initial conditions. The initial conditions were generated by running the open-loop system, with $u(0) = -1$ for Figure 41 and $u(0) = 1$ for Figure 42, then, after the open-loop system reached the associated equilibrium point, the system was switched to the closed-loop system with the proposed controller. Notice that the

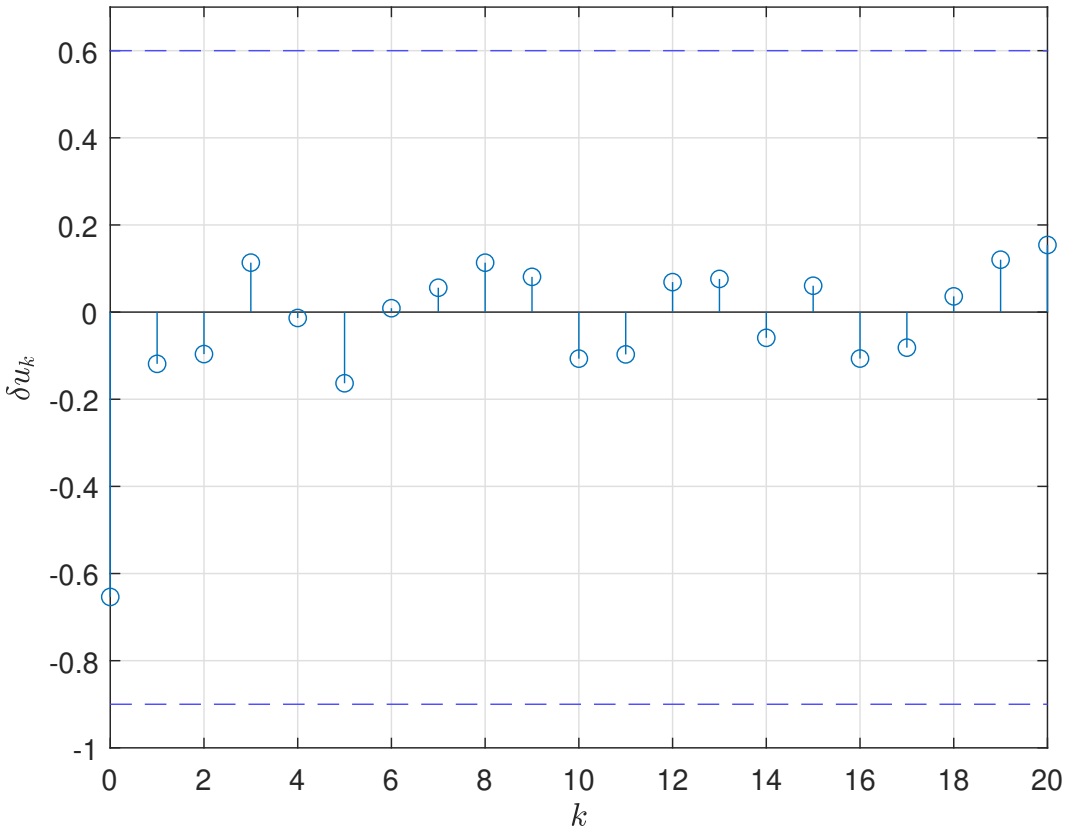

Figure 39 – δu_k evolution overtime

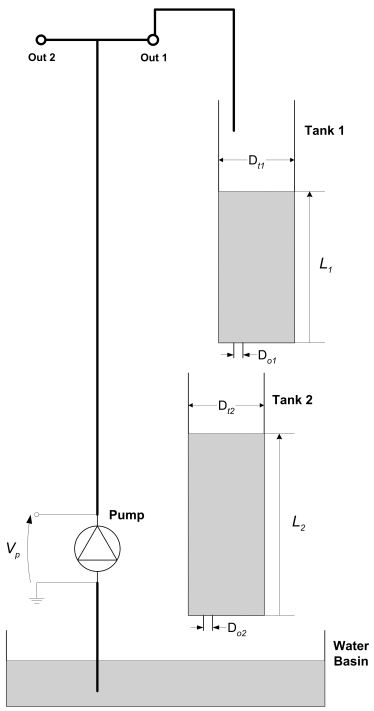

Figure 40 – Figure from Quanser®Coupled Tank Manual

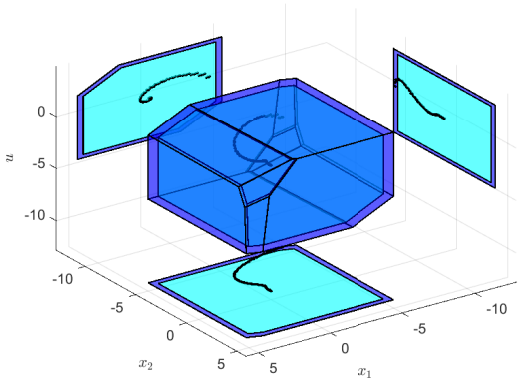

Figure 41 – $l_r = 12$, with $|\delta_u| \leq 0.5$ and for $u(0) = -1$

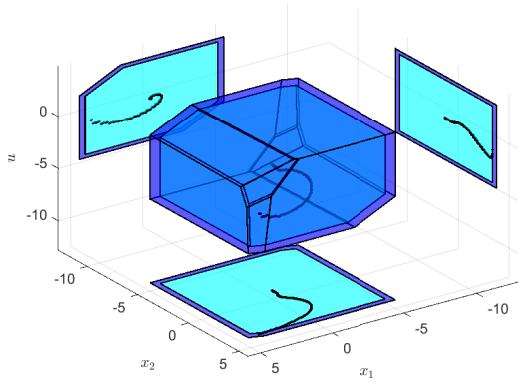

Figure 42 – $l_r = 12$, with $|\delta_u| \leq 0.5$ and for $u(0) = 1$

computed UB-set is conservative in its size because of the choice of the weight α in the objective function, which values a bigger RPI set instead of a smaller UB-set, as well as how the control input disturbance was conservatively modeled as an input disturbance.

Remark 20 *Finally, it is worth mentioning that for both the LTI and LPV examples in this section beginning, the bilinear design problem* (137) *provided non-null gains* K_1*, as shown in previous Tables 20, 21 and 22. In particular, it was possible to obtain such non-null gains in the simple LPV example, because only the system's control input matrix,* $B(\alpha_k)$*, is time-varying. On the other hand, in this coupled tank LPV application the bilinear program obtained all gains* $K_1 = 0$*, demonstrating that such constant gain* K_1 *does not provide enough degrees of freedom to improve the proposed controller* (119) *in comparison to the previous one in 4 equation* (81)*.*

5.5 CONCLUSION

In this chapter, a novel output feedback controller for constrained LPV systems subject to bounded process and measurement noises has been presented. The proposed solution utilizes the concepts of robust positive invariance to build a set of algebraic conditions that guarantee the fulfillment of the system's constraints even in the presence of bounded disturbances. Moreover, the algebraic conditions are utilized to develop a bilinear optimization problem whose objective function weights the maximization of the RPI set in a given set of directions or their projection in the system state-subspace with the minimization of an inner set where the system trajectories will be ultimately bounded. The properties of the proposed strategy have been formally proved and verified through numerical examples.

The proposed controller adds an extra degree of freedom through the constant control gain K_1. Furthermore, for even more degrees of freedom, one could consider this control gain as parameter-dependent $K_1(\alpha)$. However, by considering the parameter-

dependent version $K_1(\alpha)$, double products between parameter-dependent matrices would appear all over the algebraic conditions, particularly increasing the numerical complexity of the optimization problem and deserving of an in-depth study.

6 CONCLUSION

In this Thesis, novel control design approaches have been proposed for LTI systems subject to state, control constraints, and bounded disturbances, and for constrained LPV systems with and without bounded disturbances. The design approaches are based on set invariance, robust set invariance when necessary, and set containment conditions to build bilinear optimization problems to design the controllers. Examples were provided throughout the document in order to illustrate the proposed approaches, and each chapter can be summarized as follows.

First, in Chapter 2, we have proposed a new set of algebraic relations that jointly describe the Δ-Invariance (Robust Positive Invariance) property of a polyhedron and the convergence of the trajectories of linear discrete-time systems to an associate UB polyhedron. The algebraic conditions are then used to compose a bilinear optimization problem that allows the trade-off in maximizing the outer RPI set in some directions chosen a priori and minimizing the internal UB-set.

Next, in Chapter 3, a novel switching output feedback controller for constrained linear systems subject to bounded process and measurement noises has been presented. Then, by leveraging the extended Farkas' lemma, controllability, and set invariance arguments, we propose a set of algebraic conditions that guarantees one-step controllability to each polyhedron until the most internal set is reached, where the system's trajectories will be ultimately bounded. Finally, these algebraic conditions compose a bilinear optimization problem that aims to minimize the internal set and iteratively build a larger one-step controllable set until it is no longer able to find a bigger set.

In Chapter 4, algebraic conditions for a polyhedral set to be positively invariant for an LPV system subject to state, control, and control-rate constraints have been translated into two bilinear programming problems. Two different possibilities on the structure of the positive invariant sets are proposed and compared. Furthermore, the algebraic conditions that guarantee asymptotic stability are used to build bilinear optimization problems that aim to maximize the positive invariant set in some directions chosen a priori.

Furthermore, in Chapter 5, a novel output feedback controller for constrained LPV systems subject to bounded process and measurement noises, has been presented. By leveraging the RPI concept, we proposed a set of algebraic conditions that guarantees that any of the system's trajectories that start within the outermost set will be ultimately bounded in the innermost set. Finally, we propose a bilinear optimization problem based on these algebraic conditions that allows the trade-off in minimizing the internal set where the trajectories will be ultimately bounded and maximizing the outer set in some directions chosen a priori, representing the stabilizable initial conditions.

In all chapters, we employed the Knitro solver (BYRD et al., 2006) implemented

through AMPL (FOURER et al., 2003), which allows several different configurations, including efficient parallel processing with a high speed up, meaning that one can use multiple cores simultaneously to solve the optimization problem. Furthermore, it is important to highlight that Knitro does not guarantee global optimality. However, through its multistart configuration, the algorithm starts from multiple different initial conditions, covering a high percentage of the search space, and by comparing the resulting local minimums, the solver is able to provide satisfactory results.

6.1 PUBLICATIONS

Prior to this document, the contributions of the research throughout this PhD include the following journal articles:

- Brião, S. L., Castelan, E. B., Camponogara, E., & Ernesto, J. G. (2021). Output feedback design for discrete-time constrained systems subject to persistent disturbances via bilinear programming. Journal of the Franklin Institute, 358(18), 9741-9770.
- Lucia, W., Ernesto, J. G., & Castelan, E. B. (2023). Set-theoretic output feedback control: A bilinear programming approach. Automatica, 153, 111004.

Moreover, the following papers, published in conference proceedings, were also part of this research:

- Dórea, C. E., Castelan, E. B., & Ernesto, J. G. (2020). Robust positively invariant polyhedral sets and constrained control using fuzzy ts models: a bilinear optimization design strategy. IFAC-PapersOnLine (IFAC World Congress 2020, Germany), 53(2), 8013-8018.
- dos Santos, G. A. F., Ernesto, J. G., & Castelan, E. B. (2020, December). Controle sob Restrições de Sistemas Lineares-Projeto de Realimentação de Saídas via Programação Bilinear. In Congresso Brasileiro de Automática-CBA-2020 (Vol. 2, No. 1).
- Ernesto, J. G., Castelan, E. B., dos Santos, G. A. F., & Camponogara, E. (2021, March). Incremental output feedback design approach for discrete-time parameter-varying systems with amplitude and rate control constraints. In 2021 IEEE International Conference on Automation/XXIV Congress of the Chilean Association of Automatic Control (ICA-ACCA) (pp. 1-7). IEEE.
- dos Santos, G. A. F., Castelan, E. B., & Ernesto, J. G. (2021, March). PI-controller design for constrained linear systems using positive invariance and bilinear programming. In 2021 IEEE International Conference on Automation/XXIV Congress of the Chilean Association of Automatic Control (ICA-ACCA) (pp. 1-7). IEEE.

- Ernesto, J. G., Castelan, E. B., Lucia, W., & dos Santos, G. A. F. (2022). Alternative implementation to an incremental output-feedback design approach for constrained discrete-time parameter-varying systems. IFAC-PapersOnLine (5th IFAC Workshop on Linear Parameter Varying Systems (LPVS), Montreal, Canada), 55(35), 25-30.
- Dos Santos, G. F., Ernesto, J., Castelan, E. B., & Lucia, W. (2023). Discrete-Time Constrained PI-like Output Feedback Tracking Controllers-a Robust Positive Invariance and Bilinear Programming Approach (No. 11272). XVI Simpósio Brasileiro de Automação Inteligente (SBAI 2023, Manaus).

Finally, the contents of Chapter 5 were submitted to the 2024 Brazilian Congress of Automation (CBA - 2024).

6.2 FUTURE WORKS

Among some possible extensions to the work presented in this thesis, the following research directions can be mentioned:

- Extend the incremental control law, in Chapter 5, for LPV systems, with all control gains to be dependent on the varying parameters, enabling less conservative results.
- Propose alternative objective functions and consider saturation allowance, aiming to improve the size of the robust positive invariant sets and the closed-loop systems' time performance.
- Extend the results to discrete-time LTI systems with time-varying delays, as well as to second-order systems aiming for some mechatronics applications.

REFERENCES

ANGELI, D.; CASAVOLA, A.; FRANZÈ, G.; MOSCA, E/. An ellipsoidal off-line MPC scheme for uncertain polytopic discrete-time systems. **Automatica**, Elsevier, v. 44, n. 12, p. 3113–3119, 2008.

BERMAN, A.; PLEMMONS, R. J. **Nonnegative Matrices in the Mathematical Sciences**. [S.l.]: SIAM, 1994. v. 9.

BERTSEKAS, D. P.; RHODES, I. B. On the minimax reachability of target sets and target tubes. **Automatica**, Elsevier, v. 7, n. 2, p. 233–247, 1971.

BITSORIS, G.; OLARU, S.; VASSILAKI, M. On the Linear Constrained Regulation Problem for Continuous-Time Systems. **IFAC Proceedings Volumes**, v. 47, n. 3, p. 4004–4009, 2014. 19th IFAC World Congress. DOI: 10.3182/20140824-6-ZA-1003.02558.

BLANCHINI, F. Feedback control for linear time-invariant systems with state and control bounds in the presence of disturbances. **IEEE Transactions on Automatic Control**, v. 35, n. 11, p. 1231–1234, 1990. ISSN 0018-9286. DOI: 10.1109/9.59808.

BLANCHINI, F. Set invariance in control. **Automatica**, v. 35, n. 11, p. 1747–1767, 1999. ISSN 0005-1098. DOI: 10.1016/S0005-1098(99)00113-2.

BLANCHINI, F.; MIANI, S. **Set-Theoretic Methods in Control**. [S.l.]: Springer International Publishing, 2015. (Systems & Control: Foundations & Applications). ISBN 9783319179339. Available from: https://books.google.com.br/books?id=8a0YCgAAQBAJ.

BORRELLI, F.; BEMPORAD, A.; MORARI, M. **Predictive control for linear and hybrid systems**. [S.l.]: Cambridge University Press, 2017.

BRIAO, Stephanie L.; CASTELAN, Eugenio B; CAMPONOGARA, Eduardo. Output Feedback for Discrete-time Constrained Systems subject to Persistent Disturbances via Bilinear Programming. **Journal of The Franklin Institute**, Elsevier, 2021.

BRIÃO, S. L. **Estabilização de Sistemas Lineares com Cálculo Explícito dos Ganhos de Realimentaćão via Conjuntos Invariantes Poliédricos**. 2019. PhD thesis – PPGEAS/UFSC.

BRIÃO, S. L.; PEDROSA, M. V. A.; CASTELAN, E. B.; CAMPONOGARA, E.; ASSIS, L. S. de. Explicit Computation of Stabilizing Feedback Control Gains Using Polyhedral Lyapunov Functions. In: IEEE. 2018 IEEE International Conference on Automation/XXIII Congress of the Chilean Association of Automatic Control (ICA-ACCA). [S.l.: s.n.], 2018. P. 1–6.

BRIAT, Corentin. Linear parameter-varying and time-delay systems. **Analysis, observation, filtering & control**, Springer, v. 3, p. 5–7, 2014.

BYRD, R. H.; NOCEDAL, J.; WALTZ, R. A. Knitro: An Integrated Package for Nonlinear Optimization. In: DI PILLO, G.; ROMA, M. (Eds.). **Large-Scale Nonlinear Optimization**. Boston: Springer, 2006.

CHERIFI, Abdelmadjid; GUELTON, Kevin; ARCESE, Laurent. Quadratic design of d-stabilizing non-pdc controllers for quasi-lpv/ts models. **IFAC-PapersOnLine**, Elsevier, v. 48, n. 26, p. 164–169, 2015.

DA SILVA, JM Gomes; LIMÓN, Daniel; ALAMO, Teodoro; CAMACHO, Eduardo F. Dynamic output feedback for discrete-time systems under amplitude and rate actuator constraints. **IEEE Transactions on Automatic Control**, IEEE, v. 53, n. 10, p. 2367–2372, 2008.

DANTAS, A. D.; DANTAS, A. F.; DÓREA, C. E. T. Static output feedback control design for constrained linear discrete-time systems using data cluster analysis. **IET Control Theory & Applications**, IET, v. 12, n. 18, p. 2541–2550, 2018.

DE ALMEIDA, Tiago Alves; DOREA, Carlos ET. Output Feedback Constrained Regulation of Linear Systems via Controlled-Invariant Sets. **IEEE Transactions on Automatic Control**, IEEE, 2020. DOI: 10.1109/TAC.2020.3020100.

DING, Baocang; XI, Yugeng; CYCHOWSKI, Marcin T; O'MAHONY, Thomas. A synthesis approach for output feedback robust constrained model predictive control. **Automatica**, Elsevier, v. 44, n. 1, p. 258–264, 2008.

DÓREA, C. E. T.; CASTELAN, E. B.; ERNESTO, J. G. Robust Positive Invariant Polyhedral Sets and Constrained Control using Fuzzy T-S Models: a Bilinear Optimization Design Strategy. In: 21ST IFAC World Congress. Berlin: [s.n.], 2020. P. 8013–8018. DOI: 10.1016/j.ifacol.2020.12.2230.

DOS SANTOS, Geovana F; ERNESTO, Jackson; CASTELAN, Eugênio B; LUCIA, Walter. Discrete-Time Constrained PI-like Output Feedback Tracking Controllers-a Robust Positive Invariance and Bilinear Programming Approach. **SBAI**, 2023.

EBENBAUER, Christian; ALLGÖWER, Frank. Stability analysis of constrained control systems: An alternative approach. **Systems & Control Letters**, Elsevier, v. 56, n. 2, p. 93–98, 2007.

ERNESTO, Jackson G; CASTELAN, Eugenio B; SANTOS, Geovana A França dos; CAMPONOGARA, Eduardo. Incremental output feedback design approach for discrete-time parameter-varying systems with amplitude and rate control constraints. In: IEEE. 2021 IEEE International Conference on Automation/XXIV Congress of the Chilean Association of Automatic Control (ICA-ACCA). [S.l.: s.n.], 2021. P. 1–7.

ERNESTO, Jackson G; CASTELAN, Eugênio B; LUCIA, Walter; SANTOS, Geovana A França dos. Alternative implementation to an incremental output-feedback design approach for constrained discrete-time parameter-varying systems. **IFAC-PapersOnLine**, Elsevier, v. 55, n. 35, p. 25–30, 2022.

FENG, G. A survey on analysis and design of model-based fuzzy control systems. **IEEE Trans. Fuzzy Syst.**, v. 14, p. 676–697, 2006.

FINDEISEN, Rolf; IMSLAND, Lars; ALLGOWER, Frank; FOSS, Bjarne A. State and output feedback nonlinear model predictive control: An overview. **European journal of control**, Elsevier, v. 9, n. 2-3, p. 190–206, 2003.

FLOUDAS, C. A. **Deterministic Global Optimization: Theory, Methods and Applications**. Secaucus, NJ, USA: Springer-Verlag New York, Inc., 2005. ISBN 0792360141.

FOURER, Robert; GAY, David M; KERNIGHAN, Brian W. AMPL. A modeling language for mathematical programming. Thomson, 2003.

FRANÇA, Geovana A.; CASTELAN, Eugenio B.; ERNESTO, Jackson G. PI-controller design for constrained linear systems using positive invariance and bilinear programming. In: IEEE. 2021 IEEE International Conference on Automation/XXIV Congress of the Chilean Association of Automatic Control (ICA-ACCA). [S.l.: s.n.], 2021.

GONG, Weibo; SHI, Leyuan. **Modeling, Control and Optimization of Complex Systems: In Honor of Professor Yu-Chi Ho**. [S.l.]: Springer Science & Business Media, 2012. v. 14.

GUERRA, Thierry Marie; VERMEIREN, Laurent. LMI-based relaxed nonquadratic stabilization conditions for nonlinear systems in the Takagi–Sugeno's form. **Automatica**, Elsevier, v. 40, n. 5, p. 823–829, 2004.

GUPTA, A.; FALCONE, P. Full-Complexity Characterization of Control-Invariant Domains for Systems With Uncertain Parameter Dependence. **IEEE Control Systems Letters**, v. 3, n. 1, p. 19–24, 2019. ISSN 2475-1456. DOI: 10.1109/LCSYS.2018.2849714.

HENNET, J.-C. Discrete time constrained linear systems. **Control and Dynamic Systems**, ACADEMIC PRESS LIMITED, v. 71, p. 157–214, 1995.

HU, T.; LIN, Z. **Control Systems with Actuator Saturation: Analysis and Design**. [S.l.]: Birkhäuser, 2001. (Control Systems with Actuator Saturation: Analysis and Design).

ISIDÓRIO, Isaac D; DÓREA, Carlos ET; CASTELAN, Eugênio B. Observer-Based Output Feedback Control Using Invariant Polyhedral Sets for Fuzzy T–S Models Under Constraints. **Journal of Control, Automation and Electrical Systems**, Springer, v. 34, n. 4, p. 752–765, 2023.

KLUG, Michael. **Control of nonlinear systems using n-fuzzy models**. 2015. PhD thesis – Universidade Federal de Santa Catarina, Centro Tecnológico, Programa de Pós-Graduação em Engenharia de Automação e Sistemas.

KLUG, Michael; CASTELAN, Eugênio B; COUTINHO, Daniel. AT–S fuzzy approach to the local stabilization of nonlinear discrete-time systems subject to energy-bounded disturbances. **Journal of Control, Automation and Electrical Systems**, Springer, v. 26, n. 3, p. 191–200, 2015a.

KLUG, Michael; CASTELAN, Eugênio B; LEITE, Valter JS; SILVA, Luís FP. Fuzzy dynamic output feedback control through nonlinear Takagi–Sugeno models. **Fuzzy Sets and Systems**, Elsevier, v. 263, p. 92–111, 2015b.

KÖGEL, Markus; FINDEISEN, Rolf. Robust output feedback MPC for uncertain linear systems with reduced conservatism. **IFAC-PapersOnLine**, Elsevier, v. 50, n. 1, p. 10685–10690, 2017.

LORENZETTI, Joseph; PAVONE, Marco. A simple and efficient tube-based robust output feedback model predictive control scheme. In: IEEE. 2020 European Control Conference (ECC). [S.l.: s.n.], 2020. P. 1775–1782.

LØVAAS, Christian; SERON, Maria M; GOODWIN, Graham C. Robust output-feedback model predictive control for systems with unstructured uncertainty. **Automatica**, Elsevier, v. 44, n. 8, p. 1933–1943, 2008.

LUCIA, Walter; ERNESTO, Jackson G.; CASTELAN, Eugênio B. Set-theoretic output feedback control: A bilinear programming approach. **Automatica**, v. 153, p. 111004, 2023. ISSN 0005-1098. DOI: https://doi.org/10.1016/j.automatica.2023.111004. Available from: https://www.sciencedirect.com/science/article/pii/S0005109823001589.

LUCIA, Walter; FAMULARO, Domenico; FRANZE, Giuseppe. A set-theoretic reconfiguration feedback control scheme against simultaneous stuck actuators. **IEEE Transactions on Automatic Control**, IEEE, v. 63, n. 8, p. 2558–2565, 2017.

MAYNE, David Q; RAKOVIĆ, SV; FINDEISEN, Rolf; ALLGÖWER, Frank. Robust output feedback model predictive control of constrained linear systems: Time varying case. **Automatica**, Elsevier, v. 45, n. 9, p. 2082–2087, 2009.

MAYNE, David Q; RAWLINGS, James B; RAO, Christopher V; SCOKAERT, Pierre OM. Constrained model predictive control: Stability and optimality. **Automatica**, Elsevier, v. 36, n. 6, p. 789–814, 2000. DOI: 10.1016/S0005-1098(99)00214-9.

MCCORMICK, G. P. Computability of global solutions to factorable nonconvex programs: Part I — Convex underestimating problems. **Mathematical Programming**, v. 10, n. 1, p. 147–175, 1976. DOI: 10.1007/BF01580665.

MILANI, B. E. A.; DÓREA, C. E. T. On invariant polyhedra of continuous-time systems subject to additive disturbances. **Automatica**, v. 32, n. 5, p. 785–789, 1996. DOI: 10.1016/0005-1098(96)00002-7.

MILANI, Basílio EA; CASTELAN, Eugênio B; TARBOURIECH, Sophie. Linear regulator design for bounded uncertain discrete-time systems with additive disturbances. **IFAC Proceedings Volumes**, Elsevier, v. 29, n. 1, p. 3192–3197, 1996.

MOHAMMADPOUR, Javad; SCHERER, Carsten W. **Control of linear parameter varying systems with applications**. [S.l.]: Springer Science & Business Media, 2012.

MORATO, Marcelo Menezes. **Predictive control methods for linear parameter varying systems**. 2023. PhD thesis – Universidade Federal de Santa Catarina, Université Grenoble Alpes.

RUGH, Wilson J; SHAMMA, Jeff S. Research on gain scheduling. **Automatica**, Elsevier, v. 36, n. 10, p. 1401–1425, 2000.

SADABADI, Mahdieh S; PEAUCELLE, Dimitri. From static output feedback to structured robust static output feedback: A survey. **Annual Reviews in Control**, Elsevier, v. 42, p. 11–26, 2016. DOI: 10.1016/j.arcontrol.2016.09.014.

SANTOS, Geovana Franca dos; CASTELAN, Eugenio B; LUCIA, Walter. On the design of constrained pi-like output feedback tracking controllers via robust positive invariance and bilinear programming. **IEEE Control Systems Letters**, IEEE, v. 7, p. 1429–1434, 2023.

SANTOS, Geovana Franca dos; CASTELAN, Eugenio B.; LUCIA, Walter. **A Constrained Tracking Controller for Ramp and Sinusoidal Reference Signals using Robust Positive Invariance**. [S.l.: s.n.], 2024. arXiv: 2403.08987 [math.OC].

SANTOS, M. M. D.; CASTELAN, E. B.; HENNET, J.-C. A Linear Programming Approach for Regional Pole Placement Under Pointwise Constraints. **IFAC Proceedings Volumes**, Elsevier, v. 30, n. 16, p. 297–302, 1997.

SHAMMA, Jeff S. **Analysis and design of gain scheduled control systems**. 1988. PhD thesis – Massachusetts Institute of Technology.

SILVA, Luís FP; LEITE, Valter JS; CASTELAN, Eugênio B; KLUG, Michael; GUELTON, Kevin. Local stabilization of nonlinear discrete-time systems with time-varying delay in the states and saturating actuators. **Information Sciences**, Elsevier, v. 518, p. 272–285, 2020. DOI: 10.1016/j.ins.2020.01.029.

SILVA, Luís FP; LEITE, Valter JS; CASTELAN, Eugênio B; SOUZA, Carla de. Regional input-to-state stabilization of fuzzy state-delayed discrete-time systems with saturating actuators. **Information Sciences**, Elsevier, v. 557, p. 250–267, 2021.

SILVA JR, J. M. G. da; CASTELAN, E. B.; CORSO, J.; ECKHARD, D. Dynamic output feedback stabilization for systems with sector-bounded nonlinearities and saturating actuators. **Journal of the Franklin Institute**, Elsevier, v. 350, n. 3, p. 464–484, 2013.

STRANG, Gilbert. **Linear algebra and its applications**. Belmont, CA: Thomson, Brooks/Cole, 2006. Available from: http://www.amazon.com/Linear-Algebra-Its-Applications-Edition/dp/0030105676.

SUBRAMANIAN, Sankaranarayanan; LUCIA, Sergio; ENGELL, Sebastian. A novel tube-based output feedback MPC for constrained linear systems. In: IEEE. 2017 American Control Conference (ACC). [S.l.: s.n.], 2017. P. 3060–3065.

TAKAGI, T.; SUGENO, M. Fuzzy identification of systems and its applications to modeling and control. **IEEE Trans. Syst. Man Cybern.**, v. 15, p. 116–132, 1985.

TANAKA, K.; WANG, H.O. **Fuzzy Control Systems Design and Analysis: A Linear Matrix Inequality Approach**. [S.l.]: Wiley, 2004. ISBN 9780471465225. Available from: https://books.google.com.br/books?id=VH0AFTSmg5AC.

TARBOURIECH, Sophie; GARCIA, Germain; SILVA JR, João Manoel Gomes da; QUEINNEC, Isabelle. **Stability and stabilization of linear systems with saturating actuators**. [S.l.]: Springer Science & Business Media, 2011.

WÄCHTER, A.; BIEGLER, L.T. On the implementation of an interior-point filter line-search algorithm for large-scale nonlinear programming. **Mathematical Programming**, Springer, v. 106, n. 1, p. 25–57, 2006. DOI: 10.1007/s10107-004-0559-y.

WALTER, Gill; MICHAEL, Murray; SAUNDERS, A. SNOPT: An SQP Algorithm for Large-Scale Constrained Optimization. **SIAM Review**, v. 47, n. 1, p. 99–131, 2005. DOI: 10.1137/S0036144504446096.

WAN, Zhaoyang; KOTHARE, Mayuresh V. Robust output feedback model predictive control using off-line linear matrix inequalities. **Journal of Process Control**, Elsevier, v. 12, n. 7, p. 763–774, 2002.

WANG, H.O.; TANAKA, K.; GRIFFIN, M.F. An approach to fuzzy control of nonlinear systems: stability and design issues. **IEEE Trans. Fuzzy Syst.**, v. 4, p. 14–23, 1996.

ZHOU, Xiaojun; LI, Chaojie; HUANG, Tingwen; XIAO, Mingqing. Fast gradient-based distributed optimisation approach for model predictive control and application in four-tank benchmark. **IET Control Theory & Applications**, IET, v. 9, n. 10, p. 1579–1586, 2015. DOI: 10.1049/iet-cta.2014.0549.

Appendix

APPENDIX A – COUPLED TANK MODELLING

We will divide the coupled tank modeling into three sections. First, we show the fuzzyfication process applied to the nonlinear system (KLUG, 2015). Next, we will discretize the system, through a zero-order holder (ZOH). Finally, we will shift the system from the origin to an *a priori* chosen equilibrium point.

A.1 FUZZYFICATION

In possession of the non-linear equations (138), we proceed to utilize the following steps to describe a T-S model that describes the non-linear system for the sector within $10 \leq L_1 \leq 20$, $10 \leq L_1 \leq 20$ and $2 \leq V_p \leq 12$.

First, obtaining equations with the states and input in evidence is necessary. To this end, we multiplied the non-linear equations by $\frac{\sqrt{L_1}}{\sqrt{L_1}}\frac{\sqrt{L_2}}{\sqrt{L_2}} = 1$, resulting in

$$\begin{aligned}\dot{L}_1 &= -\frac{D_{of1}\sqrt{2g}}{D_{t1}\sqrt{L_1}}L_1 + \frac{K_m(V_p)}{D_{t1}}V_p \\ \dot{L}_2 &= -\frac{D_{of2}\sqrt{2g}}{D_{t2}\sqrt{L_2}}L_2 + \frac{D_{of1}\sqrt{2g}}{D_{t2}\sqrt{L_1}}L_1.\end{aligned}$$

Now we can write the system dynamic equations in the state space form:

$$\begin{bmatrix}\dot{L}_1 \\ \dot{L}_2\end{bmatrix} = \begin{bmatrix}-\frac{D_{of1}\sqrt{2g}}{D_{t1}\sqrt{L_1}} & 0 \\ \frac{D_{of1}\sqrt{2g}}{D_{t2}\sqrt{L_1}} & -\frac{D_{of2}\sqrt{2g}}{D_{t2}\sqrt{L_2}}\end{bmatrix}\begin{bmatrix}L_1 \\ L_2\end{bmatrix} + \begin{bmatrix}\frac{K_m(V_p)}{D_{t1}} \\ 0\end{bmatrix}V_p$$

Since, for this example, the physical parameter $D_{t1} = D_{t2}$ and $D_{of1} = D_{of2}$, we consider the nonlinear terms

$$\begin{aligned}z_1 &= \frac{D_{of1}\sqrt{2g}}{D_{t1}\sqrt{L_1}}, \\ z_2 &= \frac{D_{of2}\sqrt{2g}}{D_{t2}\sqrt{L_2}}, \\ z_3 &= \frac{K_m(V_p)}{D_{t1}},\end{aligned}$$

resulting in the system dynamic equations given by

$$\begin{bmatrix}\dot{L}_1 \\ \dot{L}_2\end{bmatrix} = \begin{bmatrix}-z_1 & 0 \\ z_1 & -z_2\end{bmatrix}\begin{bmatrix}L_1 \\ L_2\end{bmatrix} + \begin{bmatrix}z_3 \\ 0\end{bmatrix}V_p. \tag{140}$$

Next, to write the membership functions and vertices of the model, we need to compute the minimum and maximum values of the nonlinear terms

$$\max_{L_1} z_1 = a1$$

$$\min_{L_1} z_1 = a2$$
$$\max_{L_2} z_2 = b1$$
$$\min_{L_2} z_2 = b2$$
$$\max_{L_1} z_3 = c1$$
$$\min_{L_1} z_3 = c2$$

with given by the vertices

$$A_1 = \begin{bmatrix} -a_1 & 0 \\ a_1 & -b_1 \end{bmatrix}, B_1 = \begin{bmatrix} c_1 \\ 0 \end{bmatrix} \tag{141}$$
$$A_2 = \begin{bmatrix} -a_2 & 0 \\ a_2 & -b_1 \end{bmatrix}, B_2 = \begin{bmatrix} c_1 \\ 0 \end{bmatrix} \tag{142}$$
$$A_3 = \begin{bmatrix} -a_1 & 0 \\ a_1 & -b_2 \end{bmatrix}, B_3 = \begin{bmatrix} c_1 \\ 0 \end{bmatrix} \tag{143}$$
$$A_4 = \begin{bmatrix} -a_2 & 0 \\ a_2 & -b_2 \end{bmatrix}, B_4 = \begin{bmatrix} c_1 \\ 0 \end{bmatrix} \tag{144}$$
$$A_5 = \begin{bmatrix} -a_1 & 0 \\ a_1 & -b_1 \end{bmatrix}, B_5 = \begin{bmatrix} c_2 \\ 0 \end{bmatrix} \tag{145}$$
$$A_6 = \begin{bmatrix} -a_2 & 0 \\ a_2 & -b_1 \end{bmatrix}, B_6 = \begin{bmatrix} c_2 \\ 0 \end{bmatrix} \tag{146}$$
$$A_7 = \begin{bmatrix} -a_1 & 0 \\ a_1 & -b_2 \end{bmatrix}, B_7 = \begin{bmatrix} c_2 \\ 0 \end{bmatrix} \tag{147}$$
$$A_8 = \begin{bmatrix} -a_2 & 0 \\ a_2 & -b_2 \end{bmatrix}, B_8 = \begin{bmatrix} c_2 \\ 0 \end{bmatrix} \tag{148}$$

Then, the membership functions are:

$$M_1(z_1(t)) = \frac{z_1(t) - a1}{a1 - a2} \tag{149}$$
$$M_2(z_1(t)) = \frac{a1 - z_1(t)}{a1 - a2} \tag{150}$$
$$N_1(z_2(t)) = \frac{z_2(t) - b1}{b1 - b2} \tag{151}$$
$$N_2(z_2(t)) = \frac{b1 - z_1(t)}{b1 - b2} \tag{152}$$
$$P_1(z_3(t)) = \frac{z_3(t) - c1}{c1 - c2} \tag{153}$$
$$P_2(z_3(t)) = \frac{c1 - z_3(t)}{c1 - c2} \tag{154}$$

notice that

$$M_1(z_1(t)) + M_2(z_1(t)) = 1 \tag{155}$$
$$N_1(z_2(t)) + N_2(z_2(t)) = 1 \tag{156}$$
$$P_1(z_3(t)) + P_2(z_3(t)) = 1 \tag{157}$$

The defuzzification is equivalent of the multiplications of the functions h_i and the equivalent vertices $A_i,\ B_i$ where

$$\dot{L} = \sum_{1}^{8} h_i(A_i L + B_i V_p) \tag{158}$$

where

$$h_1(z(t)) = M_1(z_1(t))N_1(z_2(t))P_1(z_3(t)) \tag{159}$$
$$h_2(z(t)) = M_2(z_1(t))N_1(z_2(t))P_1(z_3(t)) \tag{160}$$
$$h_3(z(t)) = M_1(z_1(t))N_2(z_2(t))P_1(z_3(t)) \tag{161}$$
$$h_4(z(t)) = M_2(z_1(t))N_2(z_2(t))P_1(z_3(t)) \tag{162}$$
$$h_5(z(t)) = M_1(z_1(t))N_1(z_2(t))P_2(z_3(t)) \tag{163}$$
$$h_6(z(t)) = M_2(z_1(t))N_1(z_2(t))P_2(z_3(t)) \tag{164}$$
$$h_7(z(t)) = M_1(z_1(t))N_2(z_2(t))P_2(z_3(t)) \tag{165}$$
$$h_8(z(t)) = M_2(z_1(t))N_2(z_2(t))P_2(z_3(t)) \tag{166}$$

A.2 DISCRETIZATION

After obtaining the T-S model, it is numerically discretized for a sampling time $ts = 1s$ using the zero-order hold (ZOH) method, resulting in the matrices vertices given by:

$$
\begin{aligned}
A_1 &= \begin{bmatrix} 0.8925256 & 0.0000000 \\ 0.1014803 & 0.8925256 \end{bmatrix}, A_2 = \begin{bmatrix} 0.8925256 & 0.0000000 \\ 0.0991277 & 0.8514655 \end{bmatrix} \\
A_3 &= \begin{bmatrix} 0.8514655 & 0.0000000 \\ 0.1401877 & 0.8925256 \end{bmatrix}, A_4 = \begin{bmatrix} 0.8514655 & 0.0000000 \\ 0.1369125 & 0.8514655 \end{bmatrix} \\
A_5 &= \begin{bmatrix} 0.8925256 & 0.0000000 \\ 0.1014803 & 0.8925256 \end{bmatrix}, A_6 = \begin{bmatrix} 0.8925256 & 0.0000000 \\ 0.0991277 & 0.8514655 \end{bmatrix} \\
A_7 &= \begin{bmatrix} 0.8514655 & 0.0000000 \\ 0.1369125 & 0.8514655 \end{bmatrix}, A_8 = \begin{bmatrix} 0.8514655 & 0.0000000 \\ 0.1401877 & 0.8925256 \end{bmatrix} \\
B_1 &= \begin{bmatrix} 0.1364234 \\ 0.0076087 \end{bmatrix}, B_2 = \begin{bmatrix} 0.1364234 \\ 0.0074918 \end{bmatrix}, B_3 = \begin{bmatrix} 0.1333202 \\ 0.0105950 \end{bmatrix}, \\
B_4 &= \begin{bmatrix} 0.1333202 \\ 0.0104316 \end{bmatrix}, B_5 = \begin{bmatrix} 0.2250484 \\ 0.0125516 \end{bmatrix}, B_6 = \begin{bmatrix} 0.2250484 \\ 0.0123587 \end{bmatrix}, \\
B_7 &= \begin{bmatrix} 0.2199292 \\ 0.0172082 \end{bmatrix}, B_8 = \begin{bmatrix} 0.2199292 \\ 0.0174779 \end{bmatrix}.
\end{aligned} \tag{167}
$$

Since we also have access to the continuous values of the varying parameters, the membership functions can be computed utilizing its continuous form instead of discretizing both the equations and the varying parameter values.

A.3 SYSTEM SHIFT

Finally, we shifted the system from the origin to a different equilibrium point. To this end, we considered the equilibrium point $x_{eq} = [15.2\ 14.8]^T$ and $u_{eq} = 8.1$, obtained experimentally, then states $x = L - x_{eq}$ and $u = V_p - u_{eq}$ and the matrices in (167) represent the shifted discrete non-linear system in the form of (114)-(115) in Chapter 5.